CAMS Service Evolution



D6.3 Uncertainties in Sector/Source contributions

Due date of deliverable	30 June 2025
Submission date	30 June 2025
File Name	CAMEO-D6.3-V2
Work Package /Task	WP6/Task6.3
Organisation Responsible of Deliverable	TNO
Author name(s)	Jessie Zhang, Floris Pekel, Renske Timmermans, Janot Tokaya, Hilde Fagerli, Alvaro Valdebenito, Svetlana Tsyro, Augustin Colette, Palmira Messina, Blandine Raux, Elsa Real, Peter Wind
Revision number	V2
Status	Issued
Dissemination Level	Public



The CAMEO project (grant agreement No 101082125) is funded by the European Union.

Views and opinions expressed are however those of the author(s) only and do not necessarily reflect those of the European Union or the Commission. Neither the European Union nor the granting authority can be held responsible for them.

1 Executive Summary

The Copernicus Atmosphere Monitoring Service (CAMS) currently offers a number of products to support decision and policy makers regarding mitigation of air pollution at the European scale (https://policy.atmosphere.copernicus.eu/). These policy products provide information about the main sources and drivers of air pollution, through so-called source apportionment or attribution (SA) or source receptor relationships (SR). A key factor influencing the variability in the CAMS source-receptor products is the diversity of source attribution methods. The current service employs three regional chemical transport models (CTMs)—LOTOS-EUROS, EMEP, and CHIMERE— each applying different source attribution techniques: tagging (contribution estimation), brute force (impact of 15% emission reductions), and surrogate modelling (impact of variable emission reductions). Due to the nonlinear chemistry involved in secondary aerosol formation, these methods can yield different results.

This study assesses the consistency and comparability of source-specific PM contributions across the different CTMs and source attribution methods. To this end we have conducted comparative experiments across the three models (EMEP, LOTOS-EUROS, CHIMERE) and different source attribution methodologies (brute force (BF), local fraction (LF), tagging/labelling (TS) and non-linear surrogate modelling (SM)) using a harmonised set-up in terms of inputs (emissions, meteorology, boundaries) and setup (resolution and domain). Additionally, model results were compared with observational data from Positive Matrix Factorisation (PMF) and specific tracers to identify key areas of agreement, divergence, and opportunities for improvement.

Key Findings:

- Residential Biomass Combustion: Identified consistently as the dominant anthropogenic source of PM around the Mediterranean and by EMEP and LOTOS-EUROS for Eastern Europe. Model results in general align well with the PMF data, though some regional spatial allocation issues with the emissions are identified (e.g., Barcelona), which indicates the dominance of this source may be overestimated in some areas. The contributions grow with increasing PM levels and due to its dominant primary PM share this source is hardly affected by nonlinear atmospheric processes and choice of attribution method. Differences are mainly due to CTM differences in surface layer depth (results show a strong sensitivity to this parameter) and mixing processes.
- Agriculture: CHIMERE highlights agriculture as a major PM source in Central Europe and the Baltic region, while EMEP and LOTOS-EUROS suggest a mix of agriculture or industry to be dominant in parts of Germany and Benelux. Agricultural emissions contribute to PM formation through complex nonlinear chemistry, leading to larger variability across source attribution methods, especially on shorter time scales. On a yearly average method induced differences are in the same order as CTM induced differences for secondary PM. Evaluation with PMF is hindered by the inability of PMF to resolve this source, and its inclusion in broader secondary PMF profiles.
- Traffic: Identified as the major PM source only in Bern, Zürich, and Munich, and exclusively by brute force methods with 15% emission reductions. While for these cities most effective small emission reductions are thus linked to the traffic sector, tagging and surrogate models using 100% reductions identified other sources to have larger contributions, highlighting the different purposes and complementarity of the methods.

The CTM and PMF approaches are having difficulty in representing this highly spatially and temporally variable source, in a time consistent way. CTMs generally underestimate PMF traffic contributions, likely due to the model resolution, issues in spatial attribution of emissions and mixing of multiple sources in the PMF traffic profile. Notably, PMF identified traffic-related resuspension not included in the CTMs, a gap being addressed by the CAMAERA project through the development of gridded non-exhaust emission inventories.

- Industry: Dominant in several German and Iberian cities in EMEP and LOTOS-EUROS results, with differences between CTMs driven by emission injection heights and differences between attribution methods by secondary aerosol formation. Evaluation is challenging due to the low number of sites identifying an industrial source profile and the variety of industrial sources and composition of their emissions.
- Shipping: Significant around Mediterranean ports and shipping lanes, with model discrepancies influenced by emission altitude and atmospheric mixing. Evaluation with PMF is hampered due to the limited number of stations providing a heavy fuel oil PMF source, although this source can often decently be captured by tracers as nickel / vanadium.
- **Natural Sources:** Identified by the EMEP model as the main contributor to daily PM_{2.5} above 50 μg/m³. These sources are relevant in relation to the subtraction of its contributions for EU PM exceedance reporting. While these primary PM contributions show no differences between attribution methods, significant variation exists between CTMs. Comparison with PMF data confirms an overestimation of sea salt by LOTOS-EUROS, while EMEP is showing a positive bias for dust in Athens.
- Overall the source attribution results from EMEP and LOTOS-EUROS are providing
 the same major source for more than 75% of the cities, although LOTOS-EUROS
 identifies a greater number of cities where primary pollutants are the dominant
 component. There is less consistency in the main source sector and component
 between CHIMERE's surrogate model results and those from the other models,
 probably related to the large interaction terms determined by its surrogate model.

Methodological Insights:

- CAMS currently provides geographical and sectoral source attribution through separate
 products based on different methods: brute force and surrogate model for estimating
 emission reduction impacts and tagging for source contributions. Combining model
 outputs into a mini-ensemble is methodologically sound for assessing annual and
 primary PM but secondary PM attribution and total PM attribution on shorter timescales
 requires method-specific approaches used in a complementary way.
- The local fraction method is demonstrated to be an efficient substitute for brute force in EMEP, with minimal differences.
- Comparing model results to Positive Matrix Factorisation (PMF) data is complex due to differences in each PMF dataset characteristics and difficulty in isolating sources requiring thorough analysis of the PMF profiles to identify its potential match with CTM sources. Its inclusion in operational CAMS evaluation processes is furthermore hampered by delays in availability of PMF data. Alternatives like near real-time source

- specific elemental carbon or organic aerosol observations and tracer monitoring may be more suitable for this.
- Possible evaluations with PMF data can benefit from a further separation of GNFR sectors into sub sectors within the CTM models.

Recommendations:

- Provide complementary source attribution methods to leverage their strengths (e.g. the provision of more detailed information from subsectoral contributions by tagging approach) in CAMS policy support service.
- Refine spatial allocation of residential biomass emissions (and other sources) to better represent local practices.
- Consider a redistribution of the interaction terms from the surrogate model (and BF and LF) avoiding interpretation difficulties by users and improving representation of actual agriculture and other sectoral contributions influenced by non-linear chemistry.
- Develop urban source attribution modelling tools by combining the regional background information with source attribution from local models with increased resolution and more detailed local traffic emissions information, including non-exhaust sources for better attribution of the local traffic contributions.
- Evaluation of the CAMS policy support products with PMF is only recommended for PMF profiles with clear tracer species, i.e. residential biomass combustion, sea salt and to some extent dust and shipping profiles.
- Consider how to effectively communicate to policymakers the potential uncertainties and differences in source attribution results arising from the choice of CTM and source attribution method.

Table of Contents

E	Exe	cutive	Summary	3
I	ntr	oduct	ion	8
2.1		Back	ground	8
2.2	2	Scop	e of this deliverable	8
2	2.2.	1	Objectives of this deliverable	8
2	2.2.	2	Work performed in this deliverable	8
2	2.2.	3	Deviations and countermeasures	8
2	2.2.	4	CAMEO Project Partners:	9
E	Eva	luatio	n of source sector attribution products	10
3.1		Introd	luction	10
3.2	2	Chen	nistry transport models and their source attribution methods	10
3	3.2.	1	EMEP model	10
3	3.2.	2	LOTOS-EUROS model	11
3	3.2.	3	CHIMERE model	11
3.3	3	Mode	elling setup	12
3.4	ļ	Posit	ve matrix factorization	13
3	3.4.	1	European PMF datasets	14
3.5	5	Trace	er data	15
3.6	3	Com	parability of models and methods	16
3	3.6.	1	Source attribution methods	16
3	3.6.	2	CTM models	17
3	3.6.	3	CTM and PMF	17
3.7	7	Statis	tical indicators for comparisons	18
ľ	Mod	delled	concentrations evaluation	19
			•	
		-	•	
-				
-				
			•	
	3.1 3.1 3.1 3.2 3.3 3.4 3.5 5.1 5.1 6.1 6.1 6.2 6.3	Intr 2.1 2.2 2.2. 2.2. 2.2. 2.2. 3.1 3.2 3.2. 3.2.	Introduct 2.1 Backs 2.2 Scope 2.2.1 2.2.2 2.2.3 2.2.4 Evaluation 3.2 Chem 3.2.1 3.2.2 3.2.3 3.3 Model 3.4 Position 3.4.1 3.5 Trace 3.6 Comp 3.6.1 3.6.2 3.6.3 3.7 Statist Modelled Results - 1 1 1 1 1 1 1 1 1 1	2.2.1 Objectives of this deliverable 2.2.1 Objectives of this deliverable 2.2.2 Work performed in this deliverable 2.2.3 Deviations and countermeasures 2.2.4 CAMEO Project Partners: Evaluation of source sector attribution products 3.1 Introduction 3.2 Chemistry transport models and their source attribution methods 3.2.1 EMEP model 3.2.2 LOTOS-EUROS model 3.2.3 CHIMERE model 3.3.3 Modelling setup 3.4 Positive matrix factorization 3.4.1 European PMF datasets 3.5 Tracer data 3.6 Comparability of models and methods 3.6.2 CTM models 3.6.3 CTM and PMF 3.7 Statistical indicators for comparisons Modelled concentrations evaluation Results - Consistency and comparability of source sector contributions between the source attribution methods 5.1 Annual source apportionment 5.2 Seasonal variability 5.3 Daily variability 5.4 Source attribution of exceedances of limit values Results - Evaluation of CTM source attributions with observational based source tribution 6.1 Total concentrations 6.2 Biomass Burning 6.3 Road traffic 6.4 Industry

6.6	Sea salt	56
6.7	(Mineral) dust	58
6.8	Nitrate-rich & Sulfate-rich	60
7 Cc	onclusions and recommendations	64
Refere	nces	67
Appen	dix A – Annual source contributions to PM _{2.5}	71
Appen	dix B – Impact of surface layer thickness	73
Appen	dix C – seasonal variation	74
Appen	dix D - EBAS Levoglucosan, Vanadium and Nickel tracer data	75
Appen	dix E – Data Providers PMF	77

2 Introduction

2.1 Background

Monitoring the composition of the atmosphere is a key objective of the European Union's flagship Space programme Copernicus, with the Copernicus Atmosphere Monitoring Service (CAMS) providing free and continuous data and information on atmospheric composition.

The CAMS Service EvOlution (CAMEO) project is aimed at enhancing the quality and efficiency of the CAMS service and help CAMS to better respond to policy needs such as air pollution and greenhouse gases monitoring, the fulfilment of sustainable development goals, and sustainable and clean energy. This includes preparation of CAMS for the uptake of forthcoming satellite data, including Sentinel-4, -5 and 3MI, advancing the aerosol and trace gas data assimilation methods and inversion capacity of the global and regional CAMS production systems. In addition CAMEO develops methods to provide uncertainty information about CAMS products, in particular for emissions, policy, solar radiation and deposition products in response to prominent requests from current CAMS users. With this work CAMEO will contribute to the medium- to long-term evolution of the CAMS production systems and products.

The transfer of developments from CAMEO into subsequent improvements of CAMS operational service elements is a main driver for the project and is the main pathway to impact for CAMEO. The CAMEO consortium, led by ECMWF, the entity entrusted to operate CAMS, includes several CAMS partners thus allowing CAMEO developments to be carried out directly within the CAMS production systems and facilitating the transition of CAMEO results to future upgrades of the CAMS service. This will maximise the impact and outcomes of CAMEO as it can make full use of the existing CAMS infrastructure for data sharing, data delivery and communication, thus supporting policymakers, business and citizens with enhanced atmospheric environmental information.

Workpackage 6 of CAMEO is dedicated to the investigation of uncertainties in the CAMS policy products and CAMS global forecasts and analyses.

2.2 Scope of this deliverable

2.2.1 Objectives of this deliverable

The first objective of this deliverable is to evaluate the consistency and comparability of modelled particulate matter (PM) source sector contributions from the different modelling systems applied within the CAMS policy service. Here we will disentangle differences due to the use of distinct chemical transport models and differences due to the use of various source attribution methods.

The second objective of this deliverable is to evaluate the modelled PM source sector contributions with observational based source attribution using Positive Matrix Factorisation (PMF) and specific source tracers such as levoglucosan (wood combustion).

2.2.2 Work performed in this deliverable

In this deliverable the work as planned in the Description of Action (DoA, WP6 T6.3.1 and 6.3.2) was performed.

2.2.3 Deviations and countermeasures

In this work package, a 5 years run (2015-2019) with LOTOS-EUROS was originally proposed to compare with the PMF data. This has been reduced to a two-year LOTOS-EUROS run for 2018-2019, while the one year EMEP run has been extended to two years. Analysis of the available PMF datasets performed in Task 6.3.1 and beyond, showed that extending the analysis with the years 2015-2017 would enable the comparison to 6 additional PMF datasets.

The majority of these sets include locations for which we also have data for 2018-2019 and/or for which comparisons have been performed and published in other projects. An extension to the years 2015-2017 was therefore not expected to provide new or additional insights.

The decision was made to limit the LOTOS-EUROS model run to 2018-2019 and replace this effort with extended comparisons for 2018-2019, including feedback sessions with several PMF data providers.

This deviation from the original proposal does not impact the project ambitions on evaluation of CAMS source attribution results and differences, nor will it impact any other tasks in the project since there are no tasks dependent on this deliverable.

2.2.4 CAMEO Project Partners:

ECMWF	EUROPEAN CENTRE FOR MEDIUM-RANGE WEATHER FORECASTS
Met Norway	METEOROLOGISK INSTITUTT
BSC	BARCELONA SUPERCOMPUTING CENTER-CENTRO NACIONAL DE SUPERCOMPUTACION
KNMI	KONINKLIJK NEDERLANDS METEOROLOGISCH INSTITUUT-KNMI
SMHI	SVERIGES METEOROLOGISKA OCH HYDROLOGISKA INSTITUT
BIRA-IASB	INSTITUT ROYAL D'AERONOMIE SPATIALEDE
	BELGIQUE
HYGEOS	HYGEOS SARL
FMI	ILMATIETEEN LAITOS
DLR	DEUTSCHES ZENTRUM FUR LUFT - UND RAUMFAHRT EV
ARMINES	ASSOCIATION POUR LA RECHERCHE ET LE DEVELOPPEMENT DES METHODES ET PROCESSUS INDUSTRIELS
CNRS	CENTRE NATIONAL DE LA RECHERCHE SCIENTIFIQUE CNRS
GRASP-SAS	GENERALIZED RETRIEVAL OF ATMOSPHERE AND SURFACE PROPERTIES EN ABREGE GRASP
CU	UNIVERZITA KARLOVA
CEA	COMMISSARIAT A L ENERGIE ATOMIQUE ET AUX ENERGIES ALTERNATIVES
MF	METEO-FRANCE
TNO	NEDERLANDSE ORGANISATIE VOOR TOEGEPAST NATUURWETENSCHAPPELIJK ONDERZOEK TNO
INERIS	INSTITUT NATIONAL DE L ENVIRONNEMENT INDUSTRIEL ET DES RISQUES - INERIS
IOS-PIB	INSTYTUT OCHRONY SRODOWISKA - PANSTWOWY INSTYTUT BADAWCZY
FZJ	FORSCHUNGSZENTRUM JULICH GMBH
AU	AARHUS UNIVERSITET
ENEA	AGENZIA NAZIONALE PER LE NUOVE TECNOLOGIE, L'ENERGIA E LO SVILUPPO ECONOMICO SOSTENIBILE

3 Evaluation of source sector attribution products

3.1 Introduction

CAMS currently offers a number of products to support decision and policy makers with regard to mitigation of air pollution at the European scale (https://policy.atmosphere.copernicus.eu/). These policy products provide information about the causes and main drivers of air pollution, the so-called source receptor relationships (SR), and their potential evolution in the future.

Quantitative uncertainty information is needed if the products are to be used by policy makers to prioritise measures in different activity sectors and to gauge the scale of actions that must be targeted when designing air quality policies with short or long term perspectives.

However, a direct comparison of modelled source contributions from chemistry transport models (CTMs) with observations is not possible in a similar way as performed for modelled pollutant concentrations. Yet there are several studies providing PM source sector attribution information based on PM composition observations or alternatively specific source sector tracers such as levoglucosan for wood burning can be used to evaluate the modelled variability of this source. Chapter 6 presents the evaluation of the CTM source contributions with observational based data and discusses the challenges of such comparisons and possible directions for implementation in the CAMS policy service.

In the current CAMS policy service, 3 regional chemistry transport models perform source attribution calculations with different methods (answering different questions) that yield different results for species formed through non-linear atmospheric chemistry. To support policy makers, it is crucial to understand the consistency and comparability of the three systems, and to understand where differences are coming from. Are they due to the use of a different CTM or a different source attribution method? To this end a set of experiments has been performed with the three CAMS policy support models using a set of different source attribution methods (see Figure 3-1). The results and conclusions from the comparison of these model experiments are described in Chapter 5.

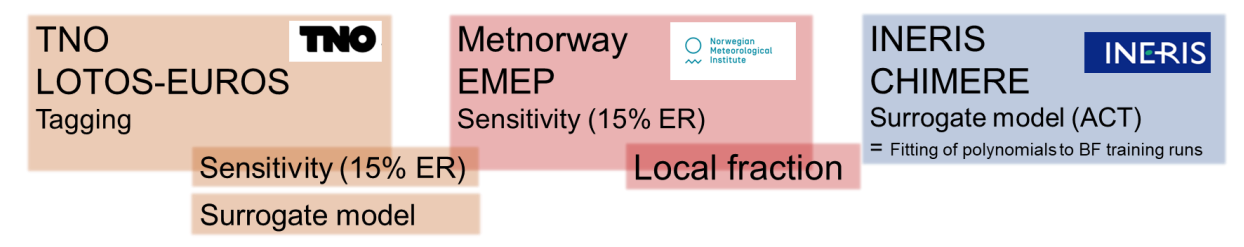


Figure 3-1 The chemistry transport models and their source attribution methods as applied in this study. ER= emission reduction.

3.2 Chemistry transport models and their source attribution methods

Below we describe the three chemistry transport models and their source attribution methods applied within this work.

3.2.1 EMEP model

Within the CAMS policy support service the EMEP model (Simpson et al., 2012) is providing Country-to-city SR and city-to-city SR using a brute force (BF) methodology (i.e. reducing emissions (ER) of NO_x , SO_x , NH_3 , VOC, PPM by 15% (at the same time) for countries and cities and scaling the effect up to 100%). This method gives the effect of emission reductions (potential impacts, e.g. (Clappier, A. et al., 2022) for instance: What happens to PM if you reduce NH_3 ? Note that in principle the result could be zero (at some specific places) when NH_3 is in excess of H_2SO_4 and no HNO_3 is available for formation of NH_4NO_3 . This method can also give negative contributions, as a result of non linear chemistry, for instance a reduction of NO_x

in a city might lead to increased ozone due to the titration of ozone by NO_x during the nights. Within the work presented here the brute force methodology is applied to emission source sectors, although source sectoral attribution by the EMEP model is not part of the current CAMS policy service.

In addition, a new method for calculating source receptor relationships has been developed at MET Norway - the local fraction (LF) methodology, also referred to as sensitivities (Wind et al., 2020; Wind & van Caspel, 2025). The LF method can be considered similar to a brute force methodology - but the emission reductions are very small (It calculates the derivative of the concentration with respect to an emission change (dC/dE) at the current concentration). Leveraging on the experience with the LF method within the work of the CAMEO project, it is planned for the near future to use the LF method within the CAMS policy user service, and therefore we include this method in our analysis.

3.2.2 LOTOS-EUROS model

The LOTOS-EUROS model is a chemistry transport model developed by TNO and used with the CAMS regional forecasts and analysis service and the CAMS policy service (for more information we refer to (Manders et al., 2016).

Within the CAMS policy support service LOTOS-EUROS is applied for the attribution of PM concentrations to countries using a tagging method (Kranenburg et al., 2013). This method has been developed to trace the origins of pollution, throughout all the processes in the model, thereby providing the contributions at any place and time under the actual conditions. By definition the method never yields negative contributions.

In the tagging method, the nitrogen and the sulphur atoms are tagged and followed in the formation of NH_4NO_3 and ammonium sulphate, $(NH_4)_2SO_4$. The formed secondary PM is attributed equally to the source of ammonium and the source of nitrate/sulphate respectively. When looking at speciated source attribution results ammonium would initially only have an agricultural contribution and nitrate would only be assigned to e.g. the traffic source. In this case we redistribute the sources of ammonium and nitrate, which are present in the form of NH_4NO_3 , by averaging the fraction of sources from both species. With this redistribution, the nitrate has some contribution from agriculture due to formation of NH_4NO_3 . Coarse nitrate formed from the reaction with sea salt is not handled this way and does not have any contribution from agriculture.

The model in this study is applied for source sector attribution calculations with this tagging method and additional experiments using the brute force (BF) method with 15% sectoral emission reductions (also referred to sensitivity calculations) and scaling the effect up to 100% have been performed to align with the EMEP brute force calculations.

Moreover, a surrogate model with the same set-up and settings as the CHIMERE ACT tool was trained and source sector apportionment results were obtained with both 15% and 100% emission reduction similar to the ACT tool and its sectors.

3.2.3 CHIMERE model

Within the CAMS policy service the CHIMERE model (Couvidat et al., 2025) is used for Sector-to-city contributions with the ACT tool which contains a parametrized concentration-emission response function updated on a hourly/daily basis. The parameterization is based on a set of brute force runs with different combinations of reductions in the different sectors (Colette et al., 2022). The sector contribution is normally based on 100% emission reductions (ER), but in this experiment also the 15% ER are considered for comparison to the other methods. The ACT surrogate model (SM) was demonstrated to be within 2% of sensitivity simulations with the full CTM CHIMERE even for secondary species (such as nitrate, sulfate, ammonium, secondary organic aerosols or ozone) for which strong chemical non-linearities occur.

3.3 Modelling setup

To be able to investigate differences due to the use of different source attribution methods we have to a large extent harmonised the set-up of all three models (see Table 3-1) in terms of inputs (emissions, meteorology, boundaries) and setup (resolution and domain). Note that while the emissions are harmonised the vertical emission profiles differ between the models.

The models with source attribution methods have been run for the year 2019. EMEP (with BF) and LOTOS-EUROS (with tagging) have additionally been run for the year 2018 for comparison with PMF data (see chapter 5).

The source attribution has been performed for the set of sources presented in Table 3-2. For LOTOS-EUROS and EMEP some GNFR sectors have been split into subsectors to allow a better matching with the identified PMF factors.

The modelled contributions have been derived for 79 out of the 80 cities included in the CAMS policy service (London is excluded here because of the city mask not being available in the Urban Audit 2021¹).

Table 3-1. Overview of models set up for this study.

	EMEP	LOTOS-EUROS	CHIMERE		
Forest fires	GFAS v1.2				
Soil NO _x	CAMS-GLOB-SOIL v2.3	(Novak & Pierce, 1993)	MEGAN V2.10 (Guenther et al., 2012)		
Model resolution	0.2x0.1				
Surface layer thickness	50m	20m	~16m		
Domain	lon: -24.9 to 44.9 by 0.2 degrees east lat : 30.05 to 71.95 by 0.1 degrees north				
Emission resolution	0.1x0.05				
Emission version	CAMS-REG v6.1 , and associated fuel splits for sectors				
Emission time factors	CAMS TEMPO v4.1(Guevara et al., 2021) , heating degree days for residential wood combustion				
City definitions	city masks and area weights corresponding to city-cores, as defined on the Urban Audit 2021².				
Initial conditions	Two weeks spinup starting from 3d interpolated IFS-COMPO (Flemming et al., 2015; Rémy et al., 2019): IFS45r1				
Boundary conditions	IFS45r1 data for all species made available for the CAMS regional validated reanalysis				
Species (focused on in this study)	PM _{2.5} , PM ₁₀ , PM components LE surrogate model results only provides PM _{2.5} , PM ₁₀				

¹ https://gisco-services.ec.europa.eu/distribution/v2/urau/urau-2021-metadata.pdf

D6.3

_

² https://gisco-services.ec.europa.eu/distribution/v2/urau/urau-2021-metadata.pdf

Table 3-2 Overview of source sectors based on GNFR subsectors identified within the different source attribution methods

GNFR (sub) sectors	LF/BF/Tagging	Surrogate models	
A_PublicPower	Power Plant Biomass	Industry	
	Power Plant Other		
B_Industry	Industry Biomass	•	
	Industry Combustion		
	Industry Other Combustion		
C_OtherStationary Comb	Residential Biomass	Residential	
(residential only)	Residential Other		
D_Fugitive; E_Solvent; I_Offroad; H_Aviation; J_Waste; M_other	Other Sectors	Other	
K_agriculture	Agriculture	Agriculture	
F1/2/3_RoadTransport _exhaust	Traffic Exhaust	Traffic	
F4_RoadTransport _nonexhaust	Trafflc Non-exhaust		
G_Shipping	Shipping	Shipping	
NA	Natural	NA	
NA	Fire		
NA	Boundary & Initial Condition (BIC)		

Note that boundary conditions for ozone and natural sources are not reduced in the BF simulations, while the boundary conditions of other species (such as SO₄, BC, OA) have been reduced. Contributions are therefore taken from a base run in LOTOS-EUROS and in EMEP the dust and seasalt from boundary conditions are labelled and outputted directly.

3.4 Positive matrix factorization

Positive matrix factorization is a source apportionment technique that uses measured species concentrations to identify an optimal number of factor profiles. It does so by statistically evaluating the optimal number of source profiles through multiple diagnostic tools. These include goodness-of-fit (Q-values) metrics, residual analysis and uncertainty estimations, while also taking into account chemical fingerprints of the identified profiles. It relies on the temporal correlation of chemical species, which allows it to identify PM profiles (Brown et al., 2015; Norris & Duval, 2014; Paatero & Tapper, 1994).

PMF output is sensitive to the selection of species used as input data, especially the inclusion or exclusion of so called tracer species and subsequently the uncertainty assigned to each species concentration. Moreover, while there are guidelines available, differences in settings used within the PMF software (e.g. constraints settings, Signal-Noise ratio, excluding species outliers) can influence profile identification.

Altogether it shows that interpretation of the identified profiles and estimated daily source concentrations of PMF depend on numerous study-specific factors. To make sure that

comparisons between CTM sources and PMF studies were conducted properly, close contact with data providers was maintained to interpret PMF profiles and the comparisons performed here

In Section 5, we will dive deeper into the interpretability of PMF profiles across studies, where we will discuss the quality of the PMF analysis and the impact on the matching. For now, an initial overview of the matches between PMF and CTMs are provided for each major source at the beginning of each subsection focusing on that source.

3.4.1 European PMF datasets

An overview of PMF studies on either $PM_{2.5}$ or PM_{10} chemical compositions in Europe was compiled through multiple sources: starting from PMF studies mentioned in existing reviews such as (Hopke et al., 2020), using search engines (e.g. Scopus) to search for European PMF studies published from 2015 onwards in Scopus, previous or currently running EU projects (e.g. RI-Urbans, Life-Remy) and personal contacts with scientific groups.

This overview served as a basis to select a focus year to run the models for the PMF-CTM comparisons. While the number of studies is quite extensive in the years of 2013-2017, a substantial proportion of these PMF datasets were already compared against CTM source contributions in France and Germany in previous work (Pekel et al., 2025; Timmermans et al., 2022; Vida et al., 2025; Weber et al., 2019). We therefore decided to focus on another time period. We have contacted the research groups which had performed PMF analysis for 2017 onwards, either published or not, and made a data request. Based on the data availability of these requests it was decided to focus the model comparisons on the year of 2019, for which all three CTMs provided data.

After receiving additional PMF data, the study period was extended to include 2018 to increase the number of stations that can be incorporated, and extend some of the datasets which were available for 2018 and 2019. In Table 3-3 an overview is provided of all PMF studies that were used for the comparison between PMF and CTM source contributions in this task, while appendix E provides an overview of the data providers for each station. Of note, the dataset from the Milan Pascal station was provided for the exercise with the understanding that the results would not yet be included in this report, as the data providers intend to first publish the accompanying results in a paper. Moreover, as elaborately discussed in source apportionment literature, the methods used for the different studies with regards to sampling, included components, PMF settings and subsequently solution criteria can have a large effect on the expected outcome (Amato et al., 2024; Borlaza et al., 2022; Brown et al., 2015; Mooibroek et al., 2022; Norris & Duval, 2014; Weber et al., 2019). We therefore consulted each PMF provider with regards to their study specific details and interpretation of the matching results and refer to the accompanying studies (Appendix E).

The study set up of the three Dutch stations requires some additional attention, worth elaborating upon. Some of the compositional data from Mooibroek et al. (2022) are derived from pooled daily samples. Filters were sampled every other day, and typically, four daily filters are combined for analysis, thereby resembling a resolution of approx. one week. Subsequently, the pooled data underwent multiple steps (e.g. detection limit determination, re-pooling data and imputation missing data) to come to a 24-hour average concentration for these species before used in the PMF analysis (see methods - Mooibroek et al. (2022)). Consequently, the dataset experiences some reduced temporal resolution compared to what would be achievable with analyses of individual daily samples. In our comparison we used the daily PMF daily estimates for these stations, but it is good to keep the underlying pooling of these samples in mind. For the other stations and studies samples were derived from daily averaged samples

Table 3-3 Overview of PMF datasets used in this study. N = number of observations

Country	Station	Start date	End date	Topology	N (2018)	N (2019)
Spain	Barcelona (BCN)	03-01-2018	31-03-2019	Urban background	78	22
	Montseny (MSY)	03-01-2018	31-03-2019	Rural background	78	23
	Payerne (PAY)	03-06-2018	29-05-2019	Rural	53	38
	Basel-Binningen (BSL)	03-06-2018	29-05-2019	Suburban	53	38
Switzerland	Zurich-Kaserne (ZRCH)	03-06-2018	29-05-2019	Urban	53	38
	Bern-Bollwerk (BERN)	03-06-2018	29-05-2019	Urban - traffic	53	38
	Magadino-Cadenazzo (MGD)	03-06-2018	29-05-2019	Rural	53	38
	Freiburg (FRB)	01-01-2018	31-12-2018	traffic	353	0
Germany	Garttringen (GRT)	01-01-2018	31-12-2019	rural	353	365
	Stuttgart Bad Cannstatt (STG)	01-01-2018	31-12-2019	urban	353	365
Germany	Melpitz - Research station (MLP_RS)	01-11-2018	31-10-2019	rural	59	290
	Melpitz – village (MLP_VIL)	01-11-2018	31-10-2019	rural	59	290
Italy	Milan Pascal (MIL)	01-01-2017	31-12-2020	urban	237	277
Greece	Athens (ATH)	01-01-2018	27-12-2019	Urban background	96	107
	ljmuiden (IJM)	01-01-2017	31-12-2019	Industrial / residential	365	365
Netherlands	Wijk aan Zee (WAZ)	01-01-2017	31-12-2019	Industrial / urban	365	365
	Beverwijk (BVW)	01-01-2017	31-12-2019	Industrial / urban	365	365

3.5 Tracer data

While PMF studies can provide valuable insights, they are relatively scarcely spread out throughout Europe, providing only limited possibility to evaluate CTM sources against a PMF derived source counterpart. This is especially true for PMF profiles that are not often identified, such as shipping. Alternatively data on the concentrations of specific source sector tracers can be used. Comparing CTM source contributions against such source specific sector tracers provides insight into the dynamics of the CTM and the species.

We therefore selected three tracers for which observational data throughout Europe was gathered, i.e. levoglucosan, which acts as a tracer for biomass combustion processes, and nickel and vanadium related to heavy fuel oil, which is mainly attributed to shipping emissions.

Observational data was obtained through the EMEP database³ where all datasets containing levoglucosan, nickel or vanadium in PM₁₀ samples within the modeling domain for the year of 2019 were selected. In Appendix D an overview of all the stations, including topology (if specified) can be found. The majority of stations providing observations on either one of the three tracers were sampling either a daily or weekly average concentration and contained a

³ https://ebas-data.nilu.no/

high number of below detection limit (DL) values, which are not excluded from the comparisons.

Only one station was identified for levoglucosan in 2019, but for nickel and vanadium multiple stations provided observational data worth comparing to the CTM output.

3.6 Comparability of models and methods

3.6.1 Source attribution methods

Designed for different purposes, tagging and BF based methods will not lead to the same source attribution results in case of non-linear relationship between emissions and concentrations (Thunis et al., 2020; Thürkow et al., 2023). Clappier et al., (2017) with theoretical examples for PM show how in case of non-linearities and either limited or nonlimited chemical regimes the different methods can lead to significantly different results. Belis et al., (2021) followed up on this study by investigating the impact of non-linearities for the source attribution of PM in a real case model application over the Po Valley in Italy. They identified that in many situations the tagging and brute force methods provide comparable results when analysing annual source contributions. Largest differences between methods were associated with contributions from the agricultural sector and the interaction of this source with road transport and to a lesser extent with industry to form secondary PM. The differences become more prominent when focusing on shorter timescales (e.g. daily averages or episodes of a few days). Additionally they found that the non-linearity was most relevant for large emission reductions connected to changes in chemical regimes. In the case of 100% emission reductions the differences with the tagging method could reach a factor of 2 for the agricultural source contributions. For smaller 20% and 50% emission reductions these differences were considerably smaller, but showed scattered results indicating spatial heterogeneity.

Since the surrogate modelling is representing brute force emission reduction impacts, similar differences can be expected between the surrogate modelling taking 15% ER and brute force runs with 15% ER. Because of the non-linearity the surrogate model results with 100% ER are however not comparable to the BF with 15% ER used in this study, but should be similar to BF results with 100% ER.

The local fraction method is also providing a potential impact of emission reduction albeit as a derivative of actual emissions. Therefore this method should be comparable to a brute force method with very small emission change.

In principle, the methods of tagging, BF, surrogate modelling, and LF should yield equivalent results for primary species that are directly emitted into the atmosphere, do not undergo chemical transformations and therefore vary linearly with respect to emission strengths. However, in practice, minor discrepancies may emerge. For instance, the LF and BF methods exhibit slight variations due to the concentration dependent advection scheme (Wind et al. 2024).

Due to the fewer number of sectors in the SM, sectors from other methods were combined for comparison with the SM results, based on Table 3-2. For tagging, contributions from subsectors are inherently additive and can be combined to get the contributions from the broader sectors, as the ones evaluated by the surrogate models. Contributions from the BF and LF methods may not be additive, and adding them up will not produce identical results as a BF method on the broad sectors. Nevertheless, the comparison between the SM and other methods can provide an insightful perspective for the users of the policy product to evaluate and understand the differences derived from different methods.

3.6.2 CTM models

Differences in source attribution results can also arise from differences in the model formulations themselves (for instance in chemistry, natural emissions, deposition and/or advection schemes, etc) and in the setup of models (for instance the use of different emissions altitudes, surface layer thickness (which is 20m in LE versus 50m in EMEP), etc).

Furthermore LE has only included secondary inorganic aerosols (SIA) in this experiment. Both CHIMERE and EMEP have also included secondary organic aerosols (SOA) in addition to SIA.

3.6.3 CTM and PMF

Comparing PMF-derived source contributions to those estimated by chemical transport models (CTMs) can potentially be a strong approach for both paradigms to learn from one another. While CTMs are based on emissions inventories, atmospheric chemistry, and transport processes, PMF provides (daily) temporal source contributions for a number of source factors/profiles identified by the chemical composition of a source. Comparing PMF outputs against CTM estimates helps check the consistency of both model (CTM and PMF) assumptions and improve source characterization.

While PMF can characterize primary sources based on ambient compositional PM data, it is important to take into account some challenges of the technique. The ability of PMF to identify certain source profiles is dependent on the chemical species included in the analysis and the uncertainty assigned to each species (Amato et al., 2024). Moreover, due to the PM mixture dynamics which PMF uses to identify profiles, it often identifies profiles which primarily are made up out of secondary (in)organic aerosols (e.g. Nitrate-rich and Sulfate-rich), making it challenging to identify the sources of the gaseous precursors of these PMF factors and match against the CTM sectors (Pekel et al., 2025; Timmermans et al., 2020; Vida et al., 2025). Similarly, whereas CTMs are able to differentiate between compositional similar sources (e.g. incomplete fossil fuel combustion processes) the PMF analysis would aggregate such sources into single factors due to the chemical similarities. Only a timing difference in the source concentrations is often not sufficient to disentangle sectors with similar profiles. For this, specific source unique tracers are required.

Therefore, it is essential to first establish an understanding of the species used as input data for the PMF, uncertainties and profiles across the PMF datasets before their comparison with CTM outputs can provide useful insights.

The matching of the CTM sectors with the PMF factors are provided per source in the respective results subsections. Note that the results from tagging which provides actual contributions for the specified time and place are the only products which are similar in definition to the contributions derived by the receptor modelling PMF data. The other CTM source attribution products are actually potential impacts of emissions translated to 100% contributions, in case of non-linear chemistry these can be different from actual contributions (see also CAMEO deliverable D6.1) and part of the differences between the PMF and CTM results can be attributed to this fact.

3.7 Statistical indicators for comparisons

Normalized Mean Bias

$$NMB = \frac{1}{N} \sum_{i}^{N} \frac{(Mod_i - Obs_i)}{Obs_i}$$

Root Mean Square Error

$$RMSE = \sqrt{\frac{1}{N} \sum_{i}^{N} (Mod_{i} - Obs_{i})^{2}}$$

Normalized Root Mean Square Error

$$NRMSE = \frac{\sqrt{\frac{1}{N}\sum_{i}^{N}(Mod_{i} - Obs_{i})^{2}}}{\overline{Obs}}$$

Temporal correlation with observations

$$r^{2} = \left(\frac{\sum (C_{model} - \overline{C_{model}})(C_{observation} - \overline{C_{observation}})}{\sqrt{\sum (C_{model} - \overline{C_{model}})^{2} \sum (C_{observation} - \overline{C_{observation}})^{2}}}\right)^{2}$$

Spearman's ranked correlation coefficient denoted as r_s is used to intercompare ranked relative contribution results

$$r_{\rm S} = \frac{cov[R(X_{model+method}),R(Y_{model+method})]}{\sigma_{R(X_{model+method})}\sigma_{R(Y_{model+method})}}$$

Where R is rank, σ is standard deviation, cov is the covariance.

Coefficient of determination

$$R^2 = 1 - \frac{SS_{res}}{SS_{tot}}$$

 SS_{tot} is the total sum of squares and SS_{res} sum of squares of residuals

4 Modelled concentrations evaluation

The modelled surface concentrations from EMEP, LOTOS-EUROS and CHIMERE have been evaluated against observations for 2019. The full evaluation with EBAS and EEA stations can be found here: https://aeroval-test.met.no/jang/pages/overall/?project=CAMEO

Figure 4-1 shows the intercomparisons of the CTM models with monthly EBAS surface concentrations for PM $_{10}$, PM $_{2.5}$, its main chemical components and precursors. All models show more or less similar performance for total PM $_{2.5}$ with small negative biases of 3.5 to 6.5%. For PM $_{10}$, CHIMERE and EMEP show larger underestimations of 34% and 25% respectively, while LOTOS-EUROS is close to the observations on the annual average.

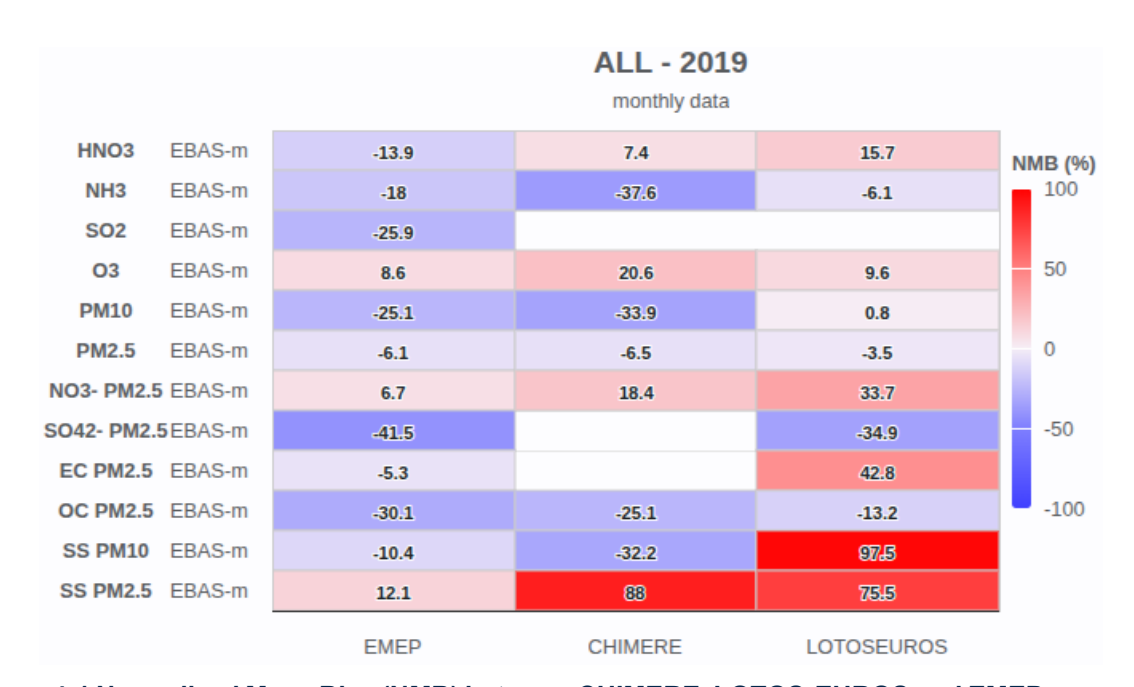


Figure 4-1 Normalized Mean Bias (NMB) between CHIMERE, LOTOS-EUROS and EMEP compared to monthly averaged EBAS observations for PM_{10} , $PM_{2.5}$ and its main chemical components.

While the yearly averaged PM_{2.5} biases are similar between the models the underlying PM composition and temporal variation show larger differences. LOTOS-EUROS overall shows higher values for the PM components leading to larger overestimations of nitrate (34%), EC (43%) and sea salt in PM_{2.5} (76%), and lower underestimations than the other models for sulfate and organic carbon.

Regarding the sea salt, LOTOS-EUROS has been shown to overestimate the concentrations in CAMS exercises before. Research is ongoing to understand the causes and improve the performance. It is believed that the deposition over land may be underestimated. Furthermore unlike the other two models, LE also has a contribution of sodium from inland industrial sources (not shown) which ends up in the sea salt component but not in the natural contributions.

For primary elemental carbon (EC), which is solely driven by dispersion and deposition, the difference between models may, amongst others, be explained by the difference in surface layer thickness between the models. The higher primary PM in LOTOS-EUROS may be influenced by the treatment of the condensables, i.e. in the applied set-up with disabled SOA formation all EC and OC emissions are considered as primary.

The reason for the similar comparison to $PM_{2.5}$, despite all chemical components being higher in LOTOS-EUROS, is partially related to the inclusion of PM water in the EMEP model results, whilst $PM_{2.5}$ in LOTOS-EUROS and CHIMERE is providing dry aerosol. Including water in the

modeling of PM $_{10}$ and PM $_{2.5}$ in CHIMERE would lead to a better partitioning between PM $_{10}$ and PM $_{2.5}$, likely improving the scores, especially for the sea salt component. The reference measurement method for EMEP observations is gravimetric where mass is collected on filters that are conditioned to relative humidity 50% and the EMEP model calculates associated PM water at 50% relative humidity. For the EEA measurements, it is less clear to which extent the PM $_{2.5}$ mass includes water.

To ensure better comparability between the source contributions from the different models, in chapters 5 and 6 the results from the EMEP model encompass only dry aerosol.

For the secondary aerosol precursors, we see an overestimation of the annual mean surface concentration of ozone (O_3) for all models, also nitric acid (HNO_3) for CHIMERE and LOTOS-EUROS. Ammonia (NH_3) is underestimated with the lowest underestimation seen for LOTOS-EUROS. The underestimation of sulphate and overestimation of nitrate indicate that the models have a bias to produce more ammonium nitrate (NH_4NO_3) instead of (NH_4)₂SO₄ than observed.

5 Results - Consistency and comparability of source sector contributions between models and source attribution methods

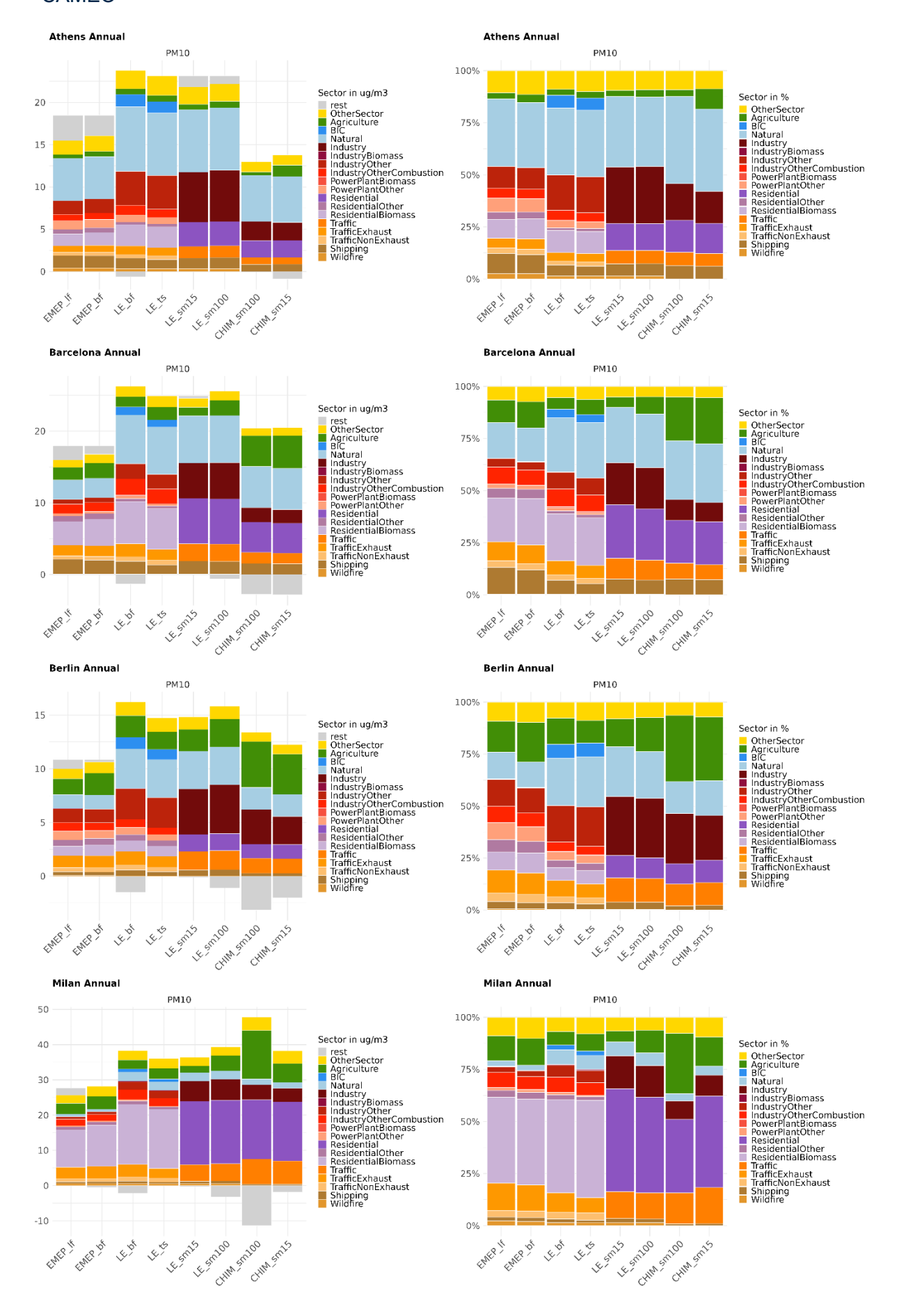
Note that in the following sections we will for simplicity refer to the source attribution from all methods as contributions, even though this nomenclature officially only applies to the tagging results. The results from all models in chapters 5 and 6 refer to dry mass PM.

5.1 Annual source apportionment

The annual mean PM₁₀ sectoral source apportionment for eight cities is shown in Figure 5-1. The "rest" category in grey is the net difference between the modelled surface concentration and the sum of the apportionment from all sources, often referred to as the closure term. This term related to the non-linearity in chemistry can be both positive as well as negative (in the latter case the source contributions add up to more than the actual concentrations). The tagging method, by definition, determines the source contributions and thus does not have a residual term. For the EMEP model, only dust and sea salt from BIC's was included. However, previous experience with the EMEP model has shown that on an annual basis contributions from PM from BICs are very small. The results for PM_{2.5} are presented in Figure A-1. It should be noted that due to the tagging set-up for PM_{2.5} the BIC category for LOTOS-EUROS tagging includes the natural contributions coming in through the model boundaries while for the BF these are included in the natural contribution, thereby leading to considerable differences for the BIC and natural contributions from these two model/methods. Similarly the rest term for the LOTOS-EUROS surrogate model includes also the BIC contributions.

When focusing on the four methods applied within the LOTOS-EUROS model we see that in general for annual average PM the different methods provide similar results.

The source apportionment results show larger discrepancies between the models. Chapter 4 already showed that LOTOS-EUROS simulated the highest sea salt concentrations, causing differences in the "Natural" category. With respect to the source apportionment of anthropogenic sources, the CHIMERE model attributes a larger fraction of anthropogenic PM_{2.5} to agricultural emissions than the other models, making this the main source in e.g. Berlin and Rotterdam. In Milan and Rotterdam the impact of non-linear processes on the results becomes clear when comparing the CHIMERE or LOTOS-EUROS surrogate model results for 15% and 100% emission reduction: especially for agriculture, the difference in calculated source contribution for different emission reductions is large. In contrast, the industrial contributions in the CHIMERE results are smaller than in the other two models. In nearly all cities, both the EMEP and LE models attribute the largest share to the residential sectors, with LOTOS-EUROS in general showing higher contributions than EMEP for cities with large biomass combustion shares.



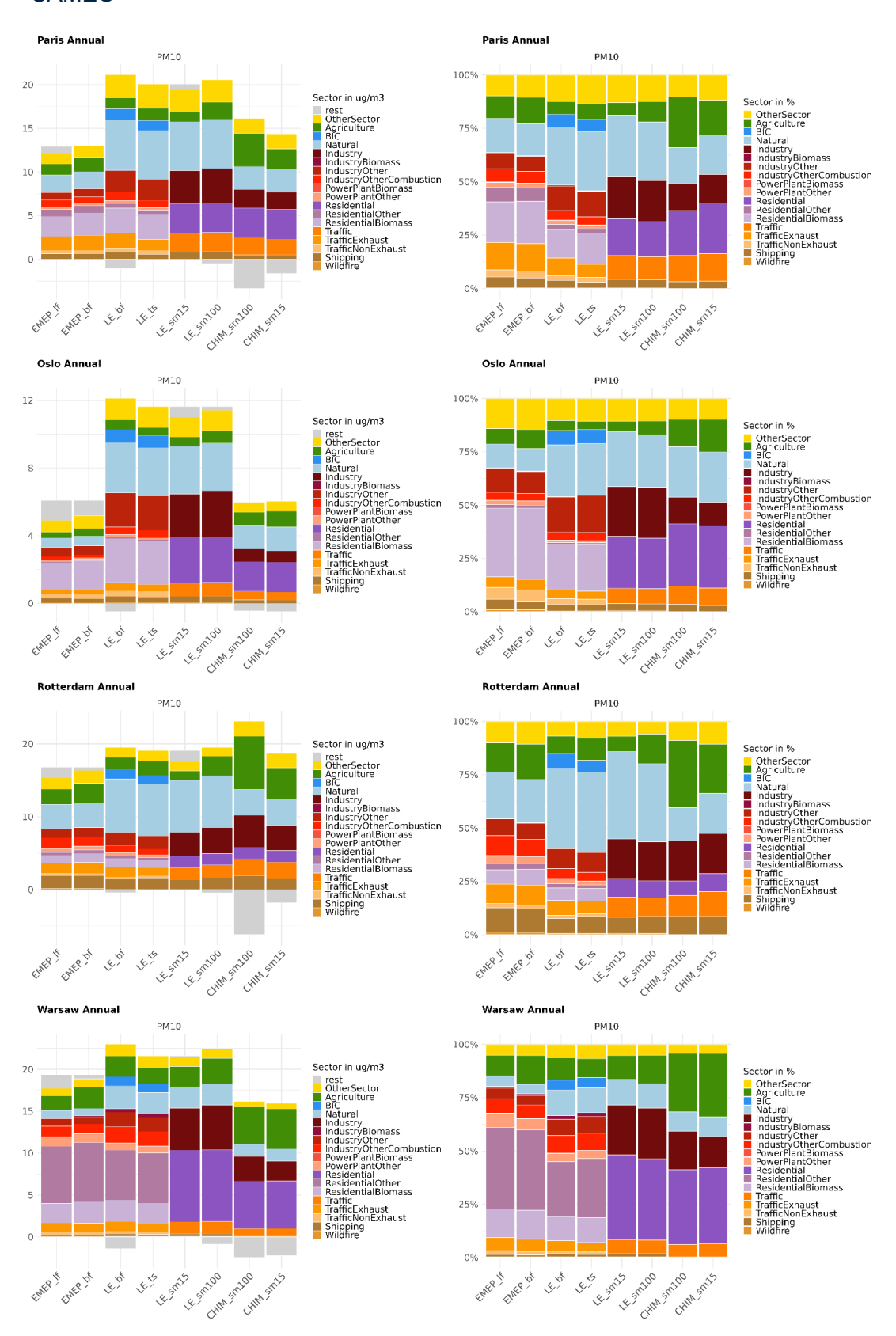


Figure 5-1 Absolute (μg/m³, left plots) and relative source sector contributions (%, right plots) to dry mass PM₁₀ in Athens, Barcelona, Berlin, Milan, Paris, Oslo, Rotterdam and Warsaw from CHIMERE (CHIM), EMEP and LOTOS-EUROS (LE) model using either Brute Force method (_bf), Local Fractions (_lf), Tagging (_ts) or Surrogate Modelling with either 15% (_sm15) or 100% (_sm100) emission reductions scenarios. Sector categories refer to Table 3-2.

When investigating the model differences for the residential sector we found that these are mainly coming from the primary components as can be seen in Figure 5-2 for Milan. While the different source apportionment methods within one model provide the same results due to the linear response of primary PM to emissions, the results between the three models differ even if the same source apportionment method is applied. This difference can be largely attributed to the surface layer thickness, which is 50 m for EMEP, 20 m for LOTOS-EUROS, and ~16 m for CHIMERE. A test experiment for January 2019 with double surface layer depth in LE shows reductions up to 30-50% in modelled PM and primary PM (Figures B-1 and B-2 in appendix B). The lower concentrations are the result of direct dilution of the emissions into a larger volume, especially in a shallow stable boundary layer in winter. This effect is most prominent in places with highly variable orography such as the Po Valley and Oslo. With smooth orography, vertical transport is more efficient in mixing and diluting the emission.

This reduced dilution is affecting all sources emitting at the surface therefore the relative contributions (Figure 5-1) show much better agreement between the different models.

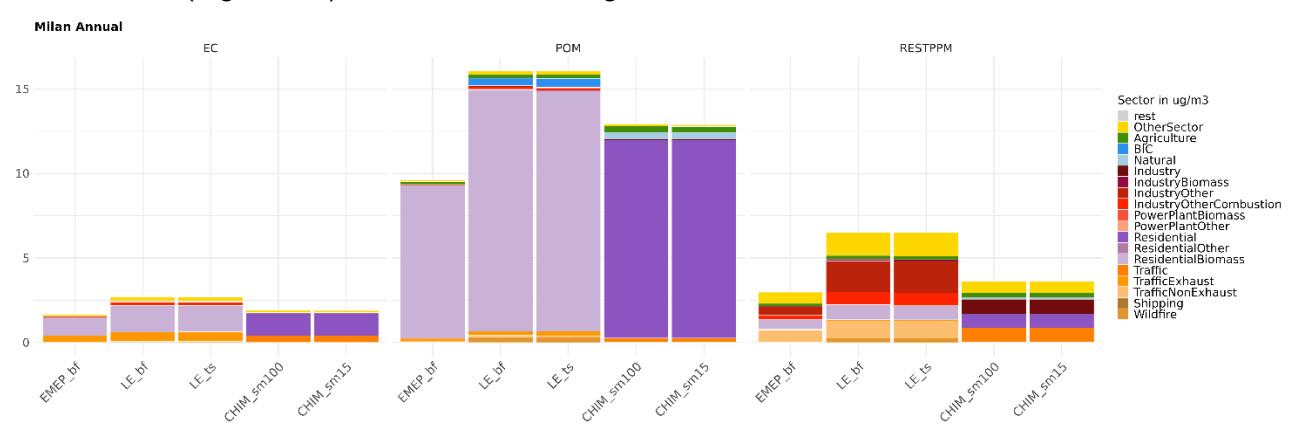


Figure 5-2 Source sector contributions (in $\mu g/m^3$) to primary PM components: Elemental Carbon (EC), Primary Organic Matter (POM) and Rest Primary PM (RESTPPM) in Milan. Note that LE_sm and EMEP_If did not deliverspeciated primary PM results, but these are almost identical to the primary results from other LE and EMEP methods respectively.

In some cities a difference between the models is also seen in the industrial contributions which may be attributed to the use of different emission altitudes. LOTOS-EUROS inserted the emissions from industrial area sources (not to be confused with the point sources) into the surface layer leading to higher concentrations than in the EMEP and CHIMERE model which applies an emission profile for area industrial sources which is similar to the one used for industrial point sources. Difference between the models can also be due to the use of different numerical advection and deposition schemes in the three CTMs.

For the secondary PM species non-linear chemistry plays a role, leading to differences between the different source attribution methods applied within the same model (Figure 5-3). For Berlin and Rotterdam, higher contributions from the CHIMERE model are again apparent, related to the large interaction between sectors, represented by the negative residual term, especially in the case of 100% emission reductions in the surrogate model. Such high residual terms are likely due to strong non-linearities when reaching large reductions. In Rotterdam all source contributions in CHIMERE are higher than for the other models. A redistribution of the residual interaction term among these sources could reduce these contributions. The relative contributions are very similar though, except for the CHIMERE surrogate model results for 100% reductions, which are higher for agriculture.

CAMEO NH4 NO3 504 100% Sector in % OtherSector Agniculture Buthural Industry IndustryOtherCombustion IndustryOtherCombustion IndustryOtherCombustion PowerPaintOther Residential ResidentialBiomass TrafficKantast TrafficKonExhaust Shipping Wildfire 75% 50% Berlin Annual NH4 NO3 504 Sector in ug/m3 rest OtherSector Agriculture BIC Outschildren Age Hadrual IndustryBiomass IndustryOtherCombustion IndustryOtherCombustion IndustryOtherCombustion PowerPlantOther Residential ResidentialOther ResidentialBiomass TrafficeNaust TrafficNaust TrafficNaust TrafficNaust Shipping Wildfire 504 Sector in % OtherSector Agriculture BIC Natural IndustryBlomass IndustryOtherCombustion PowerPlantBlomass PowerPlantOther ResidentialOther ResidentialOther ResidentialSomass TraffickAhaust TraffickOnExhaust Shipping Wildfire 25% Rotterdam Annual NH4 NO3 504 Sector in ug/m3

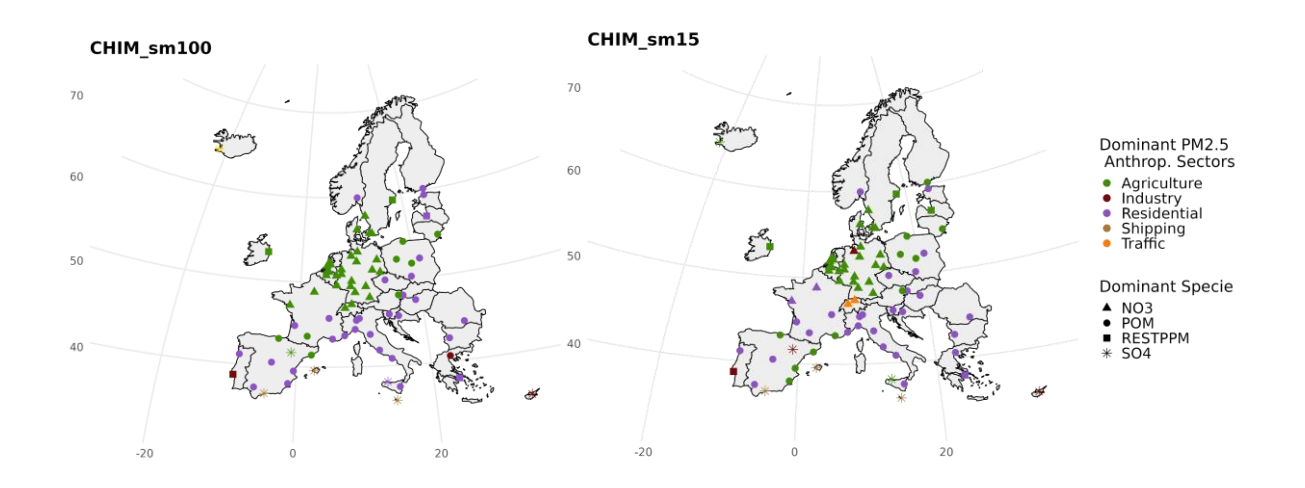
Figure 5-3 Absolute (in $\mu g/m^3$) and relative source sector contributions (in %) to secondary PM components: in Berlin (top two panels) and Rotterdam (bottom two panels).

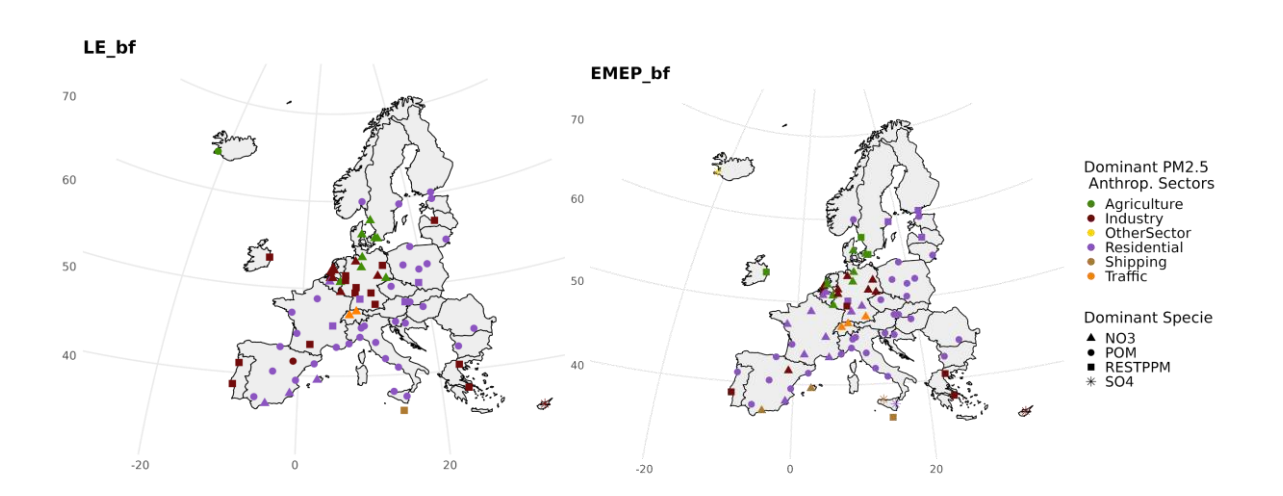
ResidentialBiomas Traffic TrafficExhaust TrafficNonExhaust

This may be explained by the formation of ammonium nitrate (NH_4NO_3) and ammonium sulfate (NH_4SO_4) aerosols from the reaction of ammonia (NH_3) (mostly from agricultural emissions) with HNO_3 that is produced from NO_x sources such as traffic and industry and H_2SO_4 produced from SO_x sources such as shipping and industry. While a 100% ammonia emission reduction in the agricultural sector will remove its entire contribution to ammonium nitrate and sulfate, a smaller emission reduction will be impacted by the availability of HNO_3 , and H_2SO_4 and the balance between the ammonium sulfate and nitrate production processes (see also CAMEO D6.1 where this is described in more detail).

There is also a difference in the sulphate contributions from LF and BF within the EMEP model. The Local Fraction method does not attribute SO_4 concentrations in the cities to agriculture emissions unlike BF. As there are almost no SO_2 emissions from agriculture, this contribution in the BF stems from the indirect effect on SO_4 when you reduce ammonia emissions, which is not yet implemented in the LF method. In the EMEP model, SO_4 is assumed to be formed from SO_2 via reactions with OH, O_3 and H_2O_2 . It then enters into equilibrium reactions with NH₃, HNO₃ etc, but that does not affect the amount of SO_4 . However, there are some indirect effects of reducing NH₃ emissions. When NH₃ is reduced, dry deposition of SO_2 is increased (and thus SO_4 decreased), as there is a parameterization for co-deposition in the EMEP model where the SO_2 dry deposition velocity depends on the NH₃/ SO_2 ratio.

The most dominant sectors and pollutants from the different models/methods are shown in Figure 5-4. All models and methods agree on the Residential emission of primary pollutants as the major anthropogenic source around the Mediterranean except for some cities influenced by volcanic emissions involved in the formation of sulfate aerosols. Note that LOTOS-EUROS does not include volcanic emissions. The Residential combustion is also identified as the major source in Eastern Europe by LOTOS-EUROS and EMEP while the CHIMERE model with its source attribution based on a surrogate model indicates an overall large impact of agriculture in a wide area in Central Europe and around the Baltic sea. Since agriculture is mostly contributing to ammonium nitrate, nitrate which is heavier than ammonium is the dominant species in these regions for the CHIMERE surrogate model (Note that for some cities CHIMERE identifies agriculture as the dominant source and POM as the dominant species, this is due to the large negative interaction residual term discussed before and/or may also be due to the sum of POM from multiple sources exceeding the NO₃ from agriculture). On the other hand both EMEP and LOTOS-EUROS suggest a mixture of industrial and agricultural sources around the Benelux and Germany. The dominant sources from the brute force approaches in EMEP and LOTOS-EUROS are very alike but LOTOS-EUROS identifies more cities with primary pollutants as dominant species.





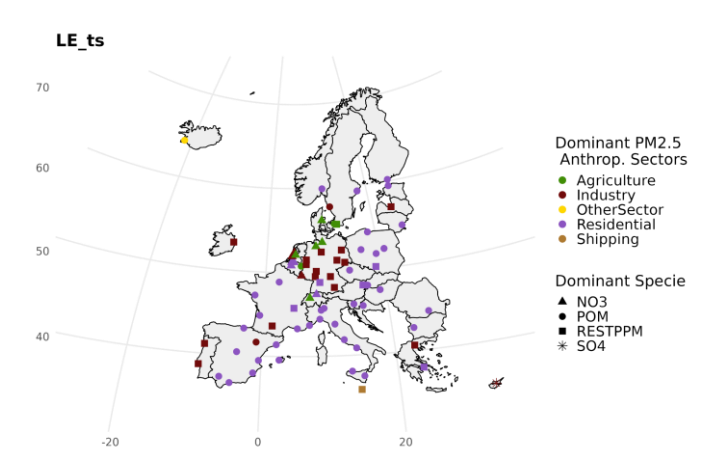


Figure 5-4 Dominant anthropogenic sectors (colors) to annual $PM_{2.5}$ surface concentration and dominant PM pollutant (shapes) to total PM surface concentration in 79 cities.

To investigate a bit further the model and method induced differences we have compared the annual average contributions from different models and different models in scatter plots.

The methods show almost identical results for primary species (not shown) as expected from a linear response to emission reductions. Small differences between TS and BF in LOTOS-EUROS still occur primarily due to numerical errors from data compression. For BF versus LF in EMEP small differences come from the advection which is flux dependent and therefore concentration changes due to the emission reduction in BF runs can result in small differences compared to the local fraction and tagging results.

Figure 5-5 shows the comparison of top three ranked relative anthropogenic contributions (natural contributions and contributions coming through the domain boundaries are excluded in this comparison due to differences in set-up between the models/methods) to the annual $PM_{2.5}$ due to the use of different source attribution methods within the same model.

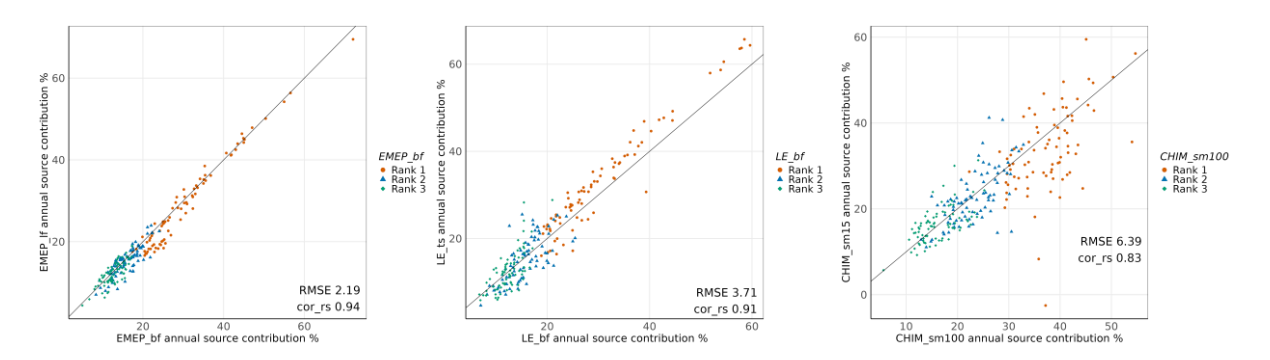


Figure 5-5 Differences in top 3 anthropogenic source contributions to PM_{2.5} due to different methods in EMEP (left panel, local fraction versus brute force), LOTOS-EUROS (middle panel, tagging versus brute force) and CHIMERE (right panel, surrogate model with 15% reduction versus 100% reduction). Ranking of sectors is based on their contribution for the method displayed on the x-axis and can be a different sector for each city represented as datapoint. First ranked contributing sector in red circles, second ranked in blue triangles, and third ranked in green diamonds. The ranking excludes natural contributions and contributions from outside the model domain due to different settings for these in the models.

Unlike primary species, aggregated PM_{2.5} contributions exhibit some variances between the source attribution methods. Within EMEP the LF and BF methods show minimal differences and the same holds for the BF and TS methods within the LE model. The difference between the 15% and 100% emission reduction results from the surrogate model in CHIMERE is larger, which is expected from the non-linear responses of the secondary PM to emission changes, while other BF sensitivity approaches in EMEP and LE are based on 15% reductions.

Figure 5-6 shows the differences due to different source attribution methods within the LOTOS-EUROS model. As indicated above the BF and tagging methods provide similar results albeit it that the first ranked anthropogenic source has slightly higher contributions in the tagging versus the BF results. The LOTOS-EUROS surrogate model shows little difference with the LOTOS-EUROS BF when 15% emission reductions are applied. The RMSE and correlation between the 15% and 100% emission reduction results from the surrogate model in LOTOS are similar to the ones seen for CHIMERE.

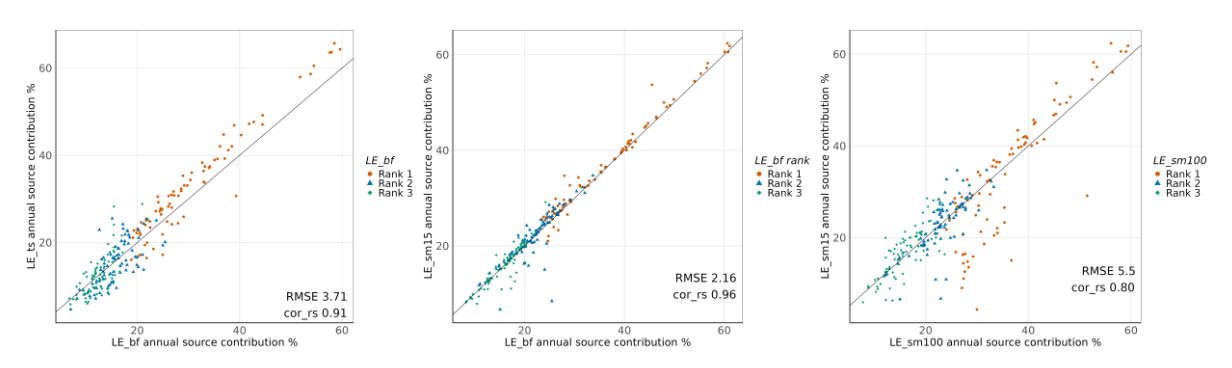


Figure 5-6 Differences in top 3 anthropogenic source contributions due to different methods in LOTOS-EUROS model. Tagging versus brute force (left panel), surrogate model with 15% reduction versus brute force (middle panel) and surrogate model 15% reduction versus 100% reduction. Ranking of sectors is based on their contribution for the method displayed on the x-axis and can be a different sector for each city represented as datapoint. First ranked contributing sector in red circles, second ranked in blue triangles, and third ranked in green diamonds. The ranking excludes natural contributions and contributions from outside the model domain.

Figure 5-7 shows the differences in source attribution results for annual mean PM_{2.5} due to the different models using the same apportionment method. It is clear that the comparison between EMEP and LOTOS-EUROS brute force (RMSE = 6.02; Rs = 0.82) and between CHIMERE and LOTOS-EUROS surrogate modelling (RMSE= 9.15 and 8.29, Rs = 0.59 and 0.75 for 15% and 100% reductions respectively) is showing larger differences than between the methods itself (Fig. 5-6: Tagging versus BF RMSE= 3.71 Rs =0.91; SM_15 versus BF RMSE= 2.16; Rs=0.96) except for the LOTOS-EUROS surrogate model 15% versus 100% reduction (RMSE=5.50; Rs =0.80). The differences between EMEP and LOTOS-EUROS seem to be smaller than between CHIMERE and LOTOS-EUROS. A further investigation of the implementation of the surrogate model in LOTOS-EUROS in comparison to the original implementation in CHIMERE is recommended to rule out implementation artifacts.

As indicated before, the difference between models is to a large extent attributed to the primary species from residential combustion, but also to industrial sources and secondary species from agriculture.

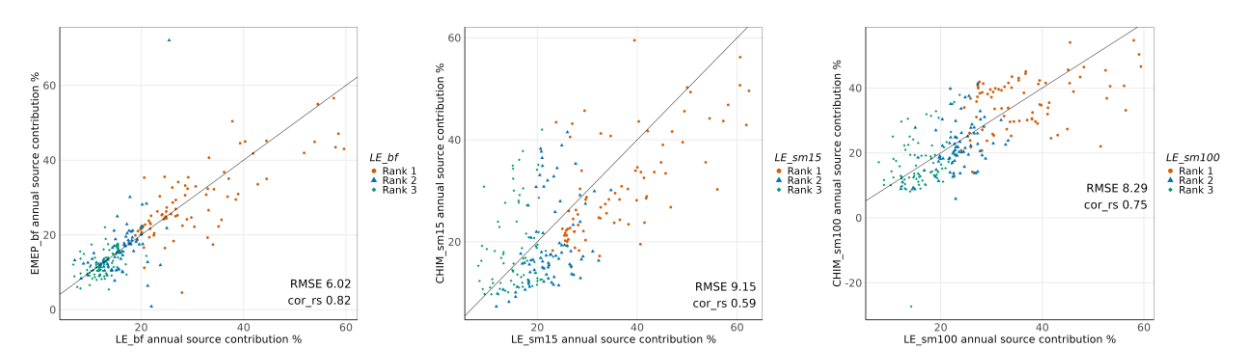


Figure 5-7 Differences in top 3 source contributions to PM_{2.5} due to different models. EMEP versus LOTOS-EUROS brute force (left panel), CHIMERE versus LOTOS-EUROS surrogate model with 15% reduction (middle panel) and CHIMERE versus LOTOS-EUROS surrogate model with 100% reduction (right panel). Ranking of sectors is based on their contribution for the method displayed on the x-axis and can be a different sector for each city represented as datapoint. First ranked contributing sector in red circles, second ranked in blue triangles, and third ranked in green diamonds. The ranking excludes natural contributions and contributions from outside the model domain due to different settings for these in the models.

For the non-linear species (e.g. NH4+, NO3-) the difference between the EMEP and LOTOS-EUROS model (Figure 5-8 right panel) is of the same magnitude as the difference between brute force and tagging within the LOTOS-EUROS model (Figure 5-8 left panel).

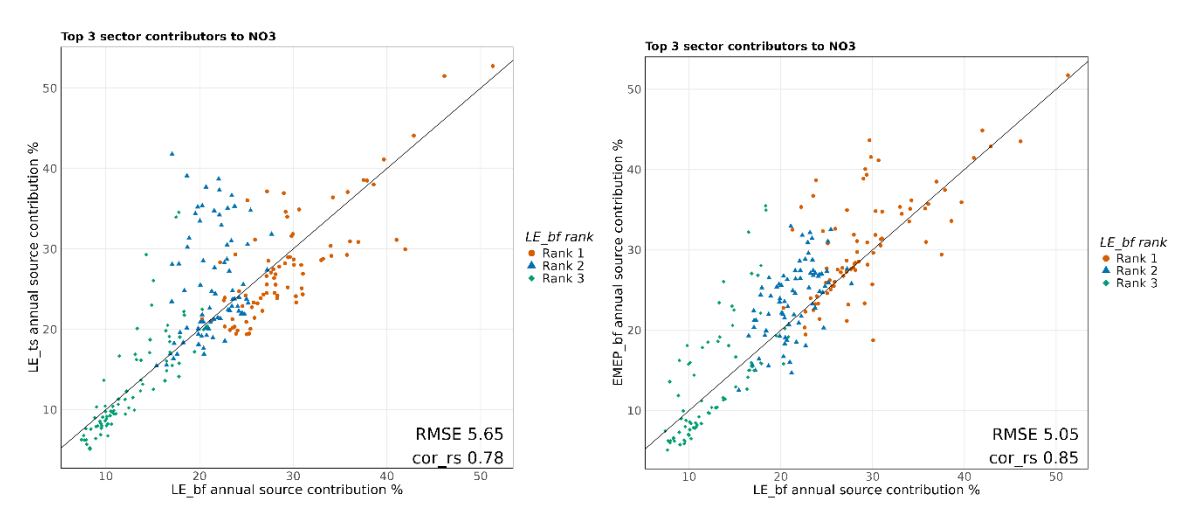


Figure 5-8 Differences in top 3 source contributions to nitrate due to different models, EMEP versus LOTOS-EUROS brute force (right panel) or different methods LOTOS-EUROS tagging vs BF (left panel). Ranking of sectors is based on their contribution for the method displayed on the x-axis and can be a different sector for each city represented as datapoint. First ranked contributing sector in red circles, second ranked in blue triangles, and third ranked in green diamonds. The ranking excludes natural contributions and contributions from outside the model domain due to different settings for these in the models.

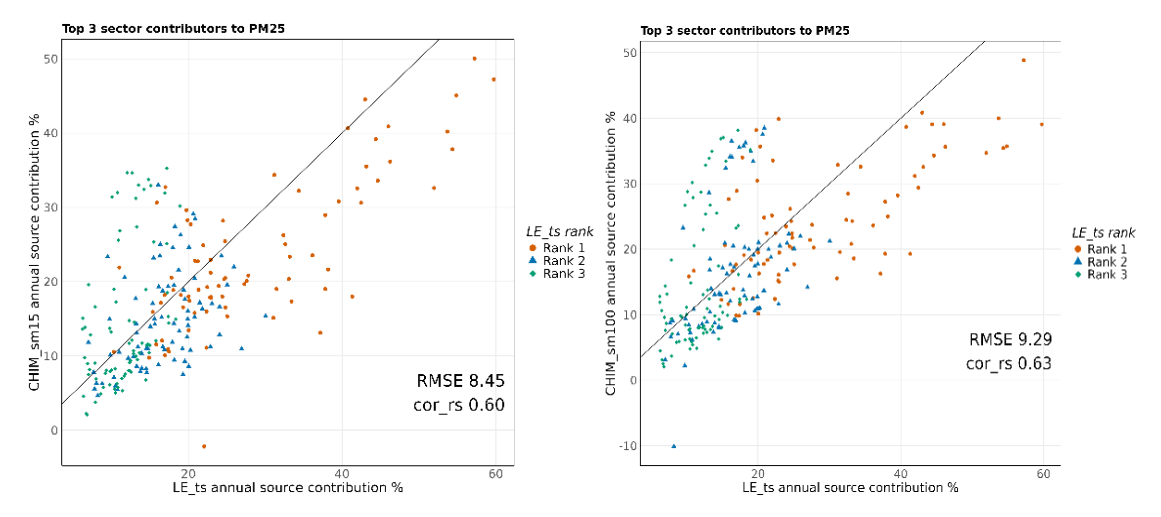


Figure 5-9 Differences in top 3 source contributions from the two systems that will be providing sector contributions in the CAMS policy service within the next phase of the CAMS policy project. CHIMERE surrogate model versus LOTOS-EUROS tagging with either 15% reduction (left panel) or 100% reduction (right panel). Ranking of sectors is based on their contribution for the method displayed on the x-axis and can be a different sector for each city represented as datapoint. First ranked contributing sector in red circles, second ranked in blue triangles, and third ranked in green diamonds. The ranking excludes natural contributions and contributions from outside the model domain due to different settings for these in the models.

Within the current CAMS policy service only the CHIMERE surrogate model is providing sector attribution. However in the next phase of the CAMS policy support project, the tagging results from LOTOS-EUROS will be added as this system can provide more detailed information on subsectors Figure 5-9 shows the differences between results from these two systems for annual PM_{2.5}. It can be seen that the different systems show substantial disparities. It is

therefore crucial to provide clear guidance accompanying the service on the purposes and application domains of the methods. It should also be mentioned that these differences are to a large extent also because of the different model process descriptions and setup and thereby also illustrate uncertainties in derived source attributions.

5.2 Seasonal variability

The main dominant source contributions show a strong variability with seasons as can be seen in Appendix C for Milan and Berlin respectively. Obviously the residential contributions are largest during winter being the dominant sector in cities with large wood combustion emissions. However, this is not true for all cities, for Berlin the residential combustion is competing with agriculture, industry and traffic sources. Natural contributions are more apparent in spring and fall due to the seasonal meteorological variability.

The seasonal variability in sector contributions is similar in all models.

5.3 Daily variability

On daily timescales the variation between the source attribution methods becomes larger, especially for sectors involved in non-linear chemistry. Figure 5-10 shows the comparison of source attribution results for PM2.5 from the different methods for the residential (biomass), agriculture and traffic exhaust sources (while Figure 5-11 shows the comparison of source attribution results for PM2.5 from between the different CAMS policy support systems. Residential (biomass combustion) contributions to PM are dominated by primary aerosols and are therefore very similar for each source attribution method. Furthermore results from another project showed that the modeled response of total OA (POA + SOA) to emission changes in residential combustion is close to linear in the range from 0-60% emission reductions (Janssen et al., 2023). On the contrary, agricultural contributions largely consist of secondary aerosols influenced by non-linear chemistry and therefore show larger deviations between potential impacts from brute force and the contributions from tagging. Similarly the sources providing NO_x and SO_x, such as traffic and industry, used in the formation of secondary aerosols also show large scatter between the BF and tagging results. In these sources the scatter is somewhat smaller since their contributions have a larger primary aerosol fraction than for agriculture.

The EMEP LF and BF results are generally quite similar, particularly for residential combustion emissions (dominated by primary PM), but also for traffic exhaust emissions. Somewhat larger variability in the results for agriculture can be attributed to the non-linearity in NH₃-HNO₃ gas/aerosol partitioning, as discussed above. Even though both EMEP BF and LF are based on emission perturbation method, in LF infinitesimal emission reduction is used compared to 15% in BF, which in some specific short-term (for hourly/daily concentrations) cases are found to yield different results. Furthermore in some cases, BF calculates negative concentrations of PM_{2.5}, which is a result of upscaling of a very effective expected PM_{2.5} decrease resulting from 15% emission reduction to 100% (for more detailed discussion see CAMEO report D6.1).

The LOTOS-EUROS surrogate model with 15% emission reduction for many sectors provides a close approximation of the LOTOS-EUROS 15% brute force results. For agriculture some larger differences can be seen, including some larger negative contributions in the surrogate model which are hardly present in the brute force runs. These differences are attributable to the different behaviour for lower concentrations of the surrogate model compared to the full model from which it is derived. Since the model is trained on a limited number of simulations, different behaviours may occur locally-especially in sectors like agriculture, which are influenced by the highly non-linear chemistry of ammonium nitrate formation.

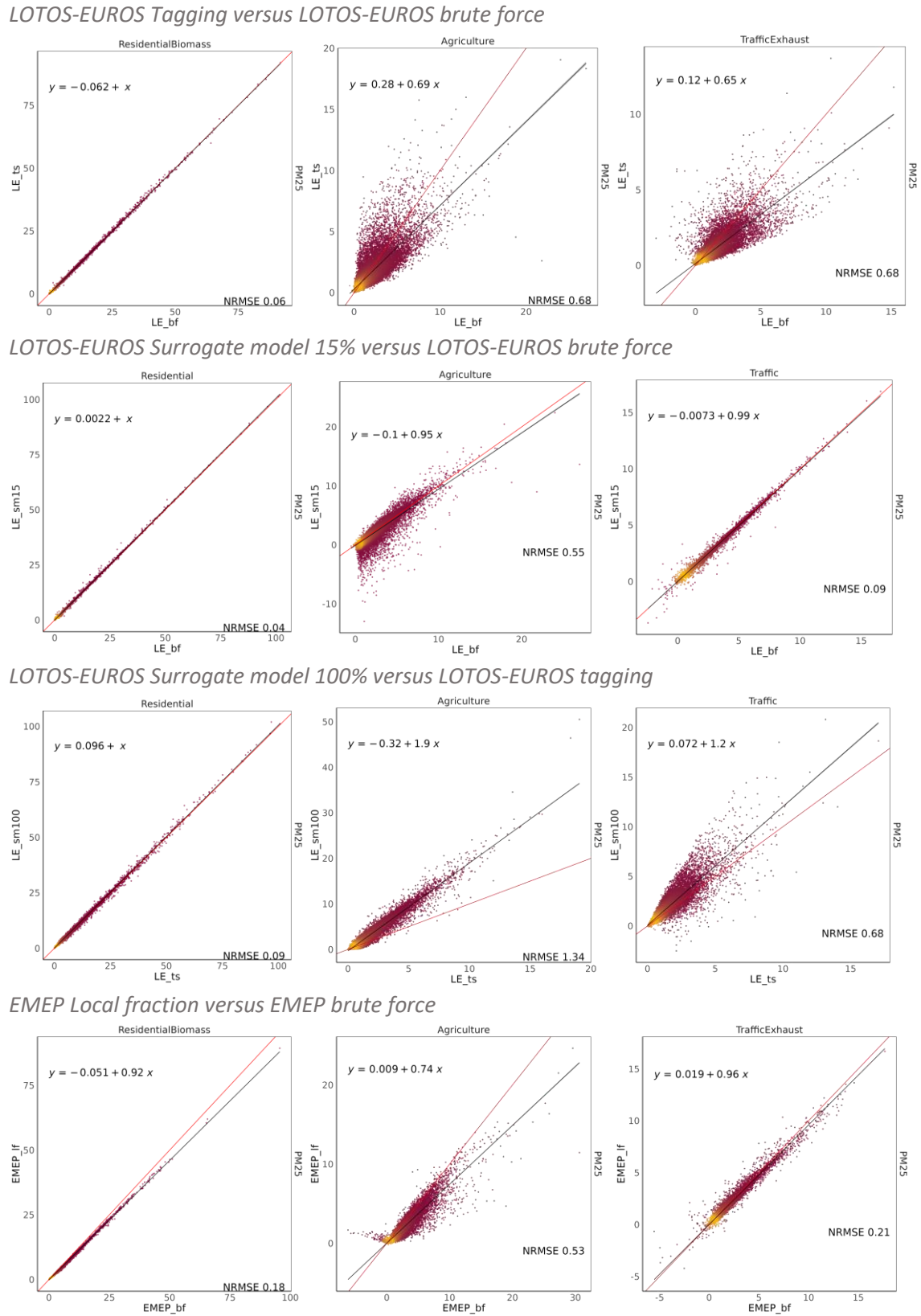


Figure 5-10 Comparison of daily $PM_{2.5}$ source contributions [µg/m³] for Residential biomass (or Residential total for surrogate model) (left panels), Agriculture (middle panels) and Traffic exhaust (right panels). In LOTOS-EUROS: BF vs TS (top row), Surrogate Model 15% vs Brute Force (second row); Surrogate Model 100% vs Tagging (third row); in EMEP: Local Fraction vs Brute Force (bottom row). The colour gradient is the density of datapoints with yellow representing highest data density, red representing lower data density. Red line = the 1:1 line.

The agricultural contribution from the LOTOS-EUROS surrogate model 100% emission reduction is nearly always larger than from tagging which can be explained by the fact that in the 100% emission reduction scenario the ammonium nitrate for example will not be formed while in the tagging approach the same ammonium nitrate is attributed not only to the agricultural source of NH₃ but also to the source of HNO₃ such as traffic.

In general the comparisons show that on a daily scale one should be considerate of the different purposes of the methods. For the assessment of source contributions to an exceedance one should consider tagging approaches, while for planning and evaluating the potential impact of policy measures one should consider methods based on impacts of emission reductions (BF, LF and surrogate models such as ACT). The methods can be used in a complementary way where tagging can be used as an efficient way for tracking many source contributions in one run, followed or accompanied by brute force/surrogate/local fraction models to identify the impact of emission reductions, potentially focusing on the main sources identified by the tagging approach.

When interpreting the brute force results one should be conscious that identified potential impacts for separate sources are not additive, i.e. the joint reduction in two source sectors may not lead to a concentration change similar to the sum of the two source contributions identified by BF. This is illustrated in Figure 5-12 and Figure 5-13 by showing timeseries of the source attribution results from four different methods applied within LOTOS-EUROS for two selected cases. The timeseries in these figures demonstrate how non-linearity and interaction between sources affects results from different source attribution methods. In the first case during late summer in Berlin, the sum of the brute force sector apportionment leads to a larger total concentration than the actual modelled concentration for most days and thus a large residual term. The largest residual terms are seen (not shown) during spring and fall when NH₄NO₃ levels are high (in summer, temperatures are too high to sustain significant ammonium nitrate levels).

This behaviour can be explained through the formation of secondary inorganic aerosols. When there is no strong limiting chemical regime, reducing either the agricultural NH $_3$ emissions or combustion related NOx emissions will both lower the NH $_4$ NO $_3$ levels. By upscaling the impacts of both NO $_x$ and NH $_3$ emission reductions one is effectively double counting the impact. Simultaneous reduction of the respective sources will however not lead to an additive impact, and the sum of the contributions calculated separately will therefore be larger than the contribution when sources are reduced together. Both SM runs in Berlin showed a similar result to the BF method. This is because in this case the 2^{nd} order polynomial equation in the SM can effectively capture the non-linear effect resulting from emission reductions, similar to the BF simulations. Note that the results from taking the 100% emission reduction from the SM approach in Berlin around the 24^{th} of September leads to smaller agricultural contributions than taking the 15% emission reduction results (Figure 5-12) due to a combination of the non-linearity derived from both chemical regime and cloud chemistry.

For the second case during winter time in Utrecht (Figure 5-13), daylight time is short and skies are mostly overcast, therefore lacking strong photochemical reactions. In this case secondary aerosol formation is restrained by insufficient hydroxyl radicals and O_3 . Due to limited oxidation, increasing or reducing NO_x and SO_2 will have limited effect on SIA formation. Hence for the BF (and SM at 15% emission reduction) method, the reduction of emission has a low impact on aerosol concentrations, despite TS demonstrated significant contributions from Agriculture and traffic.

LOTOS EUROS Tagging versus EMEP brute force

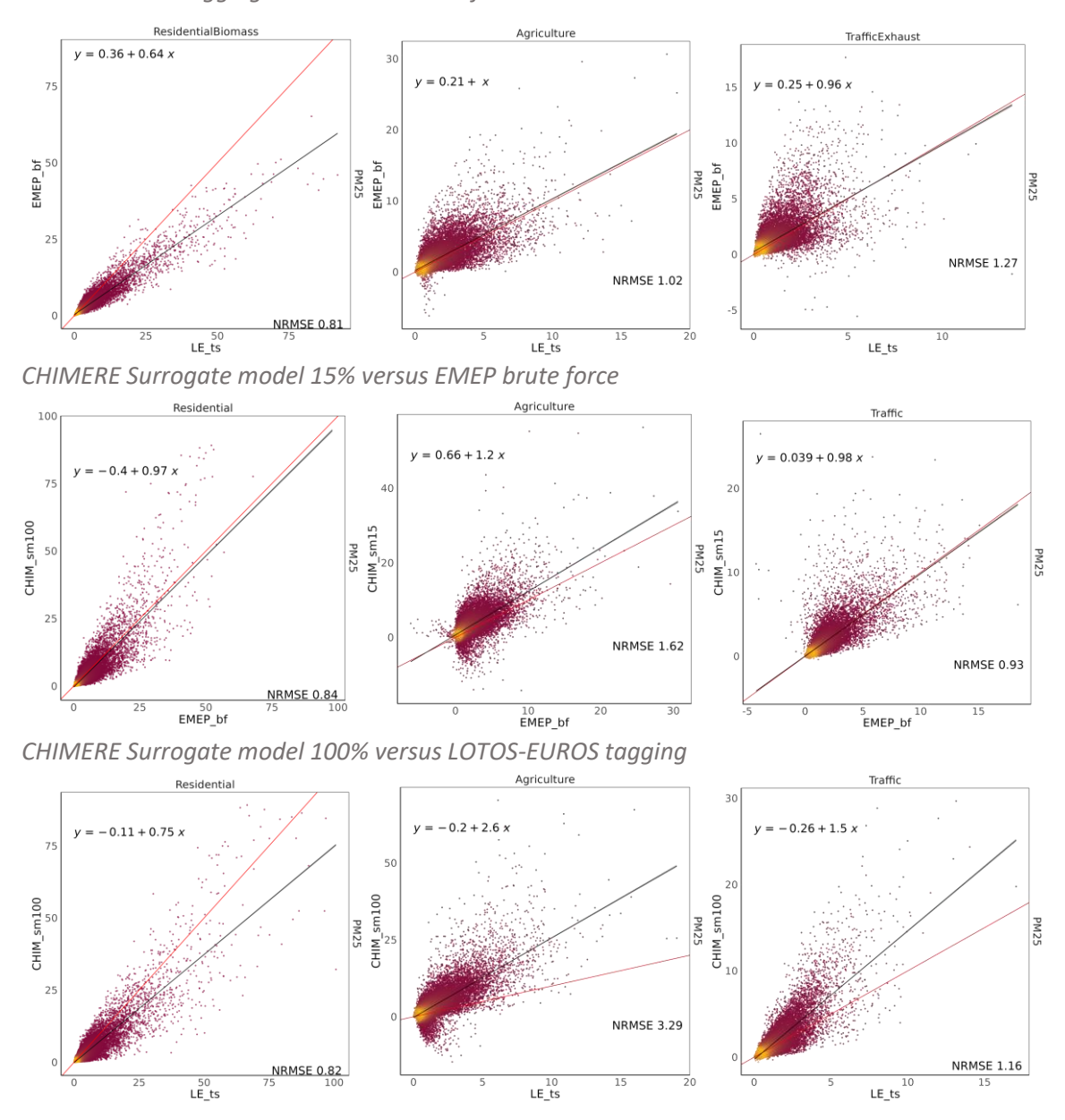


Figure 5-11 Comparison of daily $PM_{2.5}$ source contributions [μ g/m³] for Residential biomass (or Residential total for surrogate model) (left panels), Agriculture (middle panels) and Traffic exhaust (right panels). LOTOS-EUROS TS versus EMEP BF (top row), CHIMERE Surrogate Model 15% vs EMEP Brute Force (second row); CHIMERE Surrogate Model 100% vs LOTOS-EUROS Tagging (third row). The colour gradient is the density of datapoints with yellow representing highest data density, red representing lower data density. Red line = the 1:1 line.

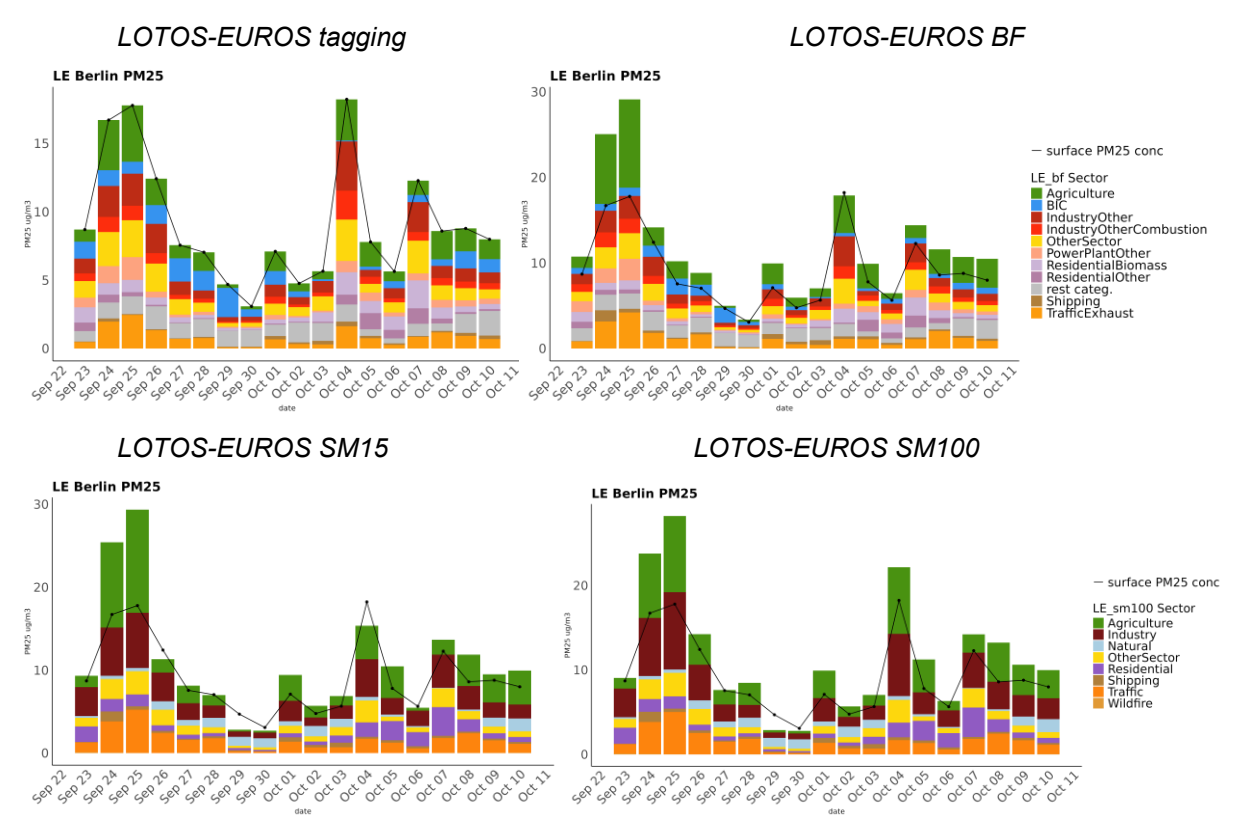


Figure 5-12 Case I Berlin: time series of surface $PM_{2.5}$ contributions [µg/m³] from LE_TS (top left panel), BF (top right panel), SM_{15} (bottom left) and SM_{100} (bottom right) from 23^{rd} September to 10^{th} October. Black line denotes the modelled $PM_{2.5}$ concentration [µg/m³].

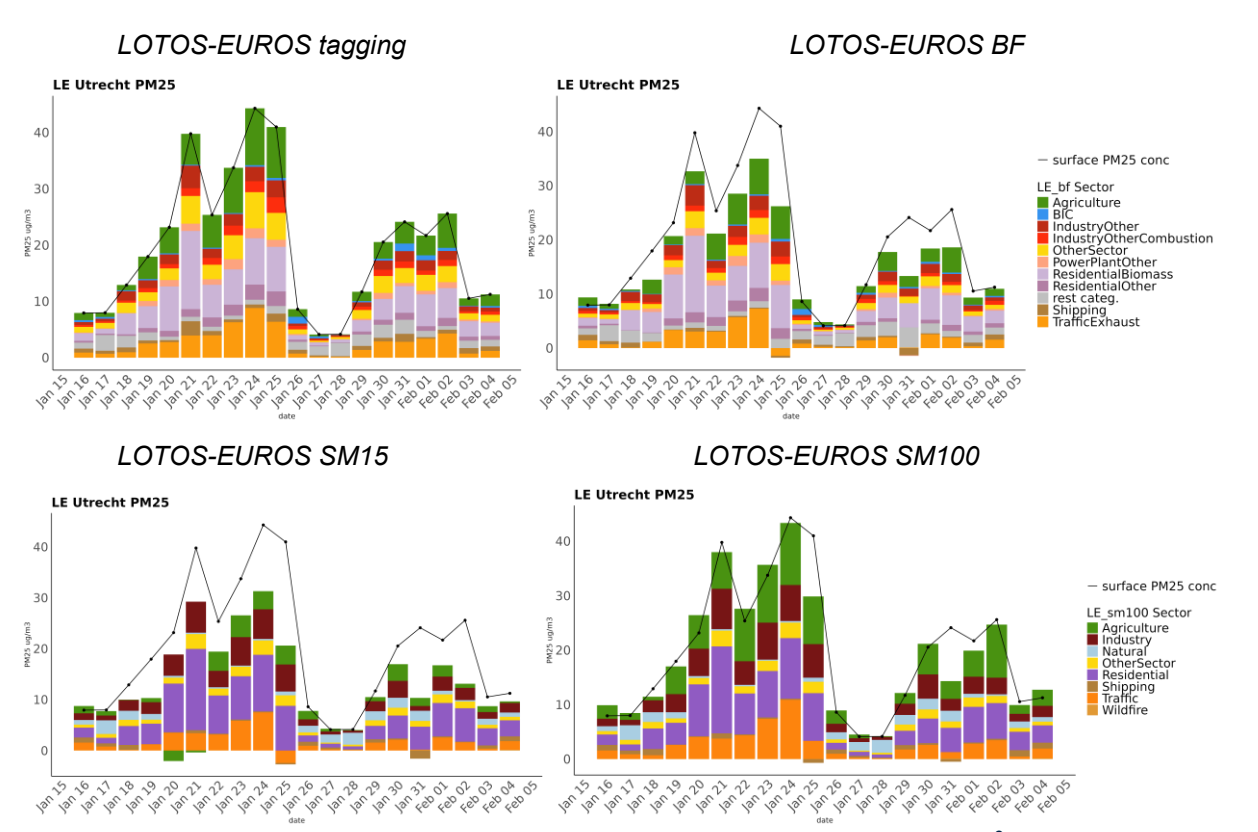
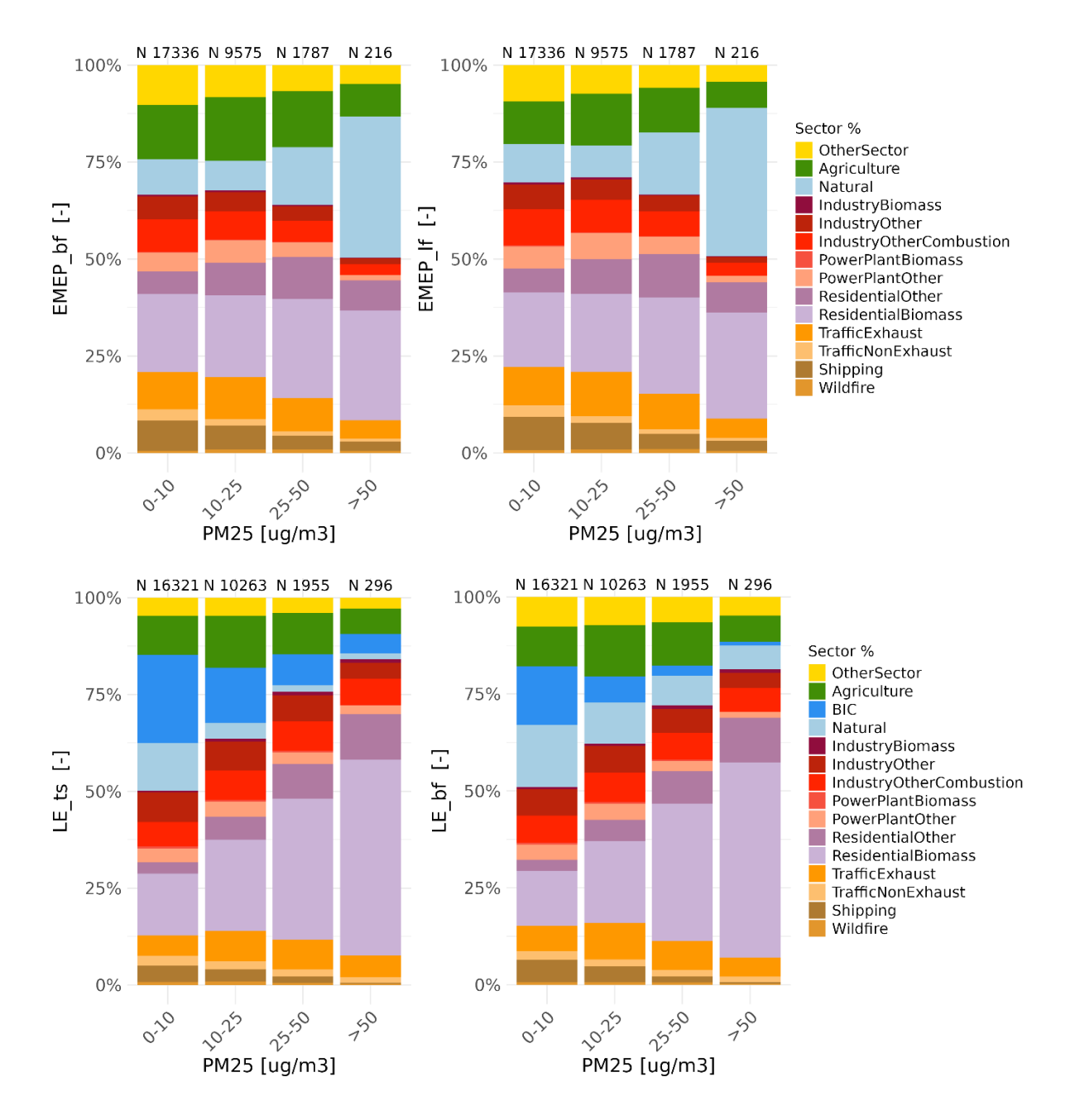


Figure 5-13 Case II Utrecht: time series of surface $PM_{2.5}$ contributions [μ g/m³] from LE_TS (top left panel), BF (top right panel), SM₁₅ (bottom left) and SM₁₀₀ (bottom right) from LE_TS, BF, SM₁₅ and SM₁₀₀ from 15th of January to 5th of February 2019. Black line denotes the modelled PM_{2.5} concentration [μ g/m³].

5.4 Source attribution of exceedances of limit values

Within the new air quality directive (EU, 2024) it is stated that the daily $PM_{2.5}$ concentration should not exceed 25 μ g/m³ on more than 18 days in the year. It is therefore interesting to evaluate the results from the different source apportionment systems for different concentration levels. Figure 5-14 shows the contributions from the different model- source attribution combinations to distinct concentration bins for all cities combined.



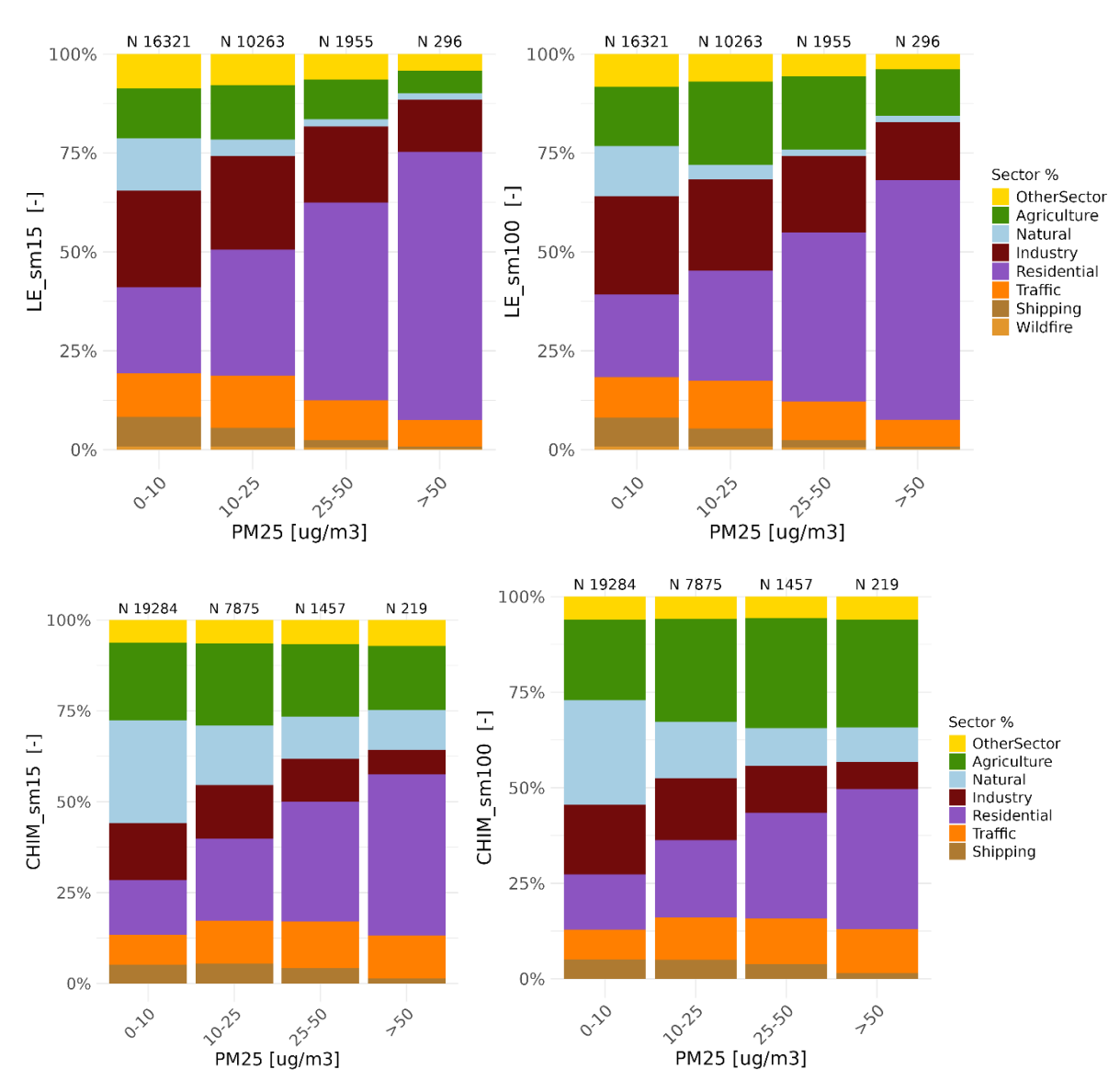


Figure 5-14 Relative source contributions [in %] to surface PM_{2.5} concentrations lower than 10 $\mu g/m^3$, between 10-25 $\mu g/m^3$, between 25-50 $\mu g/m^3$, and above 50 $\mu g/m^3$ from EMEP local fraction and Brute Force (top row), LOTOS-EUROS Tagging Species and Brute Force (second row) , surrogate model with 15 and 100% emission reduction (third row) and CHIMERE surrogate model with 15 and 100% emission reduction (bottom row). N on the top of the bars represents number of samples

All models show that the residential sector becomes more relevant with increasing concentrations. For CHIMERE and LOTOS-EUROS this sector contributes the most for concentrations above the daily limit value. For EMEP this is also the case for the concentrations above the limit values except for the highest concentrations above $50~\mu g/m^3$ where the model attributes most of the concentration to dust intrusions. Note that the sample size for this highest concentration bins is much smaller making the results less statistically significant. In the other two models the natural contribution becomes smaller when going to higher concentrations.

Exceedances of PM limit values are often seen in winter when it is cold and the shallow boundary layer hinders dilution of air pollution levels to higher altitudes. This coincides with a larger heating need and residential combustion emissions, thereby explaining the growing residential contributions with concentrations.

Categorising the exceedances by cities and occasions, LOTOS-EUROS and CHIMERE have most exceedances for Milan (number of exceedance days 68 and 76) and Bergamo (46 and 37) resulting from residential emissions. Due to the deeper surface layer, EMEP has less exceedance days driven by residential emissions (Milan 47 days) but about half of the EMEP exceedances occur in cities that are often influenced by dust intrusions (including Valletta (26 days), Catania and Palermo). LOTOS-EUROS and CHIMERE have overall less natural (dust) episodes at the surface level in the Mediterranean region. A comparison of dust contributions from all systems specifically for exceedances dominated by dust has not been performed in this study but is part of the CAMS2_71 episode reports focusing on dust episodes. There we often see variable differences in modelled dust contributions depending on the characteristics of the episode (region of emissions, extend and altitude of the dust plume).

As a consequence of the growing residential contribution, the relative contributions from other anthropogenic sectors such as traffic, industry and shipping decreases with concentrations. For shipping and industry this may also be related to the fact that part of the emissions may be emitted above the shallow boundary layer in the winter.

Interestingly, the four methods within LOTOS-EUROS show high consistency in relative source attribution results.

6 Results - Evaluation of CTM source attributions with observational based source attribution

The overarching objectives of this comparison are to evaluate the extent to which PMF derived sources align across sites with CTM (EMEP, CHIMERE, LOTOS-EUROS) source estimations and to quantify any biases or discrepancies between both source attribution approaches.

The evaluation of these approaches focuses on several aspects:

- The spatial representation (0.2 by 0.1 degrees) of CTMs for the respective area (grid-cell) in comparison to the measurement station.
- Total PM₁₀ mass contributions of sectors from CTMs compared to total PMF factor contributions.
- Seasonality / temporal profile of sources.
- Station-specific challenges that may affect PMF or CTM accuracy, due to localized meteorological conditions or local sources influencing PMF source attribution.

This work supports the broader goal of improving the CAMS modelling infrastructure by integrating observational-based information into the evaluation of source apportionment results of the CTM models.

Unless specifically mentioned the results shown in this section are based on 2019 data only to allow comparisons with all three models, in some cases we also present results for 2018-2019 to ensure broader data coverage, especially for the timeseries plots. However, all statistics plots are based on the data points present in 2019.

6.1 Total concentrations

Figure 6-1 shows the temporal correlation (R^2), Root-Mean Squared Error (RMSE) and bias ($\mu g/m^3$) between the modelled PM₁₀ and observed PM₁₀ at the PMF stations for the year of 2019.

In general the models' bias in Figure 6-1 shows that LOTOS-EUROS either underestimates or overestimates PM_{10} concentrations depending on the station, whereas CHIMERE and EMEP tend to underestimate the PM_{10} concentrations for all stations except for the Spanish stations. We will go into more details of these under- and overestimations when we compare the source specific contributions.

The temporal correlations (R²) between the CTM models and PMF profiles vary substantially across stations. On average, EMEP shows the strongest agreement with an R²of 0.49 (range: 0.23-0.74), followed by LOTOS-EUROS (LE) with an average R² of 0.41 (range: 0.14-0.68), and CHIMERE with an average R2 of 0.38 (range: 0.04-0.64). These values show that, while overall model performance is moderate, station-specific factors strongly influence the quality of the temporal match. On average we see the rural (average R²= 0.40), industrial sites (R²= 0.41) and the urban ($R^2 = 0.44$) sites have a relatively similar temporal correlation, while the traffic site shows a better performance (R²= 0.61). However when we exclude the Athens station from the comparison, the average performance of the urban stations improves to an average R²of 0.50. The station of Athens (ATH) shows a poor temporal fit for all three models (R²< 0.15). Looking at the timeseries plots for ATH (Figure 6-2), the CTMs estimate sharp PM₁₀ peaks (caused by influx events of Saharan dust) that are not captured in the PMF measurements, while contrarily two peaks around October 2019 are not captured by the CTM models. As stated previously, the number of data pairs in 2019 (Table 3-3) can differ substantially between stations and should be taken into account when interpreting these statistics.



Figure 6-1 – Metrics of the modelled PM_{10} concentrations compared to observed PM_{10} for all PMF stations for the year 2019. Bias ($\mu g/m^3$), temporal correlation (R^2) and RMSE. Green = CHIMERE against observations, Red = EMEP vs observations, Blue = LOTOS-EUROS vs observations.

From the timeseries in Stuttgart (average R²> 0.5) (Figure 6-3) one can see that the CTMs are able to reproduce the temporal variability seen in the daily observations although some of the peaks are either over or underestimated, which is in line with the evaluations in section 4. In the next sections we will go into further details when investigating the specific source sector contributions.

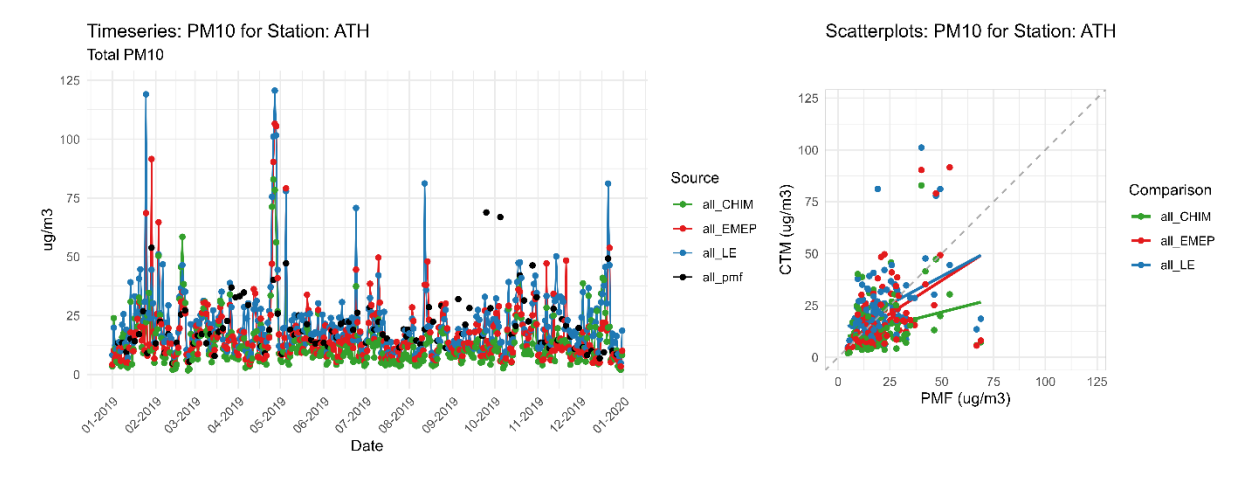


Figure 6-2 - Timeseries and Scatterplot of total observed and modelled PM_{10} for the Athens station (ATH)

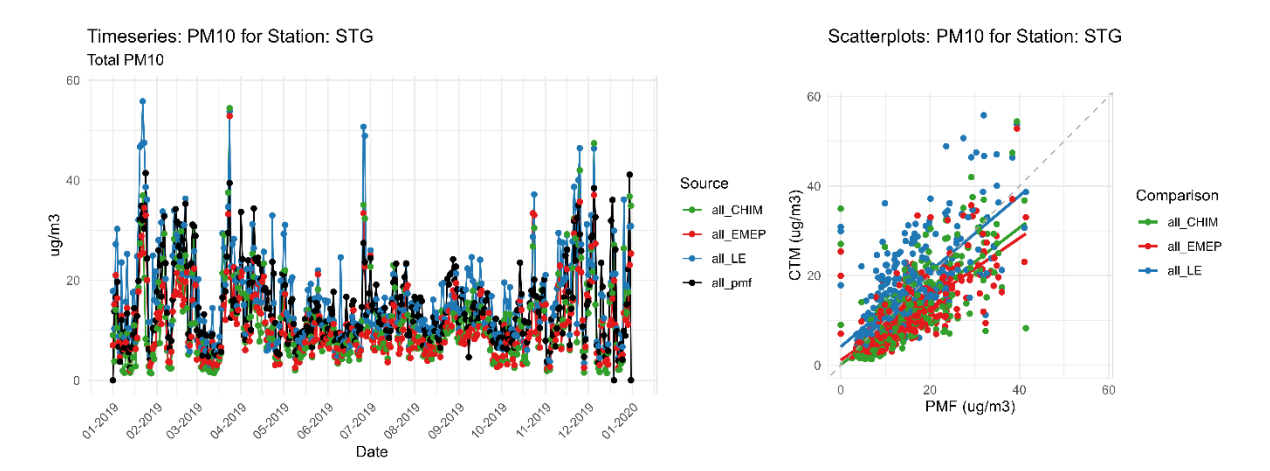


Figure 6-3 Timeseries and Scatterplot of total observed and modelled PM₁₀ for the Stuttgart station (STG)

6.2 Biomass Burning

The majority of stations (11 out of 15) identified a biomass burning-like PMF profile, often clearly manifested by the presence of levoglucosan as tracer species, since it is released during wood combustion processes (Bhattarai et al., 2019). The station in Athens applied an Aethalometer to differentiate between BC_{fossil fuel} and BC_{biomass} (Diapouli et al., 2017), however a clear biomass burning profile was not identified, but speculated to be within their 'mixed source'. The labels 'Residential combustion biomass' (EMEP and LOTOS-EUROS) and 'Residential combustion' (CHIMERE) were selected for the CTMs to compare against the PMF profiles of Biomass burning. In general the CTMs are able to represent well the temporal variability of the biomass burning source with an intermediate to good fit (Figure 6-4), with average R² for LE of 0.50, CHIMERE of 0.42, and EMEP of 0.50.

However, there is a variability in the models' performances between the stations. For example, biomass contributions in Mediterranean stations (Barcelona (Figure 6-6), Montseny and Milan (not shown)) are overestimated by the CTMS, especially during winter periods. According to the authors of (in 't Veld et al., 2023) neglectable wood burning takes place within Barcelona, which explains the fact that there is no clear biomass burning profile identified in the city. Even though the CTM models frequently calculate concentrations between 5-10 μ g/m³ of PM₁₀ during the winter months, resulting in high biases. The generic approach used for the production of the CAMS-REG emission inventory applied within the models whereby biomass driven residential emissions are determined based on population density and accessibility to forested area has been shown to be less suitable for some cities, overestimating biomass emissions in Mediterranean/Southern cities like Barcelona, Milan or Grenoble.

In contrast, we see a small underestimation by the CTM models in comparison to the biomass burning profile in the less densely populated Melpitz and Gattringen stations (Figure 6-5).

In general, EMEP provides the lowest biomass concentrations of all three models (potentially due to its relatively thicker surface layer), while also showing the smallest bias and the closest agreement with PMF concentrations. CHIMERE in general provides the highest concentrations, which can be explained by the fact that the CHIMERE residential contribution includes other fuel-types, while the other two CTM models provide the fuel specific biomass burning residential combustion contribution only (Table 3-2).

The PMF profiles related to biomass burning generally showed a clear and consistent match with their CTM counterparts. This strong alignment is largely due to the relatively stable nature of the biomass burning profile observed at most stations.

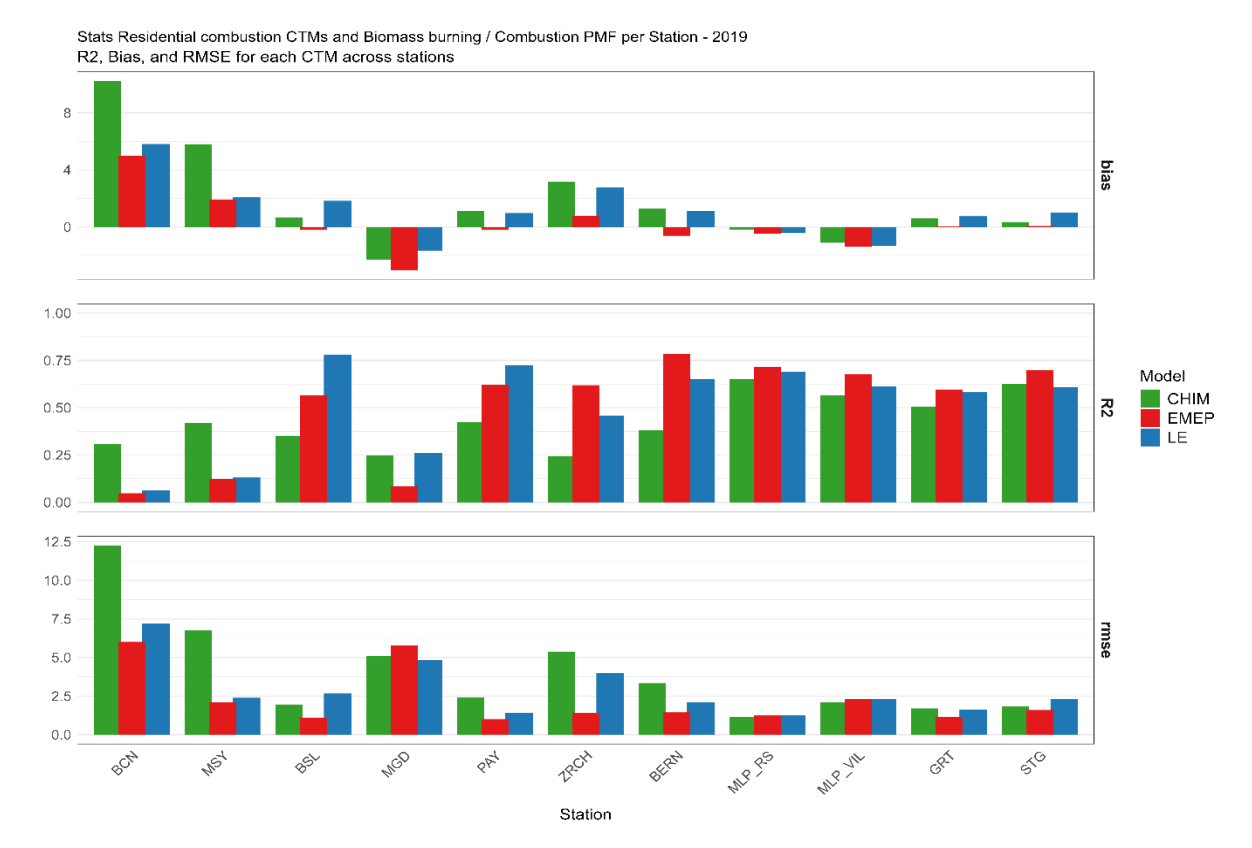


Figure 6-4 Metrics of the modelled PM_{10} concentrations for Residential combustion compared to PM_{10} concentrations equal to the 'Biomass/Wood burning' or 'Combustion' PMF factors for the year 2019. Bias ($\mu g/m^3$), temporal correlation (R^2) and RMSE. Green = CHIMERE , Red = EMEP, Blue = LOTOS-EUROS.

The EBAS database provided one station (Birkenes II - NO0002R – Appendix D) that met the data coverage criteria and measured levoglucosan. Figure 6-7 shows that the levoglucosan concentrations in the Birkenes II and 'residential combustion (biomass)' label of the LOTOS-EUROS model correlate well ($R^2 = 0.5$), which is in line with the 'biomass burning' profile comparisons.

These results illustrate that CTM models can effectively represent the temporal variability of PM from residential wood burning in many cases. However, as noted previously, performance varies per region, where especially the mediterranean stations are showing discrepancies. Nevertheless, levoglucosan remains a widely recognized robust tracer for biomass burning activities (Bhattarai et al., 2019; Simoneit et al., 1999).

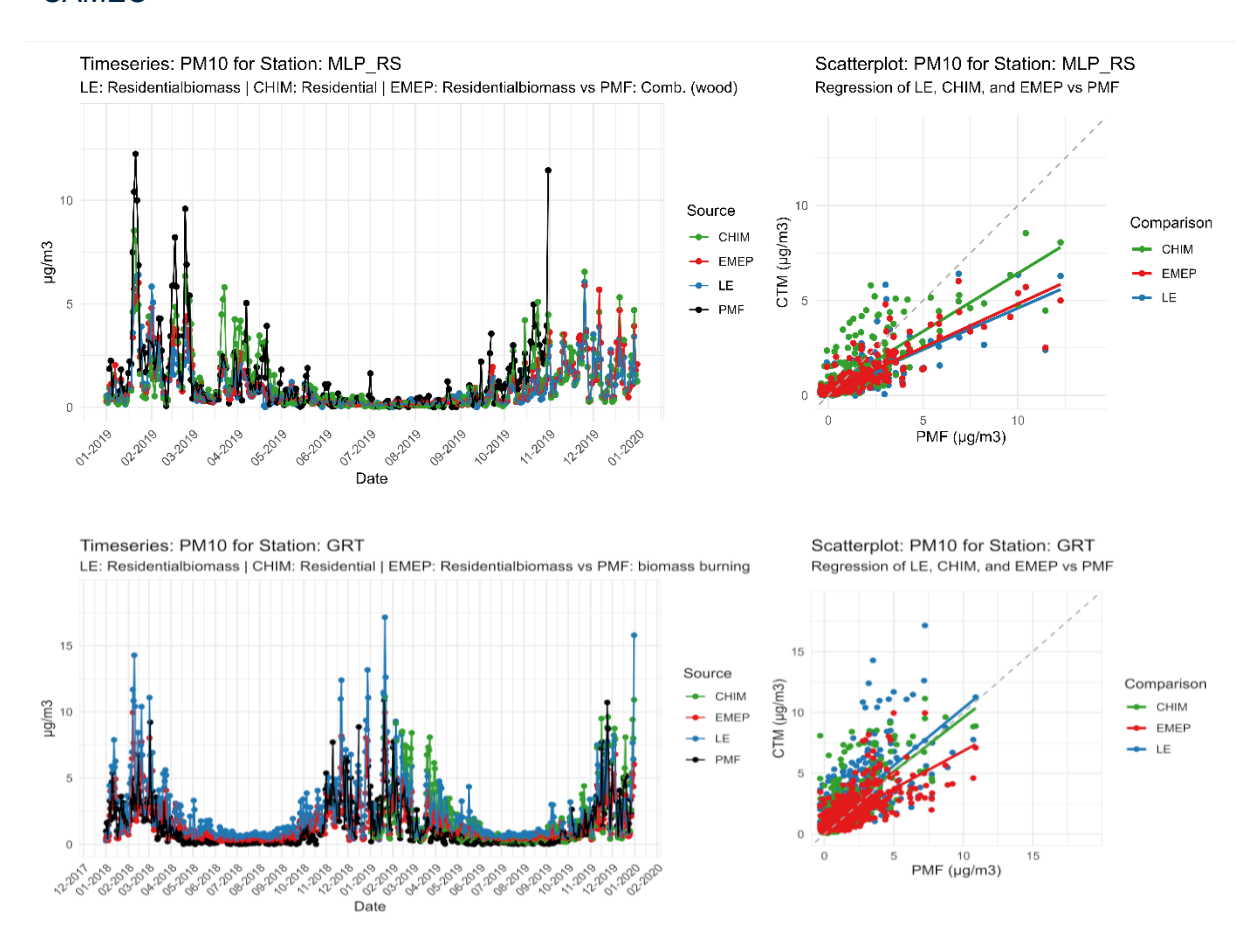


Figure 6-5 – Timeseries and scatter plot of CTM and PMF biomass burning contributions for the Melpitz research station (MLP_RS, top panel) and Gattringen (GRT, bottom panel).

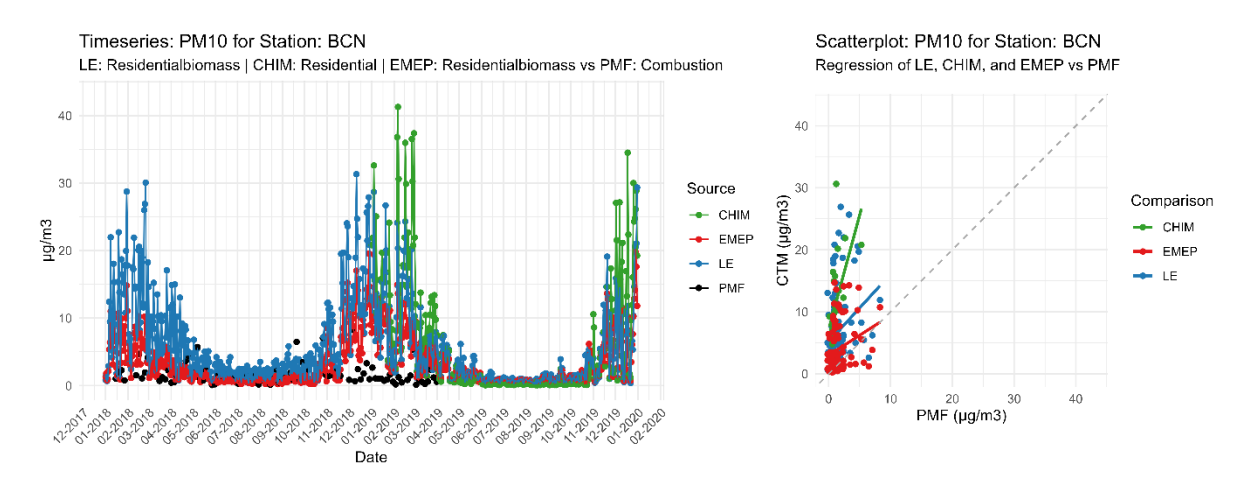


Figure 6-6 – Timeseries and scatter plot of CTM and PMF Biomass burning contributions for Barcelona (BCN).

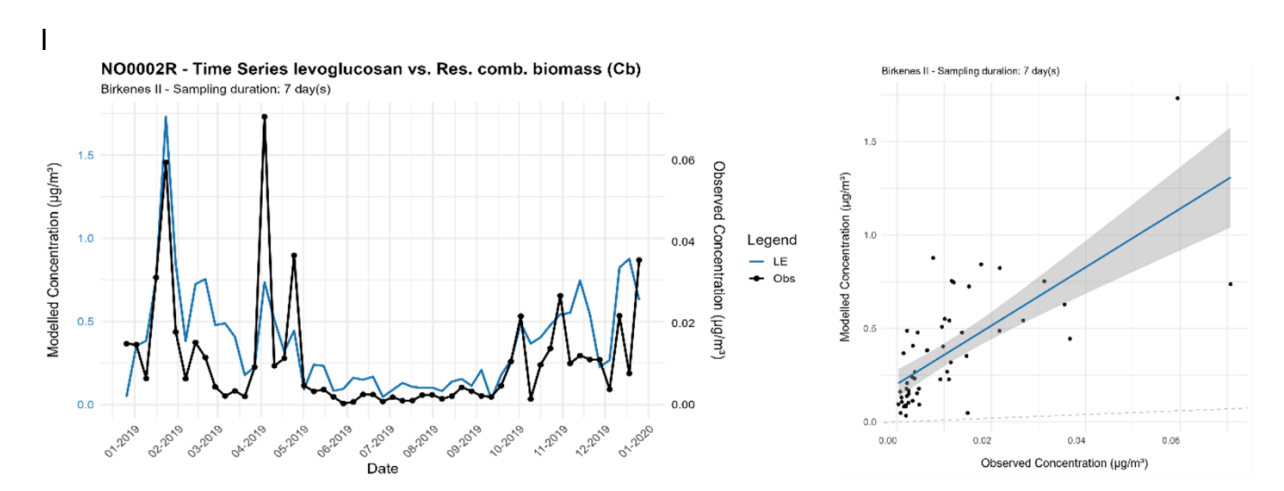


Figure 6-7 – Time series and scatterplot between levoglucosan concentrations and the Residential Combustion biomass label of Lotos-Euros at the Birkenes II station. Time Series plot; left y-axis is the modelled concentration of Lotos-Euros ($\mu g/m^3$), right y-axis is the observed levoglucosan concentration ($\mu g/m^3$). Scatterplot: y-axis is modelled concentration, while x-axis represents the observed levoglucosan concentration.

6.3 Road traffic

Road traffic emissions are in general captured in either a single 'traffic' profile identified through Elemental Carbon (EC) in combination with a number of metal components or split into an exhaust and non-exhaust profile. In those cases, the non-exhaust emissions, which represent the brake and tire wear of vehicles, often form a co-profile with dust particles due to the simultaneous resuspension of mineral particles from the road into the air (e.g. Road Dust). In the current model runs of LOTOS-EUROS, EMEP and CHIMERE the resuspension of PM was not activated, however for EMEP and LOTOS-EUROS the exhaust and non-exhaust emissions were split into two labels whereas the CHIMERE model has a single 'Traffic' source.

In contrast to the BB profile (section 6.2), road traffic proved more challenging to match. This was primarily due to the presence of exhaust and non-exhaust components, as well as a partial interference from (resuspended) mineral dust, which often ended up in the traffic-related profile.

The matching of CTM sources to traffic related PMF profiles for each station is specified in Table 6-1. For most stations a single PMF road traffic profile is provided. For these stations we aggregated the non-exhaust and exhaust contributions from EMEP and LOTOS-EUROS into a single 'traffic' contribution, while CHIMERE only provided a single traffic contribution. Moreover, the stations of BCN, MSY and ATH provided a non-exhaust or road dust profile, which were compared against the non-exhaust sectors of the EMEP and LOTOS-EUROS models and the traffic sector of CHIMERE.

Figure 6-8 shows the comparison of the traffic contributions in the CTMs and PMFs, corresponding to the matches shown in Table 6-1.

Table 6-1 - Overview comparisons between traffic sectors (CTM) and associated PMF profile

CTM model	stations	CTM source(s)	PMF Profile
LE		Traffic	
CHIM	GRT & STG	Traffic	Traffic
EMEP		Traffic	
LE		Traffic	
CHIM	BCN & MSY	Traffic	Combustion
EMEP		Traffic	
LE	(BERN / BSL/	Traffic	
CHIM	ZRCH/ MGD	Traffic	Road traffic
EMEP	/ PAY)	Traffic	
LE		Exhaust	
CHIM	ATH	Traffic	Vehicular exhaust
EMEP		Exhaust	
LE		Exhaust	
CHIM	MIL	Traffic	Vehicular exhaust
EMEP		Exhaust	

At a first glance we see that the models show larger traffic contributions than the PMF data for some Swiss stations but we should note that for Switzerland as is explained in section 6.1 these statistics are based on the limited number of observations in the winter period of 2019 giving a skewed image for these stations. All together we see mediocre to low correlation coefficients indicating the CTM and PMF models are having difficulty in representing this highly spatially and temporally variable source, in a time consistent way. This is in line with results from the RI-urbans project where a comparison was performed between the CAMS regional ensemble EC from fossil fuel versus source specific EC from aethalometer data for the year 2018. On average, the CAMS ensemble eBC attributed to traffic showed an average bias of 14.7% compared with the measurements. Which was linked to the problem of sub-grid representativeness. The average temporal correlation was R=0.50 (R² =0.25) which is somewhat higher than for most stations in our comparison for PM₁₀ traffic, which can be expected since the EC comparison is more direct focusing on one component where the PM₁₀ contributions are composed of several components.

Below we describe in more detail the comparisons for the different stations.

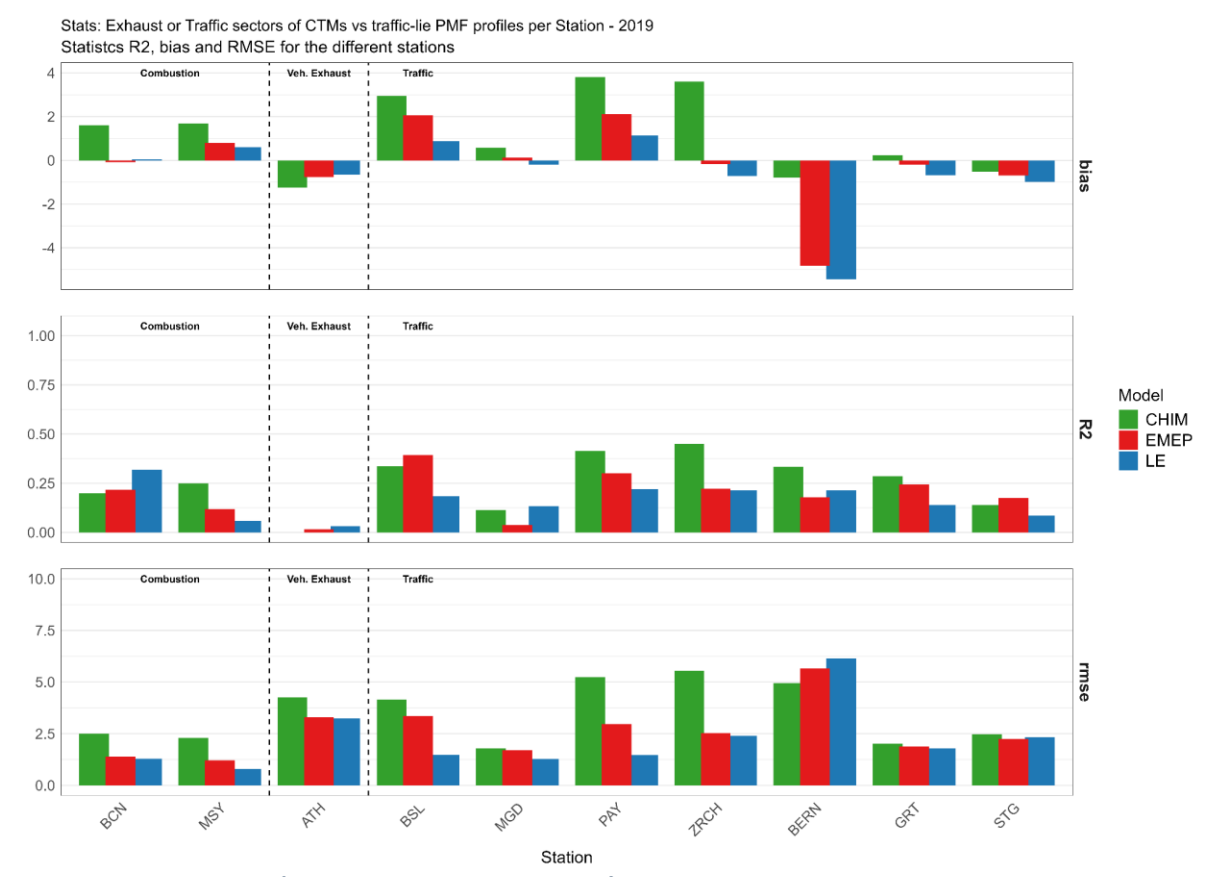


Figure 6.8- Bias (μ g/m³), temporal correlation (R²) and RMSE between the daily CTM PM₁₀ concentrations for traffic or traffic exhaust and the traffic-related (traffic, exhaust or combustion) PMF contributions for the year 2019 (see Table 6-1 for the included sources in the matching). Green = CHIMERE, Red = EMEP, Blue = LOTOS-EUROS.

For Milan and Athens the PMF identifies an '(Vehicular) exhaust' profile. We compared the exhaust labels from EMEP and Lotos-Euros against the Exhaust factors present in MIL_PAS and ATH since the definition of the profile suggests that the PMF profile mainly consists of exhaust traffic emissions. For the MIL_PAS station (not shown) the models overestimate the traffic contributions compared to PMF, with the largest overestimation by CHIMERE, which also contains non-exhaust contributions. The temporal correlation is consistently low for all models ($R^2 < 0.25$). This overestimation may be due to an overestimation of the emissions at this site, or too low mixing in the models in the Po valley.

In contrast, for the ATH station all CTMs provide lower traffic than the 'Vehicular exhaust' PMF factor contributions (LE NMB = -68%, EMEP -70%, CHIMERE -61%). When we add the nonexhaust contributions from LE and EMEP, the biases are reduced (LE NMB = -46%, EMEP -62%). The question arises if the vehicular exhaust profile in ATH consists merely of exhaust contributions, or also non-exhaust traffic or other source contributions. Especially since the ATH station also identified a non-exhaust profile. Consultation with the PMF data providers revealed that the exhaust profile contains most of the Zn and Ni species, which they relate to tire wear, but also lubricating oil. Moreover, certain caution with the PMF interpretation for Athens is required, since a number of organic compounds were not included into the analysis, which resulted in relatively high levels of unassigned mass and uncertainty (personal contact). On the other hand the underestimation of traffic-related contributions by CTMs at urban stations is not unexpected as it is observed in previous comparison work between traffic labels and PMF (Pekel et al., 2025; Timmermans et al., 2022). A major reason here is the inherent differences in comparing an area averaged value (grid-cell representing 15x15 km2) for traffic sources characterised with large subgrid variability against a point of observation representing the PM of its direct environment.

An underestimation is seen for the German stations and Bern in Switzerland. The stations in Germany (STG & GRT) identify a 'traffic' and a 'resuspension' profile, whereby the first profile contained the majority of EC, but also quantities of Fe, Ba, Zn, Sb and Cu which are all tracers related to tire and brake-wear (Grange et al., 2021; van Pinxteren et al., 2024). The resuspension profile contains large contributions of Al, V, Ca and to a lesser extent the tracer species related to (non-)exhaust emissions. Because of the inclusion of some tracers related to non-exhaust emissions in the PMF profile we included the non-exhaust contributions of EMEP and LOTOS-EUROS in the comparison to PMF data as presented in Figure 6-8. The inclusion of these non-exhaust contributions provide an improvement in the R² (average increase of 0.07 and 0.05 for LE and EMEP, respectively) and reduced biases for GRT (LE: from -1.18 to -0.75 μ g/m³ & EMEP: -0.52 to -0.26 μ g/m³) and STG (LE: from -1.76 to -0.99 μ g/m³ & EMEP: -1.23 to -0.77 μ g/m³) as compared to statistics excluding the non-exhaust contributions from these two models. The traffic contributions in CHIMERE are somewhat higher leading to a positive bias for the station GRT and lower negative bias in STG (bias_{grt} = 0.22 & bias_{STG} = -0.52 μ g/m³).

The stations in Switzerland identified one 'traffic' profile. The metrics provided in Figure 6-8 only cover a limited comparison between the observed and modelled traffic contributions, due to the limited (N=22) datapairs in 2019. However, for the winter months the daily temporal correlation for PAY, BSL, ZRCH and BERN was decent (CHIMERE R²~ 0.38), LOTOS-EUROS R²~ 0.27 and EMEP R²~0.30). For the rural MGD station a consistent low correlation was found (R² <0.11) and the lower positive bias seems to reflect a better representation of rural conditions by the model resolution. Looking at the average concentrations for 2018-2019 per station, we can see that for the PAY site (0.20 $\mu g/m^3$) the PMF contribution of traffic is very low, and the models overestimate the traffic contribution substantially. The BERN traffic station is the only station in Switzerland where we see lower CTM contributions than in the PMF for LOTOS-EUROS and EMEP (Figure 6-9). This above all shows that there is station specific variability in how well the PMF and CTM traffic estimations match within Switzerland, where the CTMs tend to overestimate rural locations and underestimate traffic stations.

Finally, the stations in Spain (BCN and MSY) describe that the 'combustion' profile represents different sources depending on the station. In Barcelona, the 'combustion' profile is mainly related to traffic (high contributions of EC), while in Montseny it represents a combination of traffic, industry and biomass burning. On top of that, both stations identify a 'Road Dust' profile, containing Fe, Cr, Cu and Sn species, which could contain part of the tire/brake-wear particles. For the BCN station (Figure 6-10) we see that the traffic exhaust contributions of EMEP (NMB = 10%) and LOTOS-EUROS (NMB = -2%) are much closer to the PMF combustion contribution than the total traffic contribution of CHIMERE (NMB = 138%). This could indicate an advantage of separating exhaust and non-exhaust sectors allowing a better fit with certain profiles. However it should be noted that only the winter months data pairs are compared here in the metrics. The CTMs traffic contributions overestimate the concentrations of the 'combustion' profile in MSY (range NMB= + 300-1200%) (Figure 6-8). This could mean that for MSY, a remote rural station, the emission inventory overestimates the emissions for traffic attributed at this location or that the spatial representativeness of the grid-cell does not properly account for such remote locations. It should also be noted that for MSY, the total average concentration of the 'combustion' profile is very low (0.19 μg/m³) considering its representing several sources.

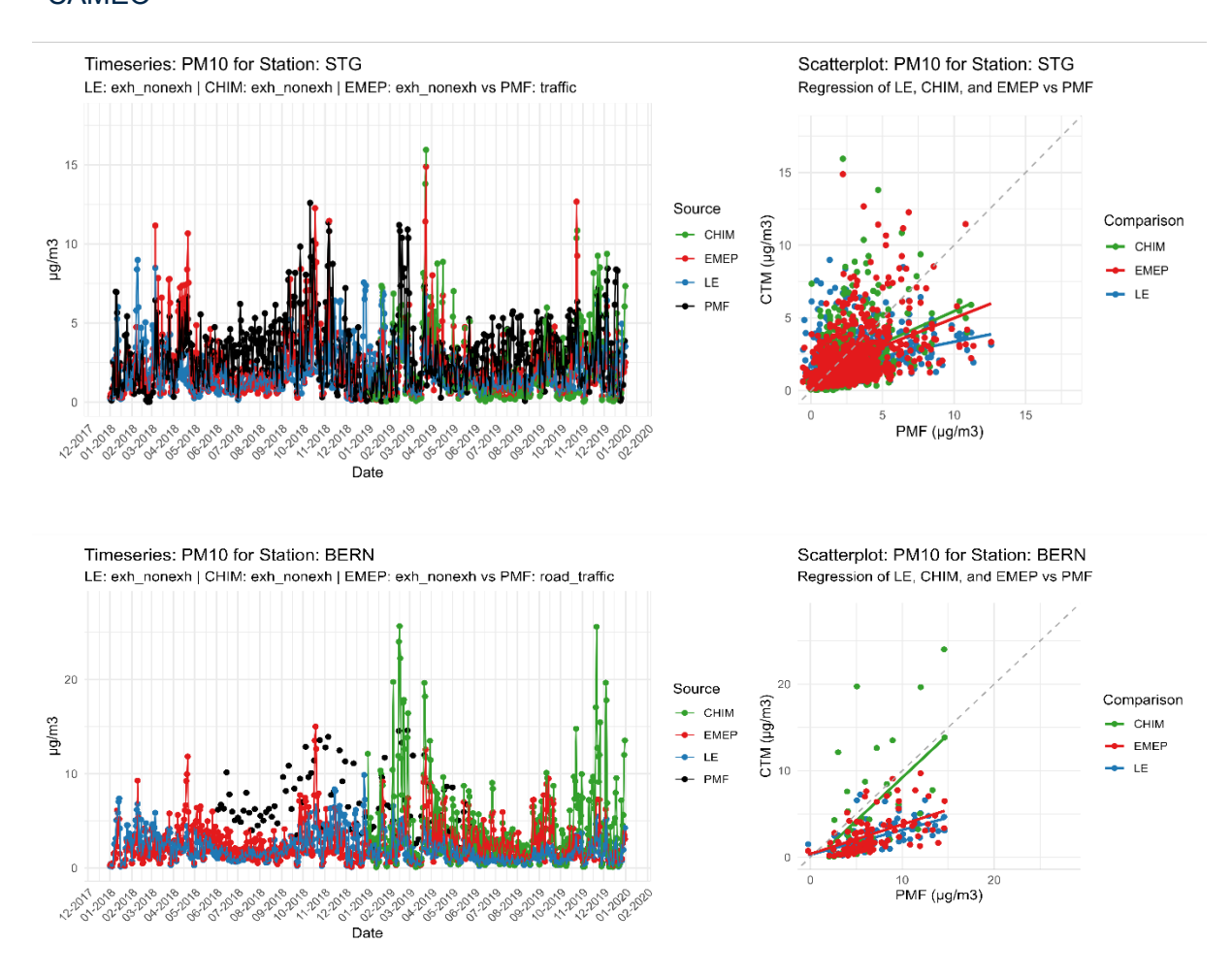


Figure 6-9 Timeseries and scatterplot of the Traffic PMF profile and Model contributions of traffic (exhaust & non-exhaust) for PM₁₀ at the STG (upper panel) and Bern (lower panel) stations. Green = CHIMERE, red = EMEP, Blue = LOTOS-EUROS, black = observations.

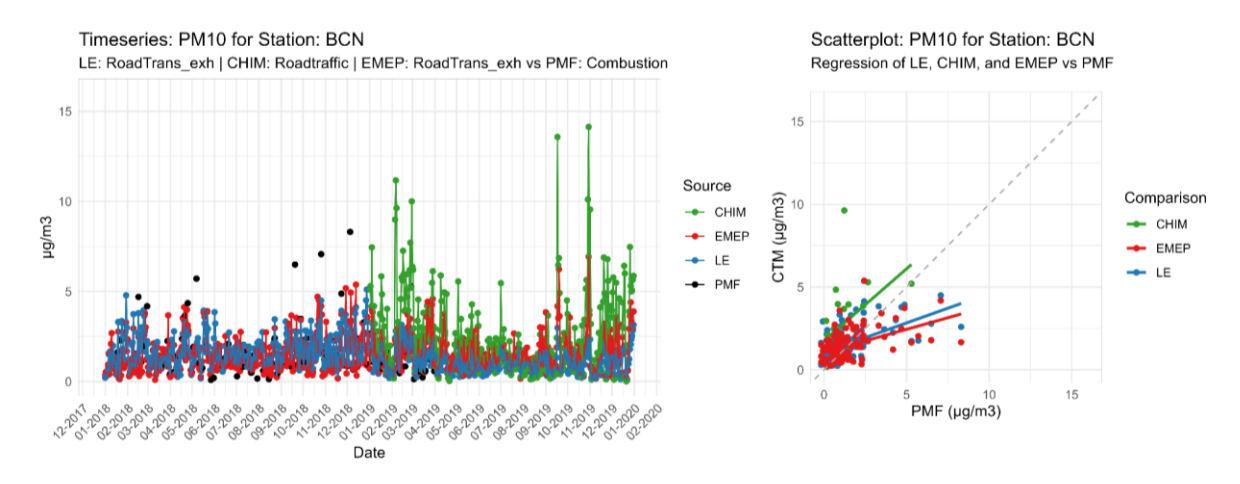


Figure 6-10 Timeseries and scatterplot of the Combustion (containing traffic) PMF profile and Model contributions of traffic (CHIMERE) and Exhaust (LOTOS-EUROS and EMEP) for PM $_{10}$ at the BCN station. Green = CHIMERE, red = EMEP, Blue = LOTOS-EUROS, black = observations.

For the BCN, MSY and ATH stations an additional comparison was made between the non-exhaust sectors of EMEP and LOTOS-EUROS, the traffic sector of CHIMERE and the Road Dust or non-exhaust profiles identified by the PMF (Figure 6-11). The temporal correlation for the ATH station was poor for all models, however, the PMF data providers emphasize the

presence of a high uncertainty surrounding the profiles and the fact that tyre-wear species were also present in their exhaust profile. For the Spanish stations, the non-exhaust sectors of EMEP and LOTOS-EUROS showed an underestimation for BCN (NMB; LE = -44%; EMEP = -50%) and were close to the observed road dust profile in MSY with an average bias of 0.04 $\mu g/m^3$, however it should be noted that the average concentration of the Road Dust profile for MSY is very low (0.07 $\mu g/m^3$). Unsurprisingly, the traffic sector of CHIMERE showed higher overestimations, since it represents both exhaust and non-exhaust emissions. Temporal correlations for BCN are reasonable (R² ~0.35-0.50), while CHIMERE shows a very low correlation for MSY.

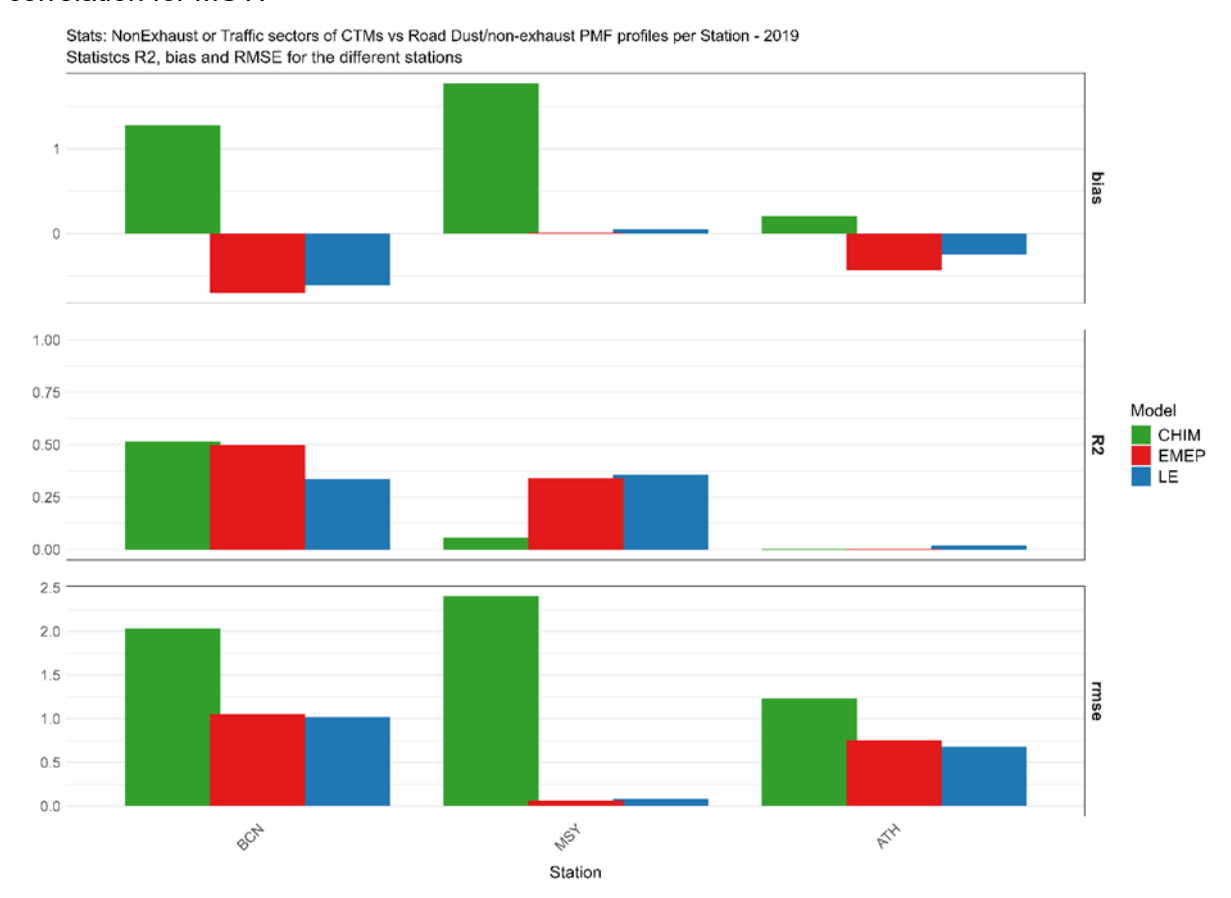


Figure 6-11 Bias (μ g/m³) temporal correlation (R²) and RMSE between the daily CTM PM₁₀ concentrations for traffic or traffic non-exhaust and the non-exhaust and road-dust PMF contributions for the year 2019 (see Table 6-1 for the included sources in the matching). Green = CHIMERE, Red = EMEP, Blue = LOTOS-EUROS.

The Dutch stations contained a 'Brake Dust or Traffic' profile, containing high contributions of Cu, Mo, Sb and Zn (all associated with brake wear emissions). The close proximity of a heavy steel and iron production plant and the associated activities (metal friction in the factory or by industry related railway transport) are likely causing contamination of the profile at these sites.

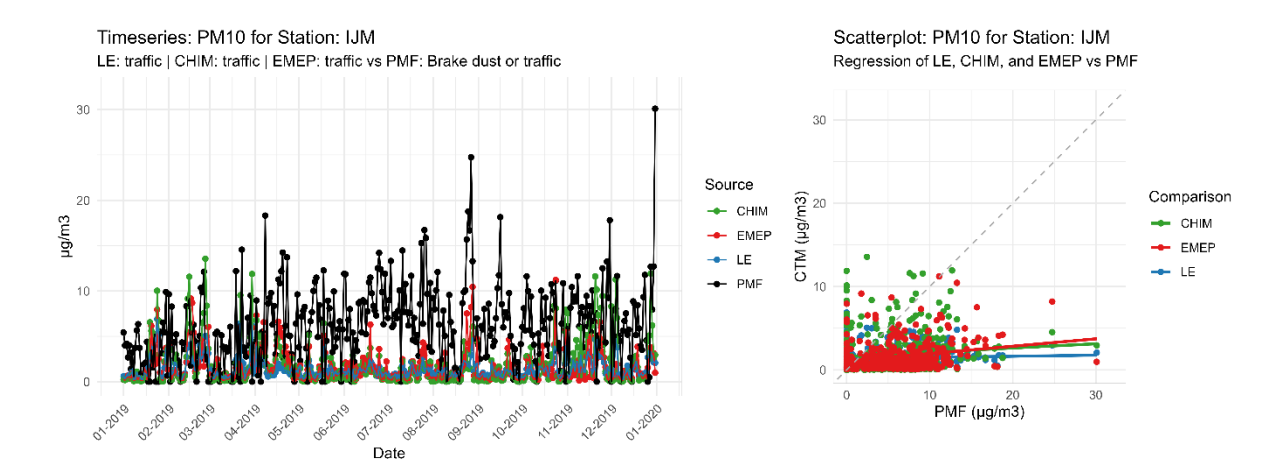


Figure 6-12 Timeseries and scatterplot of the Brake dust or traffic PMF profile and Model contributions of traffic (exhaust & non-exhaust) for PM_{10} at the IJM station. Green = CHIMERE, red = EMEP, Blue = LOTOS-EUROS, black = observations.

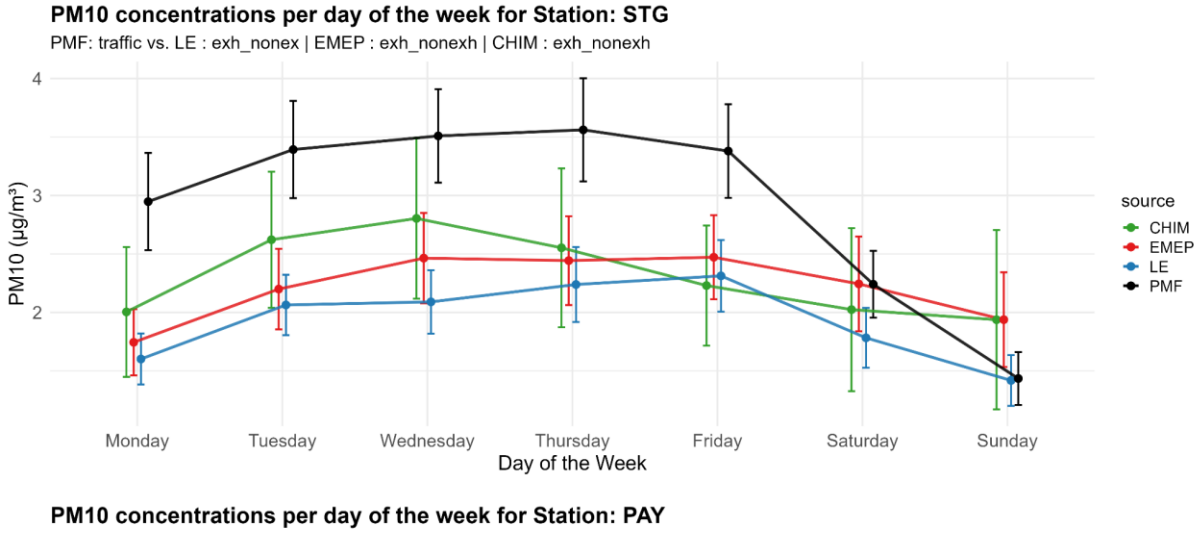
As shown in Figure 6-12 for Ijmuiden, the CTM-estimated road traffic contributions are consistently below the concentrations observed of the 'Road dust or Traffic' PMF profile for all Dutch Stations. Moreover, temporal agreement is poor across all stations and models. Comparing the PMF profiles across the stations show that the average concentrations at IJM (6.93 μ g/m³), WAZ (5.09 μ g/m³) and BVW (3.77 μ g/m³) are higher than most other European sites (other stations report < 3 μ g/m³), with values being in the same range of BERN (6.91 μ g/m³) and FRB (3.79 μ g/m³), both classified as 'traffic' stations. These high concentrations for the Dutch stations in comparison to the other traffic-related PMF profiles strengthen the suggestion of (Mooibroek et al., 2022) that contributions of railway transport, mineral dust (contaminated with metals from the industrial location and resuspended) and industry-related emissions influence this profile.

We therefore added the industrial contributions of the CTM models to the comparison, but then the CTM concentrations overshoot the PMF concentration and did not improve the match. Unfortunately resuspension of PM (through traffic) was not included in the models and could be a possible way to improve this match.

To further evaluate the ability of the models to correctly represent variations in the traffic contributions we have compared the CTM and PMF weekly profiles for this source contribution (Figure 6-13). In general we observe that for the majority of stations a similar weekly pattern for the CTMs and PMF with relatively low concentrations starting on monday that increase throughout the week, after which we see a clear drop in concentration during the weekend. There are some deviations; for some stations (e.g. Bern and Zurich, not shown) we see an increase of traffic contributions from the PMF profiles on Friday with a sharp decrease on Saturday. For the rural station of Payerne (PAY) we also see this small increase in PMF on Friday and decrease on Saturday, albeit less dynamic than for the Swiss urban or traffic locations. The CTMs seem to capture the general pattern between weekend- and working days, but for most sites the relative change is smaller in the CTM (see e.g. the weekly profile for STG in Figure 6-13 top panel), providing relevant feedback on the applied weekly cycles in the models. Depending on the station and model, the CTMs also estimate a Friday-peak (e.g. PAY, Figure 6-13 bottom panel), however there are mismatches, for example the PMF profile in Basel does not observe a Friday peak, while the EMEP and LOTOS-EUROS stations do estimate this (data not shown). These evaluations highlight the need for location dependent time profiles and can support further developments of the CAMS TEMPO emission profiles in the CAMS2 61 project.

Although all models apply the same temporal emission profiles to the emissions, differences may arise due to the different model designs and attribution method, where EMEP and CHIM

represent potential impacts and LOTOS-EUROS represents actual contributions. Especially the secondary PM from traffic is influenced by many processes and other emission sources, thereby depending on model choices and the attribution method.



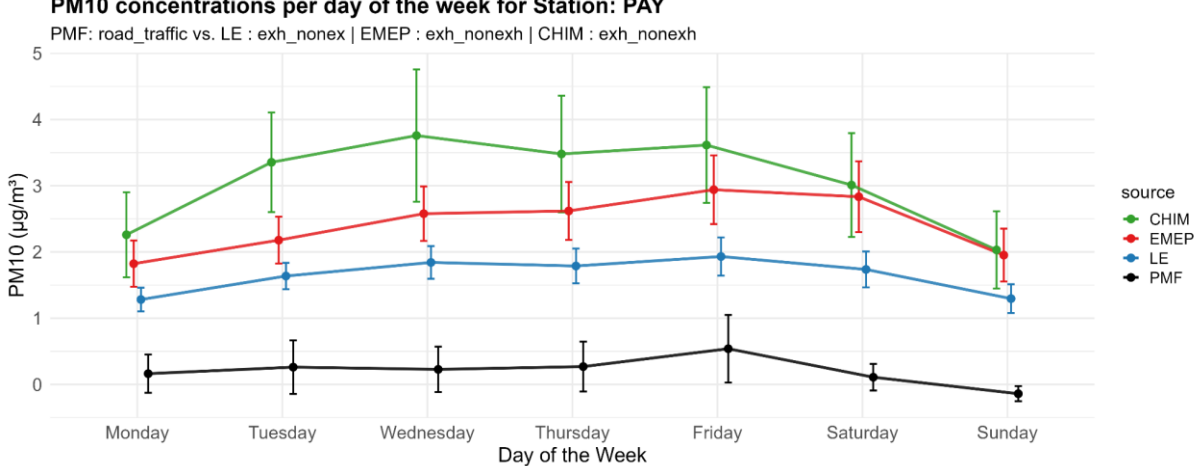


Figure 6-13 Average traffic contributions per day of the week ($\mu g/m^3$) for the stations of GRT (urban) and PAY (Rural background). Green = CHIMERE, red = EMEP, Blue = LOTOS-EUROS, black = observations. Bars represent the variability of daily mean concentrations.

6.4 Industry

Five stations (BCN, MSY, IJM, BVW and WAZ) identified a profile called industry. All these profiles were compared against the 'Industry' sources from the CTM models. Initially, we distinguished between combustion and non-combustion industrial sources for EMEP and LOTOS-EUROS, however within the PMF profiles used in this work this distinction was not clearly found. Figure 6-14 shows that the CTMs consequently overestimate industry contributions for the stations in Spain.

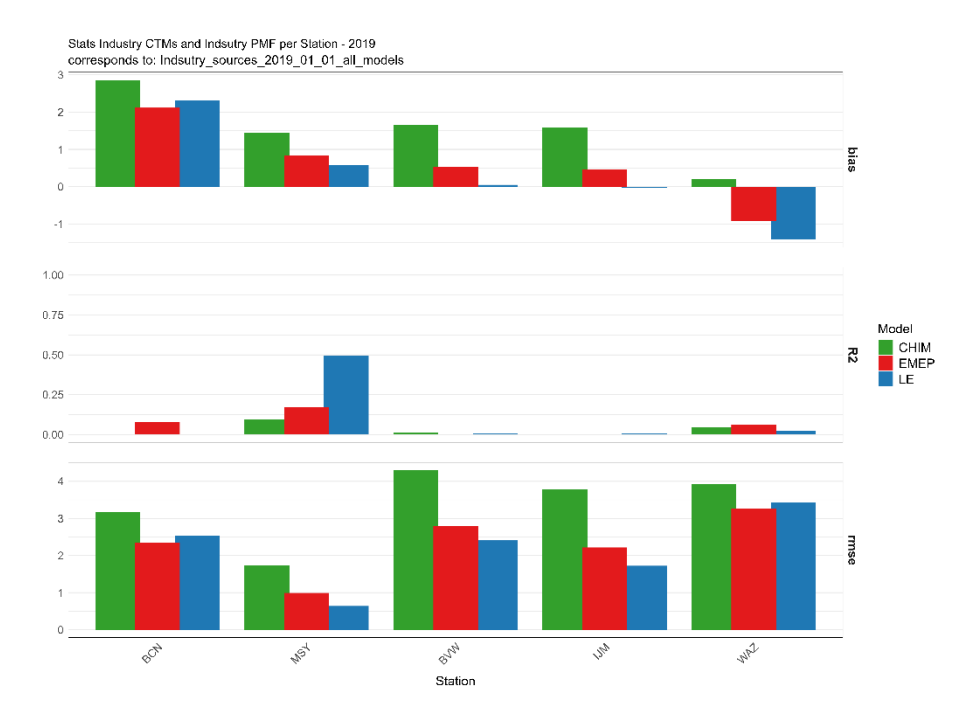


Figure 6-14 Metrics of the daily modelled PM_{10} concentrations for Industry sectors compared to PM_{10} concentration equal to the Industry PMF factors for the year 2019. Bias ($\mu g/m^3$), temporal correlation (R^2) and RMSE. Green = CHIMERE , Red = EMEP, Blue = LOTOS-EUROS.

The Industry contributions in Barcelona and Montseny are (remarkably) low throughout the year (BCN = $0.05~\mu g/m^3$ and MSY = $0.03~\mu g/m^3$), whereby it should be noted that some of the industrial contributions are expected to be present in the 'combustion' profiles. However, when we would aggregate the mass of both the industry and combustion profiles at both sites (annual average BCN = 0.81~& MSY = $0.11~\mu g/m^3$) the industrial labels of LOTOS-EUROS ($3.88~\mu g/m^3$), CHIMERE ($2.81~\mu g/m^3$) and EMEP ($2.04~\mu g/m^3$) are still substantially higher. Besides difficulties related to the PMF industrial factors this can also be related to an overestimation of emissions in the models and/ortoo low effective emissions heights. LOTOS-EUROS ($3.88~\mu g/m^3$), CHIMERE

Similarly to the road dust or traffic profiles at the Dutch stations we can observe a poor temporal correlation (R² <0.1) for the industry contributions (Figure 6-14). The stations of IJM (bias: LE = -0.03 , EMEP = 0.46, Chim = 1.59 $\mu g/m^3$) and BVW (bias: LE = 0.05, EMEP = 0.54, Chim = 1.67 $\mu g/m^3$) show an overestimation of PMF industry contributions by the models, whereas the EMEP and LOTOS-EUROS contributions underestimate the PMF industry concentrations for WAZ (bias: LE = -1.41, EMEP = -0.92, Chim = 0.20 $\mu g/m^3$) .

The three Dutch stations are closely positioned at different sides of the heavy industry plant and all fall within the same grid-cell of the CTM models. This enables a direct evaluation of how the modelled area daily averages can differ from the concentration dynamics at the three sites. Indeed, the concentration dynamics of the industry profile at WAZ and IJM are not overlapping, with peaks at WAZ not present in IJM (Figure 6-15). This is probably due to changes in wind direction, but may also partly result from the industry profile at WAZ being contaminated with slightly more crustal matter PM (Mooibroek et al., 2022) and the minor 'PAH-rich' profile could contain PM mass originating from 'Industrial activities'. A main take away from the stations closely surrounding the steel plant is that PMF-CTM comparisons for such a polluted area proves to be problematic due to the high probability of profile mixing (crustal matter, shipping, traffic and industry) and the area the CTMs represent which does not entirely represent the local dynamics.

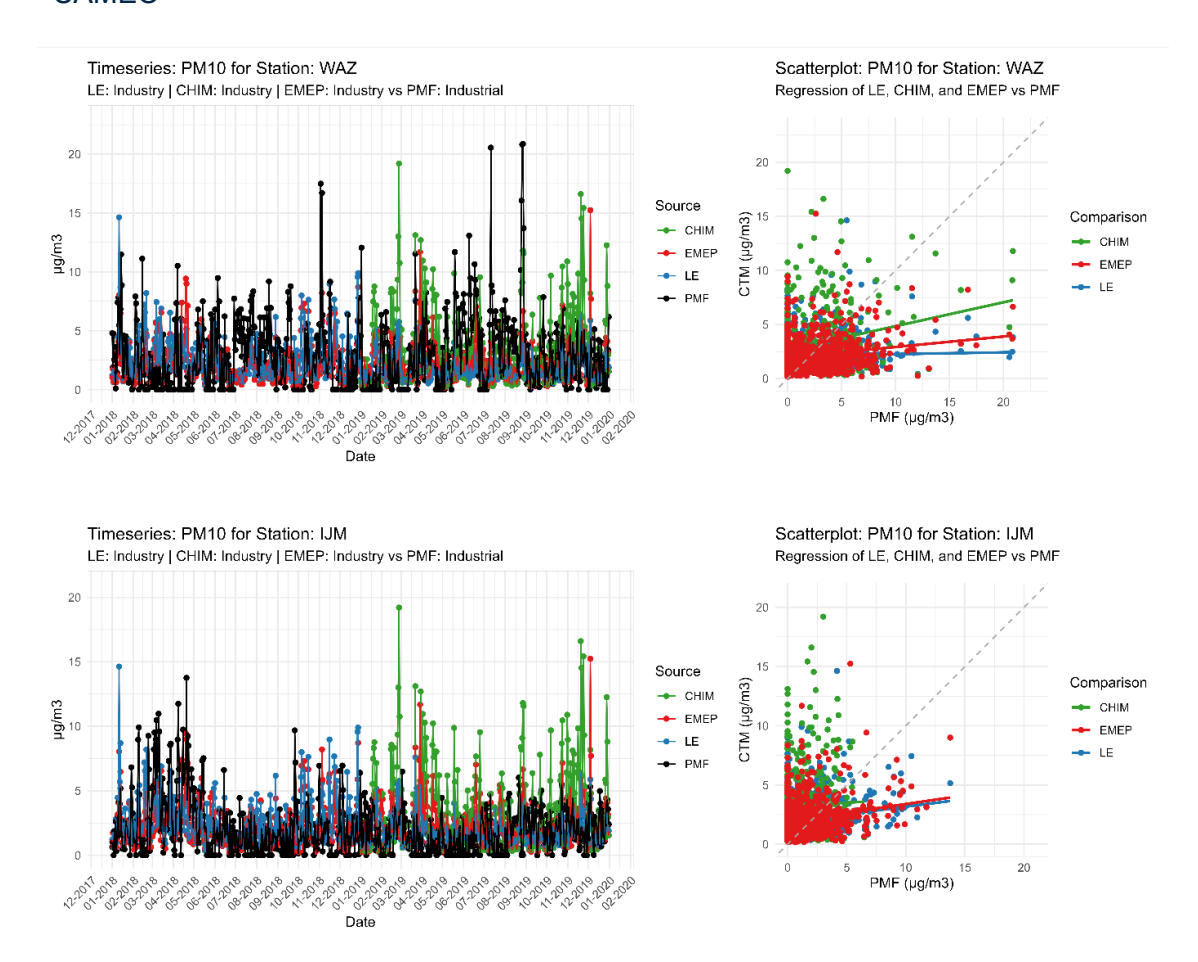


Figure 6-15 Timeseries and scatterplot of the Industrial PMF profile and Model contributions of Industry for PM_{10} at the WAZ and IJM station . Green = Chimere, red = EMEP, Blue = LOTOS-EUROS, black = observations.

6.5 Shipping

Only three stations identified a 'heavy oil (combustion)' profile: Barcelona, Montseny and Athens. These Heavy Oil profiles are frequently identified at harbor-cities and can largely be associated with shipping emissions, therefore we match the CTM labels of shipping against this profile. The profile is identified through the tracer specie of Vanadium (V) and could also be identified by making use of the daily wind directions.

For the station of Athens we observe that the annual CTM concentrations of shipping show a small relative bias in comparison to the Heavy Oil profile (Figure 6-16 top panel) (EMEP = -0,19 $\mu g/m^3$, CHIMERE = -0,77 $\mu g/m^3$ and LOTOS-EUROS = -0,18 $\mu g/m^3$), while a good temporal match is more difficult to achieve (all models, $R^2 < 0.25$). Looking at the BCN station (Figure 6-16 bottom panel) we show the period of 2018-2019, since this allows us to include all data points from the PMF analysis. Here, we observe a higher overestimation of the EMEP (bias = 3.52 $\mu g/m^3$ & NMB = 33.3%) and LOTOS-EUROS model (bias = 1.36 $\mu g/m^3$ & NMB = 11,9%)). On average, at BCN and MSY, the heavy oil profile contributed ~2.5% and 0.7% respectively to the total PM $_{10}$ concentration. In comparison we can see that the shipping contributions in EMEP (15.23% and 8.96%), LOTOS-EUROS (8.35% and 6.43%) and CHIMERE (10,1% and 7.32%) are relatively larger contributors to annual PM $_{10}$ concentrations. Looking at the Athens station, the PMF profile contribution is on average 7.4% and is more similar to the CTM shipping contributions (EMEP = 7.09% , CHIMERE = 5.98% ,LOTOS-EUROS = 5.69%).

When looking at other studies we can see that heavy oil (Shipping) contributions reported in Spain and France are slightly higher than the concentrations reported in this PMF study (annual Heavy oil concentration BCN = $0.38 \, \mu g/m^3$), however it should be noted that the measurement periods of these studies were before 2011 (Ledoux et al., 2023; Toscano, 2023; Weber et al., 2019).

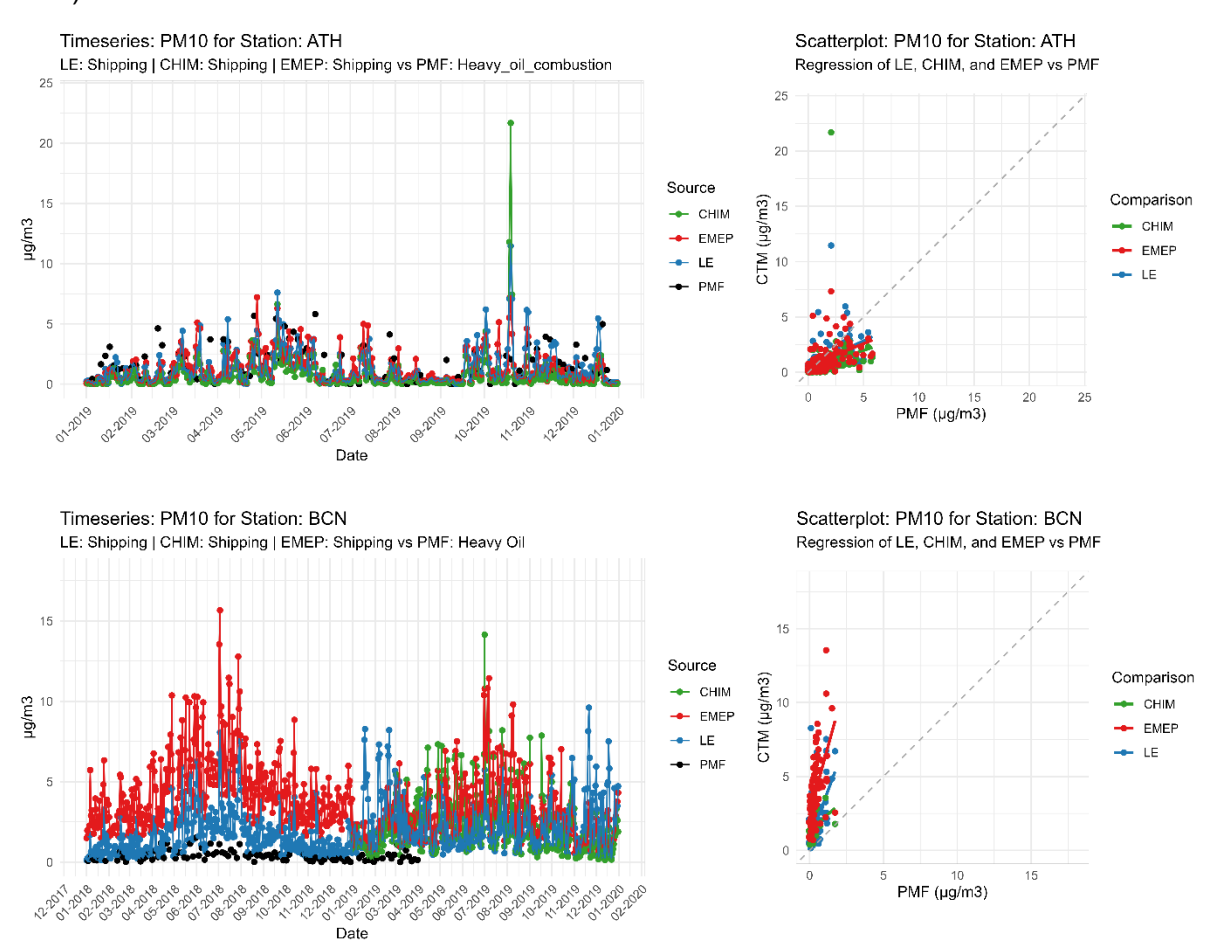


Figure 6-16 – Time series and scatterplot of the Heavy Oil combustion PMF profile and Model contributions of Shipping for PM₁₀ at the ATH (top panel) and BCN (bottom panel) station. Green = CHIMERE, red = EMEP, Blue = LOTOS-EUROS, black = observations.

Interpreting the potential uncertainty in the CAMS tools for the shipping and heavy fuel profile comparisons remains challenging with the currently limited number stations available for evaluation. Since both studies used vanadium and nickel in their PMF to identify the shipping/heavy fuel profiles the stability of the profile is relatively good. After consultation with the data providers of the BCN and MSY stations, the stability of the profile indeed seems within their expectations. Using an emission inventory containing more detailed local emission would likely improve the match with the profile in BCN. It would be useful to further investigate the impact and differences between European shipping inventories and more local inventories.

The better agreement for Athens could indicate that the European emission inventory for shipping is better represented in Athens than it is in Barcelona. Also the model resolution may play a role since it is known that the Barcelona harbour air masses do not always impact directly the measurement station (personal communication). Altogether, the poor match observed in BCN and MSY are not easy to attribute to one methodological choice in the CTM, nor to the PMF estimates. Rather, it underlines the high site (and time period)-specific variability in the CTM-PMF evaluations, making it even unfortunate that we only have three sites. Integrating additional observational data from monitoring networks, especially for certain tracers such as

V for shipping, can greatly enhance the number of stations which allows us to evaluate the temporal dynamics of the CAMS tools.

Both Nickel and Vanadium are tracers which are emitted by heavy fuel oil combustion. Appendix D shows the stations providing nickel and vanadium observations in 2019, either with a low- or high-volume sampler, sampled with filters representing a daily until an average concentration of several days.

The comparison of shipping contributions from LOTOS-EUROS against the daily (or weekly) concentrations of nickel and vanadium showed a wide range of correlations with the observations across stations (appendix D). Pearson correlations (R) ranged between 0.01 to 0.74 for vanadium and 0.00 to 0.84 for nickel, indicating poor to decent agreements depending on the site and likely its topology. Some of the stations showing very low correlations (R < 0.05), including EE0009R, NO0047R, NO0090R and FI0036R, are located Estland, Norway and Finland. These stations are located in isolated rural places with a large proportion of either the vanadium or nickel observations set below or to a detection limit. However, the FI0018R, (Figure 6-17) located relatively close to the gulf of Finland and possibly exposed to regional shipping lanes, also exhibits weak correlation with the shipping source contribution with a correlation of 0.04 for nickel and 0.20 for vanadium (N=52). Unlike some other poorly correlated stations, this station does not report any nickel or vanadium concentrations below the detection limit. While some dynamics are corresponding in the timeseries we can see that some V peaks are not overlapping with the modelled shipping contributions.

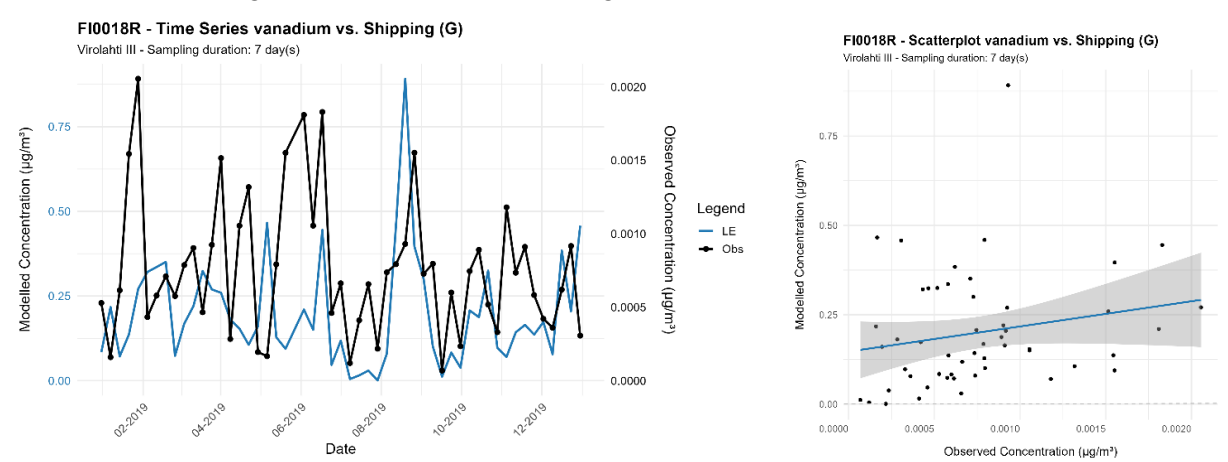


Figure 6-17 – Time series (left panel) and scatterplot (right panel) of 7 days averaged vanadium concentration against the Shipping source contribution of the LOTOS-EUROS model at the Fl0018R station. Left y-axis in time series plot shows the modelled PM_{10} concentration and the right y-axis shows the observed levoglucosan concentration.

On the other hand, we find multiple stations near coastal areas, such as DE0001R and DE0009R (Figure 6-18) that show a similar dynamics over time between modelled shipping contributions and Vanadium, again based on a 7 day averaged sample.

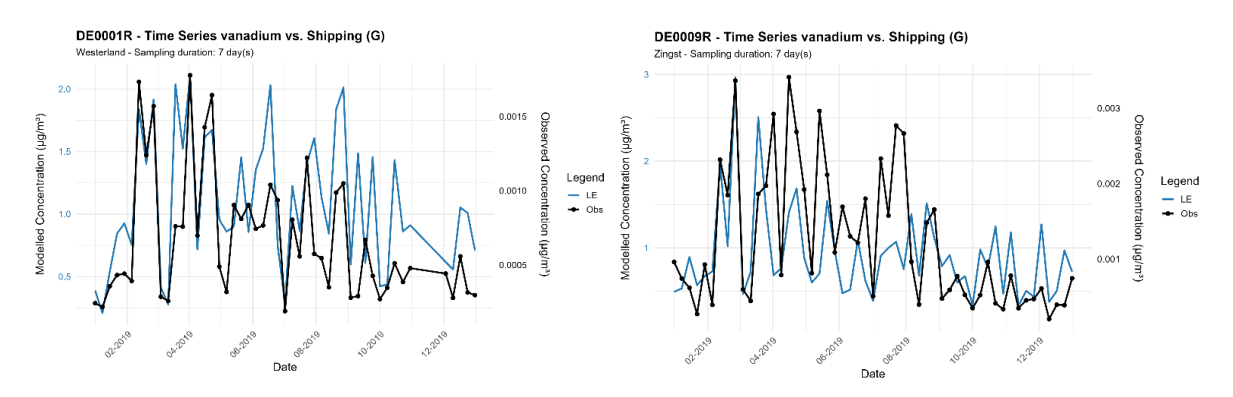


Figure 6-18 Timeseries of 7 days averaged vanadium concentration against the Shipping source contribution of the LOTOS-EUROS model at the DE0001R and DE0009R stations. Left y-axis shows the modelled PM_{10} concentration and the right y-axis shows the observed levoglucosan concentration.

6.6 Sea salt

The majority of stations identify a single sea salt profile (e.g. 'sea salt'), identified through large contributions from CL⁻, Na⁺, but also Mg²⁺. There are several stations that identify two factors per station, separating between a fresh (primary emitted) and 'aged' counterpart in which secondary formed aerosols or contaminations from other sources are present (Tab 6-3). Moreover, the resuspension of salt particles present on road surfaces could cause the coemission of salt, mineral dust and traffic tire/brake wear particles. This could especially be the case for stations where salt is used against road icing, but previously deposited sea salt particles in warmer areas could also be subject to resuspension. As a result, PMF profiles can contain an aggregate of particles from these sources and are subsequently identified as such (e.g. STG – Road and Sea Salt).

For the stations that identified multiple PMF factors containing the majority of seasalt species (GRT, STG, and the stations in Melpitz), we decided to aggregate them into a single Sea Salt profile, making the comparison with the seasalt species in the CTM models more straightforward. Table 6-2 shows the PMF profiles that are compared against all seasalt species within the CTM models.

Table 6-2 - Overview of PMF factors identified and compared against CTM source

Station	PMF Factor Identified	Compared against CTM species:
ATH	Sea Salt	Total seasalt in the
BCN & MSY	Sea Spray	models including all labels
BERN / MGD / PAY/ ZRCH/BSL	Aged Sea Salt	
IJM / BVW / WAZ	Sea salt	
GRT / STG	'Road and Sea salt' & 'Aged Road and Sea Salt'	
Melpitz stations	'Salt (Fresh)' & 'Salt (aged)'	

The GRT, STG and Melpitz stations all showed that there was a good temporal correlation between sea salt species in the CTM models and the combined mass of the aged and fresh salt profiles (Figure 6-19). It is interesting to note that the aged sea salt profiles described at the locations in Melpitz do find a satisfactory fit with seasalt of the CTM models while also being a mixture of both anthropogenic and natural sources. The '(fresh) salt' profile in Melpitz

contributes on average 1% to the total PM_{10} , whereas the '(aged) Salt' contributes 10.4%. A possible explanation for this observation is the relatively small contribution of the anthropogenic sources to the aged sea salt mass in Melpitz (rural stations), while the contribution in the Swiss stations is more substantial.

Moreover, the observed bias at the particular stations was relatively low: EMEP and CHIMERE often slightly underestimating PM_{10} concentrations, while LOTOS-EUROS tended to overestimate the observed PM_{10} concentration. The tendency of LOTOS-EUROS to simulate higher seasalt concentrations then EMEP and CHIMERE is partly discussed in section 4. This leads to larger overestimations for LE in the stations of ATH, MSY and in particular all three Dutch stations.

In contrast to the good fit of the stations located in Germany, all five stations in Switzerland show very poor temporal correlation ($R^2 < 0.2$) as can be seen in the example for MGD (Figure 6-20). Grange et al. (2021) mention that their aged sea salt profile contained contributions from metals, indicating that the profile was probably influenced by anthropogenic (traffic) emissions or resuspension of dust, containing metals. This could partly explain the poor fit for these stations with sea salt species in the CTM models.



Figure 6-19 Metrics of the daily modelled Seasalt concentrations compared to PM $_{10}$ concentration equal to the (fresh) and (aged) seasalt PMF factors for the year 2019. Bias ($\mu g/m^3$), RMSE and temporal correlation (R^2). Green = CHIMERE , Red = EMEP, Blue = LOTOS

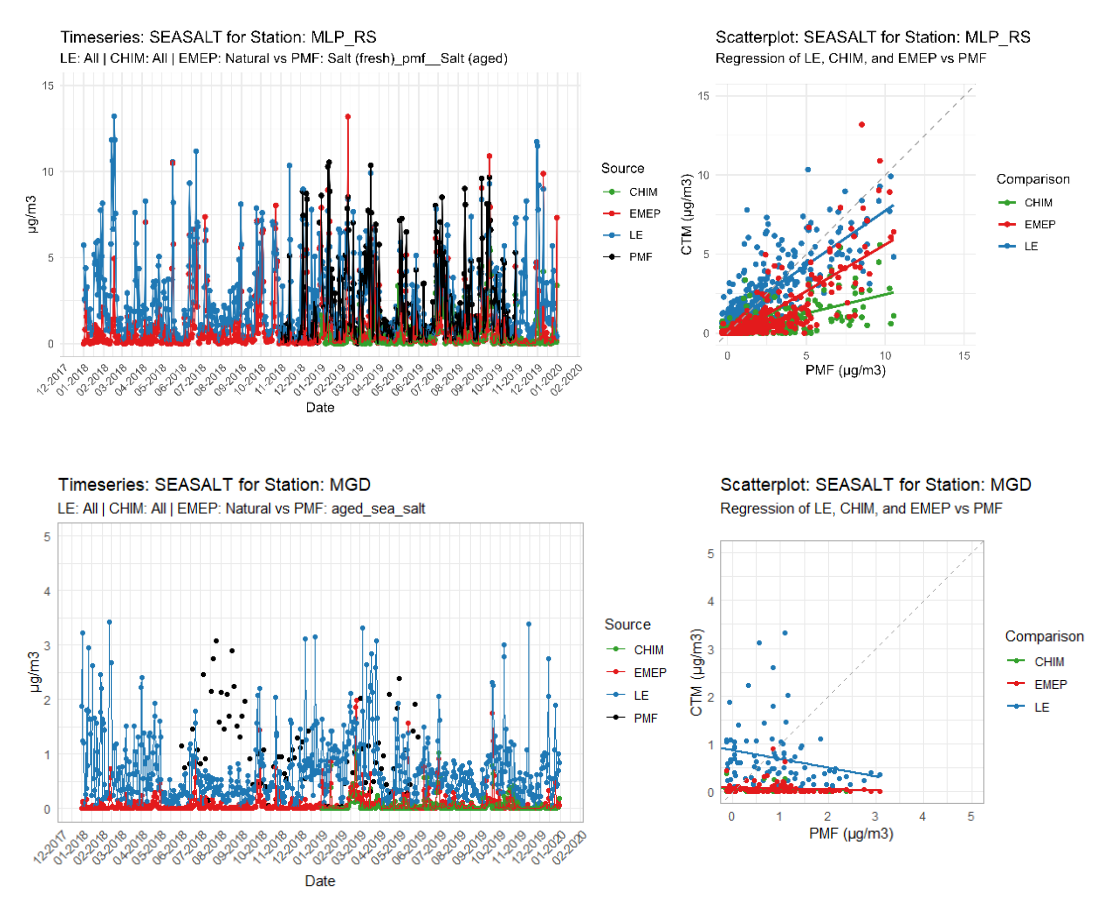


Figure 6-20 Timeseries and scatterplot of (fresh) and (aged) Seasalt PMF profile and Model contributions seasalt at the MLP_RS station (top panel) and MGD station (bottom panel). Green = Chimere, red = EMEP, Blue = LOTOS-EUROS, black = observations.

6.7 (Mineral) dust

Table 6-3 shows an overview of the stations containing profiles that correspond to mineral dust. In general, mineral dust profiles are identified by species like Al, Mg, V, Ti, Ca²⁺, Na (Glojek et al., 2024; Grange et al., 2021; in 't Veld et al., 2023; Mooibroek et al., 2022; van Pinxteren et al., 2024). PMF profiles containing (mineral) dust contributions obtain these species from longterm transport mineral dust, blown-up dust from local sources (e.g. due to agricultural activities) or from resuspension of dust particles from roadsides by traffic induced turbulence or wind. In the latter case, species from previously emitted sources could be mixed with the tracer species for mineral dust. A similar discussion as the 'Aged seasalt' mixtures could be held about the definition of the profiles regarding mineral dust. As seen in Table 6-3, only a limited number of stations identifies a 'clear' (mineral) dust profile, while stations as GRT and STG found tracer species to be present within their traffic or resuspension profiles, rather than finding a clear profile. Moreover, the stations of IJM and BVW found both a 'road dust or traffic' profile as well as a 'Crustal matter' profile. As previously mentioned, Mooibroek et al. (2022) point out that the mineral dust in the region is likely mixed with other sources, either from the metal industry activities therefore naming one profile; road dust or traffic, while the crustal matter profile contains, next to the Al, Ca, Si, Ti and Li, high levels of Na that could be derived from sea salt particles. To make matters more complex, material used in steel production can contain elements that are similar to crustal material (Al, Si, Ti) and were also identified within the industry profile of the station. As an initial comparison we decided to compare the Crustal matter profile of this station with all the mineral dust present in the CTM models. In the CTM models, the vast majority of the dust species is emitted from Saharan dust events in outer boundary areas. Dust particles from agricultural activities or resuspension is limitedly available in the models. For the LOTOS-EUROS and EMEP models dust emissions are strictly attributed

to the natural, boundary and Saharan dust sectors. In the CHIMERE model the vast majority is also allocated to the natural emissions or long-range transport influx sectors, however a small contribution of dust is allocated to other sectors (on average 3% of all dust). This may be explained by the influence of changes in other particle concentrations on the size distribution and concentrations of dust

Table 6-3 Overview comparison PMF factors identified per station against total dust present in the model.

Station	PMF Factor Identified	Compared to CTM
ATH	Soil dust	All dust components in
BCN & MSY	Mineral	models; of which main
BERN / MGD / PAY/ ZRCH/ BSL	Mineral Dust	contributors are : boundary
IJM / BVW / WAZ	Crustal Matter	influx, Saharan sand

Figure 6-21 provides an overview of the Bias and R^2 for each station. It is not surprising that the station of Athens, closest located to the Saharan region, shows a good fit and overlapping peaks that correspond to Saharan dust influx events (LOTOS-EUROS $R^2 = 0.63$, EMEP $R^2 = 0.60$, CHIMERE $R^2 = 0.43$, Figure 6-22 top panel). We do see that the EMEP and LOTOS-EUROS model, and to a lesser extent CHIMERE, calculate high dust peak concentrations that are not observed in the PMF profile, while in between the peak periods of the models underestimate the (more local) mineral dust profile concentrations. This pattern is similar at all other stations, where sharp peaks (influx Saharan or boundary dust) in the models fall close to zero afterwards. Overall this results in an observation that the bias of almost all comparisons shows to be negative, implying an underestimation of the CTMs (Figure 6-21).

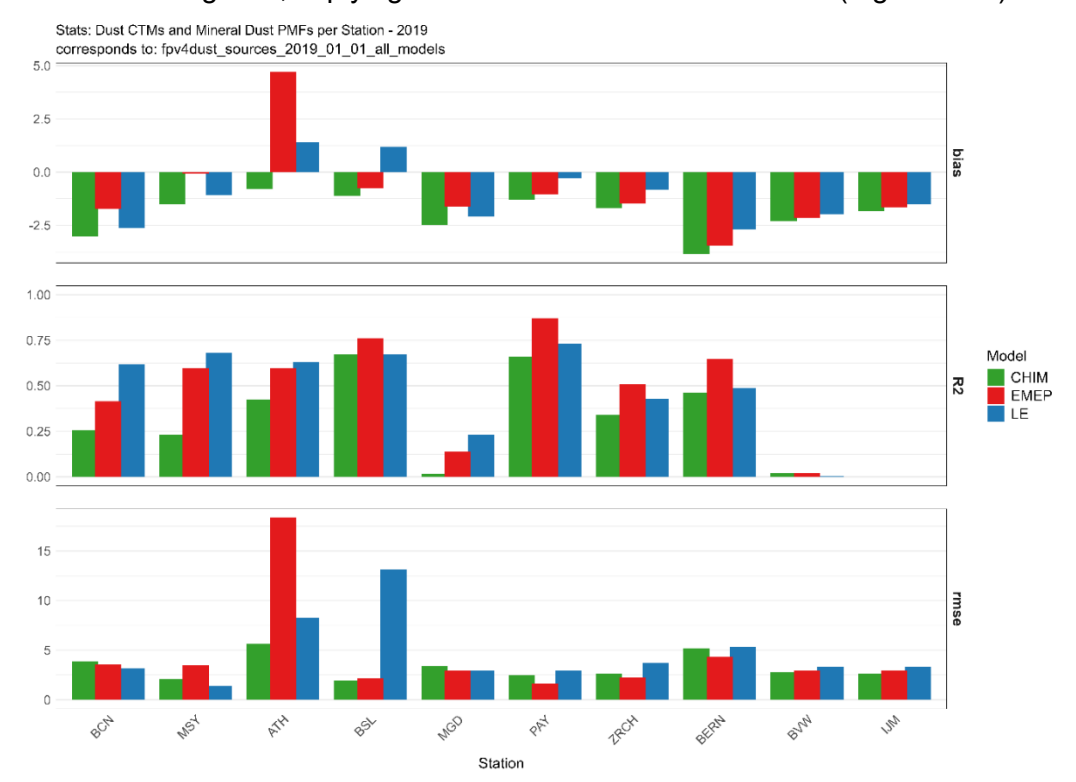


Figure 6-21 Metrics of the daily modelled dust concentrations compared to PM₁₀ concentration equal to the (mineral) dust PMF factors (Table 6-3) for the year 2019. Bias (μ g/m³), temporal correlation (R²) and RMSE. Green = CHIMERE, Red = EMEP, Blue = LOTOS-EUROS.

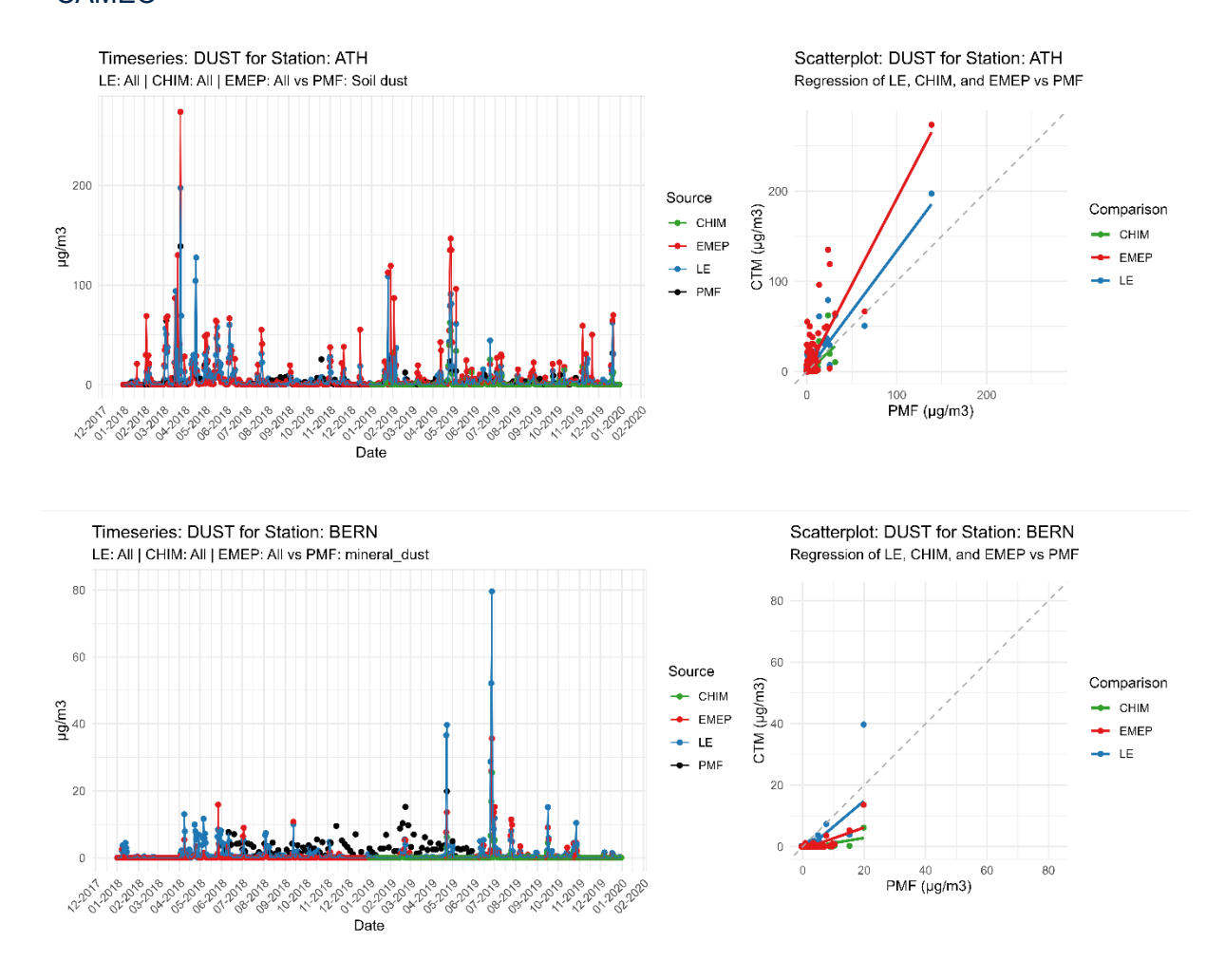


Figure 6-22 Time series and scatterplot of Soil Dust PMF profile and Model contributions of dust at the ATH (top panel) and BERN (bottom panel) station. Green = CHIMERE, red = EMEP, Blue = LOTOS-EUROS, black = observations.

The crustal matter profiles located in IJM and BVW show a particularly bad fit with the natural dust species. Which is in line with the possibility that the crustal matter profile, in addition to the industry and road dust profiles of these locations are contaminated with one and another's sources. The high volumes of coal and iron transport at the steel facility possibly contributing to crustal matter profile could explain the consistently low levels of the CTMs.

6.8 Nitrate-rich & Sulfate-rich

Across multiple locations (all except the stations in the Netherlands), PMF consistently identifies Nitrate-rich profiles characterized by high concentrations of ammonium and nitrate, often accompanied by smaller amounts of sulfate. These profiles represent the presence of secondary inorganic aerosol (SIA) formed in the atmosphere through chemical reactions of precursor gases such as NO_x and NH_3 . Additionally, Sulfate-rich profiles, identified at the stations in Barcelona, Montseny, Switzerland and Germany, consist of high concentrations of sulfate and ammonium. Depending on the station (e.g. Melpitz) the sulfate-rich profile contributes substantially to the OC concentrations which is likely due to secondary organic aerosol formation (van Pinxteren et al., 2024). At some stations, such as Milan and Melpitz, this is reflected in the definition of the profile (e.g. 'Sulfate and SOA-rich').

Table 6-4 - The average percentage of the total measured concentration of: ammonium, nitrate, sulfate and organic carbon aerosols included in the nitrate-rich and sulfate-rich PMF profiles. These values are based on the stations (N=12) where these profiles were identified with PMF.

	Nitrate-rich profile NH ₄ NO ₃ SO ₄ OC				Sulfate-rich profile			
					NH ₄	NO ₃	SO ₄	ОС
Average	54%	71%	15%	4%	41%	0%	60%	25%
min	32%	64%	0%	0%	28%	0%	51%	7%
max	63%	80%	23%	18%	68%	2%	70%	47%

Unfortunately, these nitrate- and sulfate-rich profiles do not contain specific information on the primary sources contributing to their profiles. The CTM models attribute the nitrate, sulfate and ammonium concentrations to the sources of their gaseous precursors, i.e. ammonia (NH_3), nitrate-oxides (NO_x) and sulfur dioxide (SO_2) (mainly agricultural, traffic and combustion-related sectors).

To be able to compare the PMF contributions with contributions simulated by the CTMs, we looked at the Nitrate-rich and Sulfate-rich profiles of all stations and determined how much of the total SIA and OC concentrations at that station ended up in these secondary profiles. For example, for the STG station, 60% of the observed ammonium was attributed to the nitrate-rich profile. By averaging these contributions across all relevant stations, we derived a generalized profile representing the nitrate-rich and sulfate-rich profiles. This method estimated that, on average, the nitrate-rich profile contained approximately 54%, 71% and 15% of all ammonium, nitrate and sulfate concentrations, respectively (Table 6-4). For the Sulfate-rich profile, this was 41% of ammonium, 60% of sulfate and 25% of OC. For the stations in the Netherlands (BVW, IJM, WAZ) a single combined 'Nitrate- and Sulfate' profile was identified, containing on approx. >95% of ammonium, 75% of Nitrate and 40% of sulfate.

In most cases, the majority of secondary inorganic aerosols are captured in the Nitrate- and Sulfate rich profiles, but the origin of its precursors remains unclear. Depending on the site, PMF indicates some SIA contributions in other 'primary' or 'secondary' profiles. Conversely, we find some components (e.g. organics) included in these secondary profiles, believed to be caused by the mixing of some profiles, indicating that a general approach for matching these nitrate-rich and sulfate-rich profiles is a challenge. Although probably large variability is present between sites, we attempted to find such a suitable, generalizable, match between PMF profile and CTM sectors. We matched the Nitrate-rich and Sulfate-rich mass of each site against the aggregated concentration of all SIA species present in the CTM models, whereby we selected the proportion of the species contributing to the profiles (Table 6-4). Initially we disregarded the OC contribution, after which we later on added the SOA species of EMEP and CHIMERE models (missing in LOTOS-EUROS) to the evaluation to see if the comparison would improve for the Sulfate-rich profiles for the stations of MLP_RS, MLP_VIL, GRT and STG.

It should be noted that this approach closely resembles a conventional comparison between observed pollutant concentrations and modelled SIA species, without accounting for the specific PMF-derived source contributions. Which could be more informative than this indirect comparison between profiles and sources.

Figure 6-23 and 6-24 shows the results of the comparison against the nitrate-rich and sulfate-rich profile respectively.

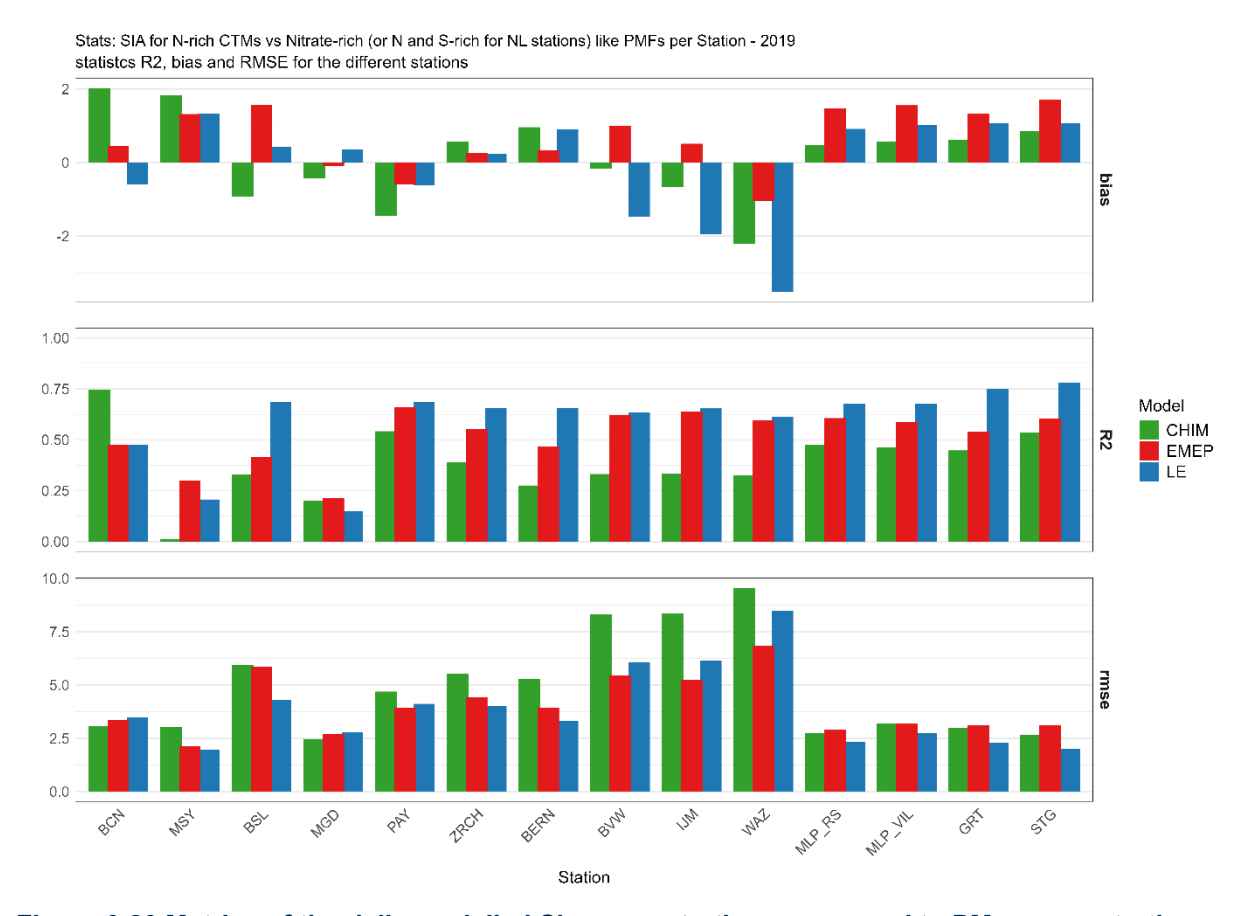


Figure 6-23 Metrics of the daily modelled Sia concentrations compared to PM_{10} concentration equal to the Nitrate-rich PMF factors (Table 6-4) for the year 2019. Bias ($\mu g/m^3$), temporal correlation (R^2) and RMSE. Green = CHIMERE, Red = EMEP, Blue = LOTOS-EUROS.

That being said, the PMF Nitrate-rich contributions showed a reasonably good agreement for all stations were more than the start of 2019 could be compared (BVW, IJM, WAZ, MLP, GRT and STG) with the SIA components in the CTMs LOTOS-EUROS (mean $R^2 = 0.68$, range = 0.61 - 0.78) and EMEP ($R^2 = 0.60$, range = 0.54-0.63), and CHIMERE also performed reasonable for these stations ($R^2 = 0.48$, range = 0.45 - 0.54). The dynamics of winter months in Switzerland and MSY were less well captured for CHIMERE.

On average, EMEP overestimated the contributions to nitrate-rich the most (bias = $1.52 \,\mu g/m^3$), whereas CHIMERE (bias = $0.63 \,\mu g/m^3$) and Lotos-Euros (bias = $1.01 \,\mu g/m^3$) do this to a lesser extent.

Looking at the Dutch stations, in which a single nitrate-sulfate profile was identified and the subsequent concentration of SIA from the CTM models was in accordance to the PMF profiles the CTMs matched well with respect to temporal variability for Lotos-Euros (R^2 = 0.63) and EMEP (R^2 = 0.62), while here CHIMERE shows only moderate correlation (R^2 = 0.33). A consistent underestimation from Lotos-Euros (bias= 2.31 µg/m³) and CHIMERE(bias CHIMERE= -1.01 µg/m³), while EMEP on average showed a slight overestimation (bias = 0.15 µg/m³).

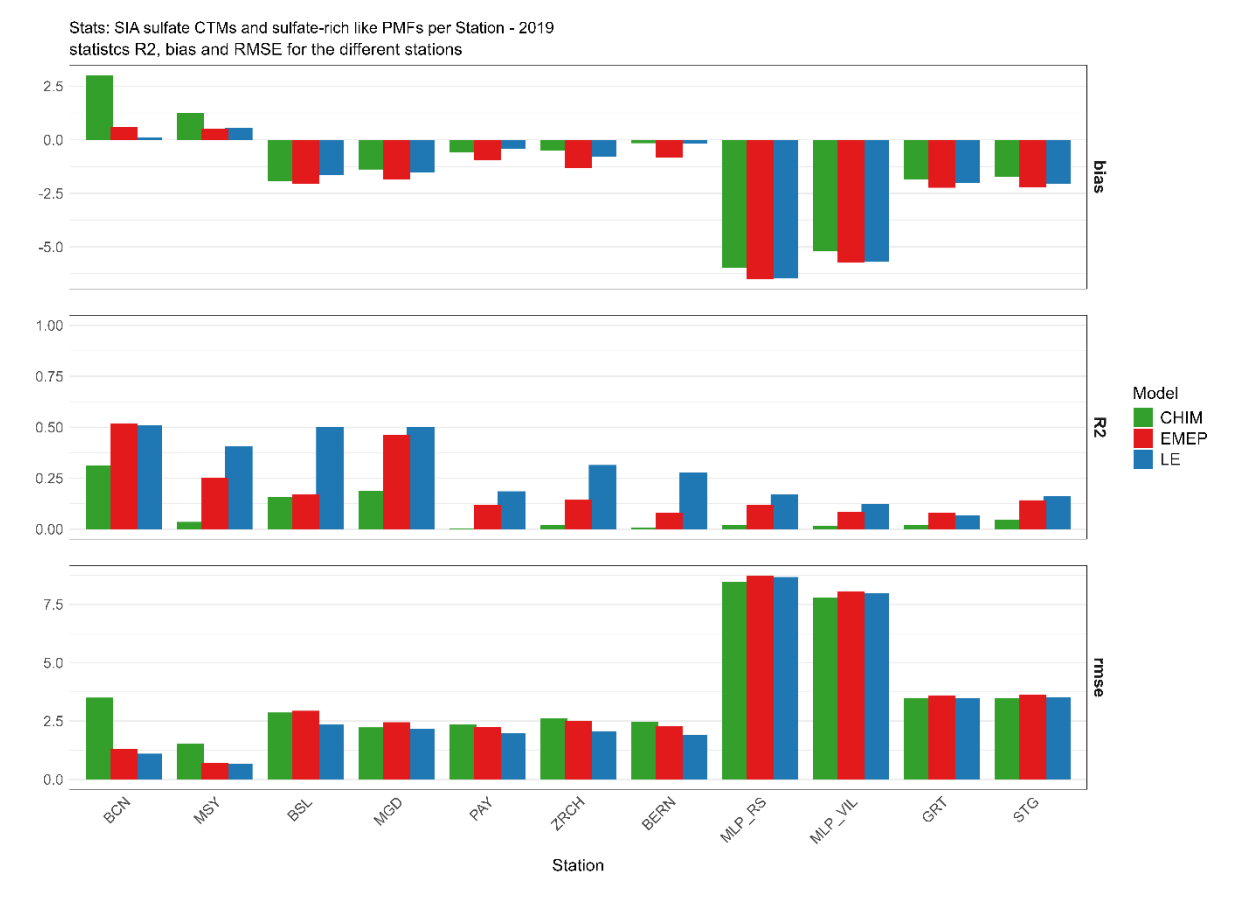


Figure 6-24 Metrics of the daily modelled Sia concentrations compared to PM₁₀ concentration equal to the Sulfate-rich PMF factors (Table 6-4) for the year 2019. Bias ($\mu g/m^3$), temporal correlation (R²) and RMSE. Green = CHIMERE, Red = EMEP, Blue = LOTOS-EUROS.

For the sulfate-rich comparison we can observe a poorer temporal fit then the Nitrate-rich comparisons (LOTOS-EUROS R²= 0.27, EMEP R² = 0.19, CHIMERE R² = 0.07) for all stations and an underestimation for all stations, except for BCN and MSY. This is not entirely surprising for a number of stations that explicitly discuss the possibility of SOA components that are integrated into their sulfate-rich like profiles, which is also shown in Table 6-4. When adding the SOA from the EMEP and CHIMERE models in the comparison against the Sulfate/SOA-rich profiles of the MLP_RS, MLP_VIL, GRT and STG stations the average bias for these four locations improved from -4.17 to -3.05 $\mu g/m^3$ (EMEP) and from -3.69 to -2.65 $\mu g/m^3$ (CHIMERE), while the temporal resolution clearly improved for EMEP (from 0.11 to 0.47) and for CHIMERE (from 0.03 to 0.26) due to increased concentrations during the summer period which overlaps with the higher SOA formation in this period.

7 Conclusions and recommendations

In this work we have evaluated the consistency and comparability of modelled particulate matter (PM) source sector contributions from different modelling systems applied within the CAMS policy service. We have disentangled the differences due to the use of distinct chemical transport models and differences due to the use of various source attribution methods. In addition, we have evaluated the modelled PM source sector contributions with observational based source attribution using Positive Matrix Factorisation (PMF) and specific source tracers such as levoglucosan (a marker of wood combustion).

All models and their source attribution methods agree on the residential (biomass) combustion emission of primary pollutants as the major anthropogenic source around the Mediterranean except for some cities influenced by volcanic emissions. Residential combustion is also identified as the major source in Eastern Europe by LOTOS-EUROS and EMEP. The relative contribution is shown to grow with increasing PM concentrations. This source which is mainly contributing to primary PM is not much influenced by non-linear effects and therefore by the source attribution methods used. Contrarily we see considerable differences between the CTM's used due to differences in surface layer height and mixing parametrisations. The CTM contributions generally correspond well with the PMF data, providing confidence in the modelled CTM contributions and underlying emissions, although for some sites the general approach for spatial attribution of residential wood combustion emissions in CAMS-REG seems inappropriate (e.g. Barcelona) and requires refinements. This also indicates that the dominance of this source modelled around the Mediterranean may be overestimated. For eastern Europe no PMF datasets were available preventing the evaluation of the reliability of this source being the dominant in that region. The relatively high certainty in identifying biomass combustion through PMF—thanks to well-defined tracers in observations-makes PMF data for this sector a strong candidate for inclusion in routine evaluation exercises within CAMS.

The CHIMERE model with its source attribution based on a surrogate model identifies agriculture as the main anthropogenic source of PM in a wide area in Central Europe and around the Baltic sea while EMEP and LOTOS-EUROS suggest a mixture of industrial and agricultural sources to be dominant around the Benelux and Germany. The relative impact of agriculture decreases for highest PM concentrations. This source which is mainly contributing to the formation of ammonium nitrate is highly influenced by non-linear effects and shows larger differences between the source attribution methods especially on daily timescales. But also differences in model descriptions influencing secondary PM formation led to differences in the source attribution results. On an annual scale the differences in secondary PM due to source attribution method is within the same range as differences due to the CTM.

Since the models overestimate nitrate concentrations a proper evaluation of the contributions for this source is worthwhile. Unfortunately, within the PMF data the agricultural source contributions are included within broader secondary source profiles (mainly the nitrate-rich profile) preventing a direct evaluation.

The larger agricultural contributions in CHIMERE are linked to high negative interaction terms between several sources. To avoid large interaction terms which are difficult to interpret by users and to better represent the actual contribution of agriculture to PM a redistribution of the interaction terms to the relevant sources is deemed worthwhile and is currently being investigated by the CHIMERE team.

Traffic has only been identified in Bern, Zürich and Munich as the major anthropogenic source of PM pollution and only by brute force based methods with 15% emission reductions. The tagging and surrogate model with 100% emission reduction do not identify any locations with

traffic as dominant source indicating that while traffic may not be the dominant contributor, considering 15% emission reductions may be most efficient when applied to traffic. This further highlights the complementarity between tagging and brute force based methods. The comparison with PMF data in Bern and Zürich shows lower contributions by the CTMs than from the PMF (except for CHIMERE in Zürich). Low correlations over all sites indicate that the CTM and PMF models are having difficulty in representing this highly spatially and temporally variable source, in a time consistent way. This is partly related to the mixing of other combustion sources and dust resuspension within the PMF traffic source. The model resolution may be the main reason that this source is underrepresented as a relevant source by the models. To improve modelled traffic contributions for locally influenced locations an increase in spatial resolution is recommended and the use of local emission information. An investigation of the added value of increased model resolution using u-EMEP is undertaken and will be presented in D6.2. The separation of total traffic contributions into subsectoral contributions is recommended as it allows better evaluation with observational data and identification of ways for improving the model results. Several PMF stations identified a traffic resuspension profile, but this component was not included in the three CTMs used in this study. The CAMAERA project is addressing this gap by developing gridded hourly non-exhaust emission inventories to support improved modelling of this important source.

The EMEP and LOTOS-EUROS models identify **industry** as the dominant anthropogenic source sector for several cities in Germany and across or close to the Iberian Peninsula. For this source we see considerable differences between the CTM models connected to the altitude at which these emissions are inserted into the models. But this source is also involved in the formation of secondary aerosols and thereby shows some differences due to the attribution method. Evaluation of this source with PMF is hampered by the low number of sites identifying an industrial source profile and the variety of industrial sources and composition of their emissions.

Shipping is identified by some models/methods as the dominant anthropogenic source for some sites around the Mediterranean close to shipping routes or large harbours. Also, here the emission altitude and mixing parametrisations may play a role in the difference seen between models. Evaluation with PMF data is challenging due to the limited number of stations providing a heavy fuel oil PMF source, although this source can often decently be captured by tracers as nickel / vanadium. The performance is good for Athens but worse for Barcelona, possibly hinting to uncertainties in the emission data.

While we did not put a lot of focus to the **natural** contributions in this study, these contributions are very relevant with respect to the allowed subtraction of these contributions from PM exceedances of limit values in the reporting by EU Member States. Furthermore, the EMEP model identifies these natural sources as the main contributor to PM2.5 above 50 µg/m³, although comparisons with PMF dust contributions in Athens show that EMEP may be overestimating dust in the mediterranean region. Because of the primary nature of natural contributions, we do not see differences between the source attribution methods. However, differences between the CTMs are considerable related to the difficulty in correctly representing the relevant processes (online emission, deposition and transport). LOTOS-EUROS is showing largest and overestimated sea salt contributions. Comparison with PMF sea salt and especially dust data provide a valuable tool to extend common model evaluation and identify areas for improvements. Although it would be valuable to consider such evaluations in CAMS2_83, PMF datasets are scarcely available and usually provided with large time delays.

At present, the **CAMS Policy Support Service** separates the source attribution into different products based on the different methods: potential impact of emission reductions (BF, done with the EMEP model for spatial allocation, and ACT/CHIMERE for sectoral allocation) and contribution (tagging, done with LOTOS-EUROS for spatial allocation and within the next

phase also for sectoral allocation). The present study demonstrates that integrating the three modeling systems into a mini-ensemble is methodologically sound when assessing annual mean or primary PM contributions. However, for daily or even hourly attribution of secondary PM it is important to consider the purpose of the chosen source attribution method, i.e. tagging for the provision of source contributions and brute force based approaches for the provision of potential impacts of emission reductions, and use the methods in a complementary way.

For future evolutions of the service the local fraction is considered as an efficient substitute for the brute force method within the EMEP model. The comparisons in this work shows that in most cases the differences between those methods is small and such a replacement is justified.

The **evaluation** of CTM source contributions with PMF data proved challenging due to the distinct characteristics of each PMF dataset depending also on user settings (identifying the need for harmonisation of PMF applications) and the difficulty to resolve source sectors into singular profiles. Such an evaluation requires thorough analysis of the PMF profiles to identify its potential match with CTM sources. Furthermore, uncertainties surrounding the PMF profiles make it difficult to pinpoint whether the CTM or PMF contribution, or both, require improvements. Moreover, the difference spatial representation between the CTMs (area average) and the sampling stations remains a challenge. This, together with delays in availability of the PMF analysis, prevents its inclusion in automatic CAMS evaluation processes. Here, alternatives to total PM source evaluation should be considered such as evaluation of EC from biomass and fossil fuels with near real time source contributions from aethalometer data as demonstrated in the RI-Urbans project. Another complementary option is the use of tracer data from monitoring networks to evaluate the CTM spatial-temporal concentration dynamics for certain sources.

For offline evaluation however such comparisons can be used to gain confidence in models and used emission input, but also provides useful information on missing/underestimated/ overestimated sources.

References

- Amato, F., van Drooge, B. L., Jaffrezo, J. L., Favez, O., Colombi, C., Cuccia, E., Reche, C., Ippolito, F., Ridolfo, S., Lara, R., Uzu, G., Ngoc, T. V.D., Dominutti, P., Darfeuil, S., Albinet, A., Srivastava, D., Karanasiou, A., Lanzani, G., Alastuey, A., & Querol, X. (2024). Aerosol source apportionment uncertainty linked to the choice of input chemical components. *Environment International*, *184*. https://doi.org/10.1016/j.envint.2024.108441
- Belis, C. A., Pirovano, G., Villani, M. G., Calori, G., Pepe, N., & Putaud, J. P. (2021). Comparison of source apportionment approaches and analysis of non-linearity in a real case model application. *Geoscientific Model Development*, *14*(7), 4731–4750. https://doi.org/10.5194/GMD-14-4731-2021
- Bhattarai, H., Saikawa, E., Wan, X., Zhu, H., Ram, K., Gao, S., Kang, S., Zhang, Q., Zhang, Y., Wu, G., Wang, X., Kawamura, K., Fu, P., & Cong, Z. (2019). Levoglucosan as a tracer of biomass burning: Recent progress and perspectives. *Atmospheric Research*, 220, 20–33. https://doi.org/10.1016/J.ATMOSRES.2019.01.004
- Borlaza, L. J., Weber, S., Marsal, A., Uzu, G., Jacob, V., Besombes, J. L., Chatain, M., Conil, S., & Jaffrezo, J. L. (2022). Nine-year trends of PM10sources and oxidative potential in a rural background site in France. *Atmospheric Chemistry and Physics*, 22(13), 8701–8723. https://doi.org/10.5194/acp-22-8701-2022
- Brown, S. G., Eberly, S., Paatero, P., & Norris, G. A. (2015). Methods for estimating uncertainty in PMF solutions: Examples with ambient air and water quality data and guidance on reporting PMF results. *Science of the Total Environment*, *518–519*, 626–635. https://doi.org/10.1016/j.scitotenv.2015.01.022
- Clappier, A., Thunis, P., Pirovano, G., Riffault, V., & Gilardoni, S. (2022). Source apportionment to support air quality management practices A fitness-for-purpose guide (No. EUR 31222 EN). JRC, Publications Office of the European Union, Luxembourg. https://doi.org/10.2760/781626
- Clappier, A., Belis, C. A., Pernigotti, D., & Thunis, P. (2017). Source apportionment and sensitivity analysis: Two methodologies with two different purposes. *Geoscientific Model Development*, 10(11), 4245–4256. https://doi.org/10.5194/GMD-10-4245-2017
- Colette, A., Rouïl, L., Meleux, F., Lemaire, V., & Raux, B. (2022). Air Control Toolbox (ACT_v1.0): A flexible surrogate model to explore mitigation scenarios in air quality forecasts. *Geoscientific Model Development*, 15(4), 1441–1465. https://doi.org/10.5194/GMD-15-1441-2022
- Couvidat, F., Lugon, L., Messina, P., Sartelet, K., & Colette, A. (2025). Optimizing computation time in 3D air quality models by using aerosol superbins within a sectional size distribution approach: Application to the CHIMERE model. *Journal of Aerosol Science*, *187*, 106572. https://doi.org/10.1016/J.JAEROSCI.2025.106572
- Diapouli, E., Kalogridis, A. C., Markantonaki, C., Vratolis, S., Fetfatzis, P., Colombi, C., & Eleftheriadis, K. (2017). Annual variability of black carbon concentrations originating from biomass and fossil fuel combustion for the suburban aerosol in Athens, Greece. *Atmosphere*, *8*(12). https://doi.org/10.3390/atmos8120234
- Directive (EU) 2024/2881 of the European Parliament and of the Council of 23 October 2024 on ambient air quality and cleaner air for Europe (recast), 2881 (2024).
- Flemming, J., Huijnen, V., Arteta, J., Bechtold, P., Beljaars, A., Blechschmidt, A. M., Diamantakis, M., Engelen, R. J., Gaudel, A., Inness, A., Jones, L., Josse, B., Katragkou, E., Marecal, V., Peuch, V. H., Richter, A., Schultz, M. G., Stein, O., & Tsikerdekis, A. (2015). Tropospheric chemistry in the integrated forecasting system of ECMWF. *Geoscientific Model Development*, 8(4), 975–1003. https://doi.org/10.5194/GMD-8-975-

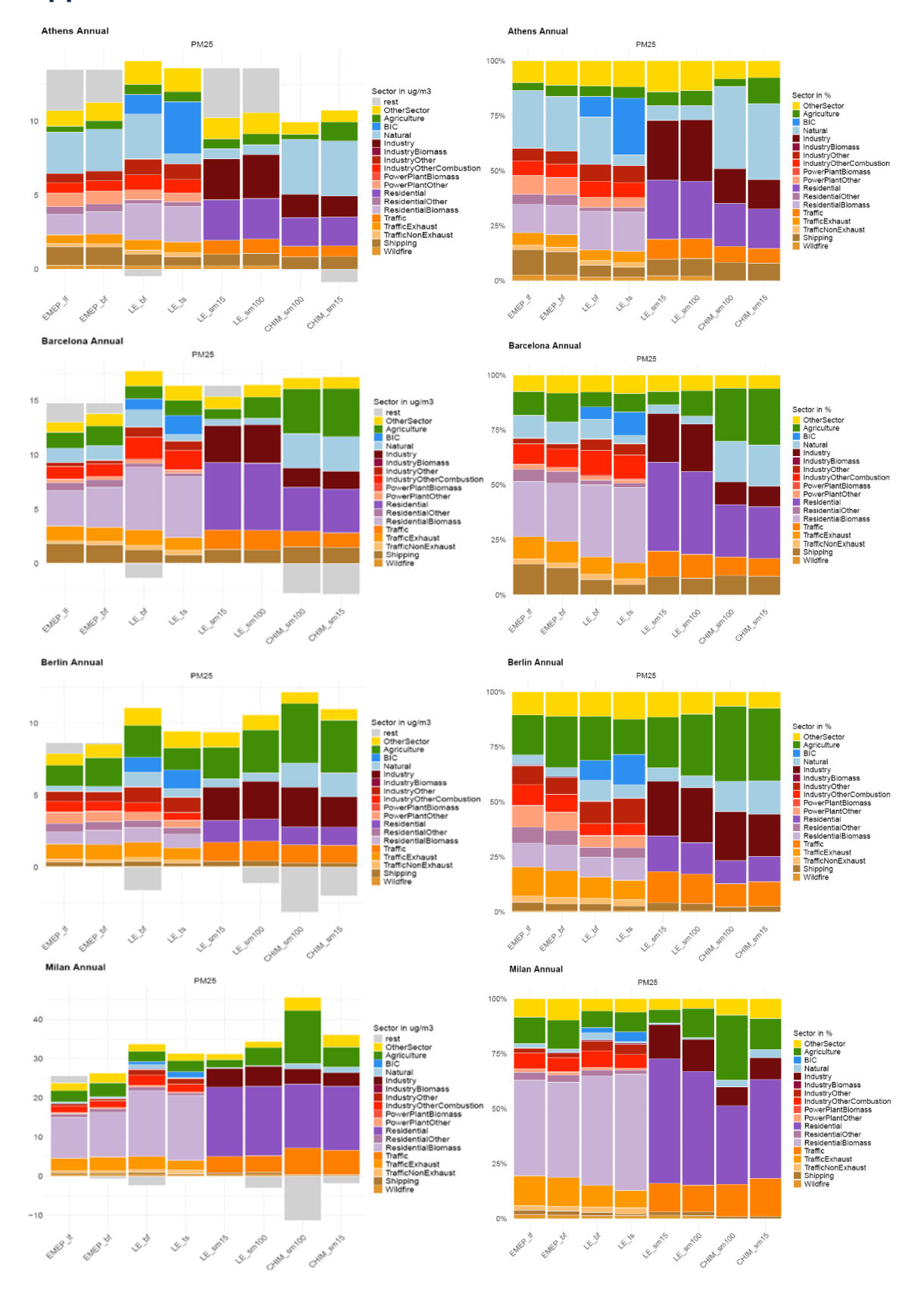
2015

- Glojek, K., Dinh Ngoc Thuy, V., Weber, S., Uzu, G., Manousakas, M., Elazzouzi, R., Džepina, K., Darfeuil, S., Ginot, P., Jaffrezo, J. L., Žabkar, R., Turšič, J., Podkoritnik, A., & Močnik, G. (2024). Annual variation of source contributions to PM10 and oxidative potential in a mountainous area with traffic, biomass burning, cement-plant and biogenic influences. *Environment International*, 189(March). https://doi.org/10.1016/j.envint.2024.108787
- Grange, S. K., Fischer, A., Zellweger, C., Querol, X., Jaffrezo, J., & Hueglin, C. (2021). Switzerland's PM 10 and PM2 .5 environmental increments show the importance of non-exhaust emissions. *Atmospheric Environment: X*, 12(100145). https://doi.org/https://doi.org/10.1016/j.aeaoa.2021.100145
- Guenther, A. B., Jiang, X., Heald, C. L., Sakulyanontvittaya, T., Duhl, T., Emmons, L. K., & Wang, X. (2012). The model of emissions of gases and aerosols from nature version 2.1 (MEGAN2.1): An extended and updated framework for modeling biogenic emissions. *Geoscientific Model Development*, *5*(6), 1471–1492. https://doi.org/10.5194/GMD-5-1471-2012
- Guevara, M., Jorba, O., Tena, C., Denier Van Der Gon, H., Kuenen, J., Elguindi, N., Darras, S., Granier, C., & Pérez García-Pando, C. (2021). Copernicus Atmosphere Monitoring Service TEMPOral profiles (CAMS-TEMPO): Global and European emission temporal profile maps for atmospheric chemistry modelling. *Earth System Science Data*, *13*(2), 367–404. https://doi.org/10.5194/ESSD-13-367-2021
- Hopke, P. K., Dai, Q., Li, L., & Feng, Y. (2020). Global review of recent source apportionments for airborne particulate matter. *The Science of the Total Environment*, 740. https://doi.org/10.1016/J.SCITOTENV.2020.140091
- in 't Veld, M., Pandolfi, M., Amato, F., Pérez, N., Reche, C., Dominutti, P., Jaffrezo, J., Alastuey, A., Querol, X., & Uzu, G. (2023). Discovering oxidative potential (OP) drivers of atmospheric PM10, PM2.5, and PM1 simultaneously in North-Eastern Spain. *Science of The Total Environment*, 857, 159386. https://doi.org/10.1016/J.SCITOTENV.2022.159386
- Janssen, R. H. H., Geers, L. F. G., Kranenburg, R., Coenen, P. W. G. H., & Schaap, M. . (2023). Particulate matter formation potential of gas-phase emissions over Germany, Umweltbundesambt, FKZ 3719 51 201 0.
- Kranenburg, R., Segers, A. J. J., Hendriks, C., & Schaap, M. (2013). Source apportionment using LOTOS-EUROS: module description and evaluation. *Geoscientific Model Development*, 6(3), 721–733. https://doi.org/10.5194/gmd-6-721-2013
- Ledoux, F., Roche, C., Delmaire, G., Roussel, G., Favez, O., Fadel, M., & Courcot, D. (2023). Measurement report: A 1-year study to estimate maritime contributions to PM10 in a coastal area in northern France. *Atmospheric Chemistry and Physics*, *23*(15), 8607–8622. https://doi.org/10.5194/acp-23-8607-2023
- Manders, A., Builtjes, P., Curier, L., Denier van der Gon, H., Hendriks, C., Jonkers, S., Kuenen, J., Timmermans, R., Wichink Kruit, R. A., van Pul, A., Sauter, F., van der Swaluw, E., Douros, J., Eskes, H., van Meijgaard, E., van Ulft, B., Mues, A., Banzhaf, S., & Schaap, M. (2016). Curriculum Vitae of the LOTOS-EUROS chemistry transport model (v1.11). *Geoscientific Model Development, submitted.*
- Mooibroek, D., Sofowote, U. M., & Hopke, P. K. (2022). Source apportionment of ambient PM10 collected at three sites in an urban-industrial area with multi-time resolution factor analyses. Science of the Total Environment, 850(July). https://doi.org/10.1016/j.scitotenv.2022.157981
- Norris, G., & Duval, R. (2014). EPA Positive M atrix Factorization (PMF) 5.0 Fundamentals and User Guide. In *Environmental Protection Agency Office of Researc and Development*,

- Publishing House Whashington, DC 20460.
- Novak, J., & Pierce, T. (1993). Natural Emissions of Oxidant Precursors. *Water, Air and Soil Pollution*, *65*, 57–77.
- Paatero, P., & Tapper, U. (1994). Positive matrix factorization: A non-negative factor model with optimal utilization of error estimates of data values. *Environmetrics*, *5*(2), 111–126. https://doi.org/10.1002/env.3170050203
- Pekel, F., Uzu, G., Weber, S., Kranenburg, R., Tokaya, J. P., Schaap, M., Dominutti, P., favez, O., Jaffrezo, J.-L., & Timmermans, R. (2025). *Unravelling Source Contributions to Pm10 Oxidative Potential Through Comparison of Modelled and Experimental Source Apportionment Approaches*. https://doi.org/10.2139/SSRN.5202636
- Rémy, S., Kipling, Z., Flemming, J., Boucher, O., Nabat, P., Michou, M., Bozzo, A., Ades, M., Huijnen, V., Benedetti, A., Engelen, R., Peuch, V. H., & Morcrette, J. J. (2019). Description and evaluation of the tropospheric aerosol scheme in the European Centre for Medium-Range Weather Forecasts (ECMWF) Integrated Forecasting System (IFS-AER, cycle 45R1). *Geoscientific Model Development*, 12(11), 4627–4659. https://doi.org/10.5194/gmd-12-4627-2019
- Schwarz, P., Scheinhardt, S., & Witzig, C. (2019). Identifizierung und Quantifizierung von Feinstaubquellen im Raum Stuttgart anhand von Inhaltsstoffanalysen und Positivmatrix-Faktorisierung (PMF). *Immissionsschutz*, *24*(3), 127–132. https://doi.org/1430-9262
- Simoneit, B. R. T., Schauer, J. J., Nolte, C. G., Oros, D. R., Elias, V. O., Fraser, M. P., Rogge, W. F., & Cass, G. R. (1999). Levoglucosan, a tracer for cellulose in biomass burning and atmospheric particles. *Atmospheric Environment*, 33(2), 173–182. https://doi.org/10.1016/S1352-2310(98)00145-9
- Simpson, D., Benedictow, A., Berge, H., Bergström, R., Emberson, L. D., Fagerli, H., Flechard, C. R., Hayman, G. D., Gauss, M., Jonson, J. E., Jenkin, M. E., Nyúri, A., Richter, C., Semeena, V. S., Tsyro, S., Tuovinen, J. P., Valdebenito, A., & Wind, P. (2012). The EMEP MSC-W chemical transport model Technical description. *Atmospheric Chemistry and Physics*, 12(16), 7825–7865. https://doi.org/10.5194/ACP-12-7825-2012
- Thunis, P., Clappier, A., & Pirovano, G. (2020). Source apportionment to support air quality management practices. *Publications Office of the European Union*, 57. https://doi.org/10.2760/47145
- Thürkow, M., Banzhaf, S., Butler, T., Pültz, J., & Schaap, M. (2023). Source attribution of nitrogen oxides across Germany: Comparing the labelling approach and brute force technique with LOTOS-EUROS. *Atmospheric Environment*, 292, 119412. https://doi.org/10.1016/J.ATMOSENV.2022.119412
- Timmermans, R., Kranenburg, R., Hendriks, C., Thürkow, M., Kirchner, I., van Pinxteren, D., & Schaap, M. (2020). Establishing the Origin of Particulate Matter in Eastern Germany Using an Improved Regional Modelling Framework. *Springer Proceedings in Complexity*. https://doi.org/10.1007/978-3-030-22055-6_1
- Timmermans, R., van Pinxteren, D., Kranenburg, R., Hendriks, C., Fomba, K. W., Herrmann, H., & Schaap, M. (2022). Evaluation of modelled LOTOS-EUROS with observational based PM10 source attribution. *Atmospheric Environment: X*, *14*, 100173. https://doi.org/10.1016/J.AEAOA.2022.100173
- Toscano, D. (2023). The Impact of Shipping on Air Quality in the Port Cities of the Mediterranean Area: A Review. *Atmosphere*, 14(7). https://doi.org/10.3390/atmos14071180
- van Pinxteren, D., Engelhardt, V., Mothes, F., Poulain, L., Fomba, K. W., Spindler, G., Cuesta-Mosquera, A., Tuch, T., Müller, T., Wiedensohler, A., Löschau, G., Bastian, S., &

- Herrmann, H. (2024). Residential Wood Combustion in Germany: A Twin-Site Study of Local Village Contributions to Particulate Pollutants and Their Potential Health Effects. *ACS Environmental Au*, *4*(1), 12–30. https://doi.org/10.1021/acsenvironau.3c00035
- Vida, M., Foret, G., Siour, G., Jaffrezo, J. L., Favez, O., Cholakian, A., Cozic, J., Dupont, H., Gille, G., Oppo, S., Zhang, S., Francony, F., Pallares, C., Conil, S., Uzu, G., & Beekmann, M. (2025). Modelling oxidative potential of atmospheric particle: A 2-year study over France. Science of the Total Environment, 967(January). https://doi.org/10.1016/j.scitotenv.2025.178813
- Weber, S., Salameh, D., Albinet, A., Alleman, L. Y., Waked, A., Besombes, J. L., Jacob, V., Guillaud, G., Meshbah, B., Rocq, B., Hulin, A., Dominik-Sègue, M., Chrétien, E., Jaffrezo, J. L., & Favez, O. (2019). Comparison of PM10 Sources Profiles at 15 French Sites Using a Harmonized Constrained Positive Matrix Factorization Approach. *Atmosphere 2019, Vol. 10, Page 310, 10*(6), 310. https://doi.org/10.3390/ATMOS10060310
- Wind, P., Rolstad Denby, B., & Gauss, M. (2020). Local fractions-a method for the calculation of local source contributions to air pollution, illustrated by examples using the EMEP MSC-W model (rv4_33). *Geoscientific Model Development*, 13(3), 1623–1634. https://doi.org/10.5194/GMD-13-1623-2020
- Wind, P., & van Caspel, W. (2025). Generalized local fractions a method for the calculation of sensitivities to emissions from multiple sources for chemically active species, illustrated using the EMEP MSC-W model (rv5.5). https://doi.org/10.5194/EGUSPHERE-2024-3571

Appendix A – Annual source contributions to PM_{2.5}



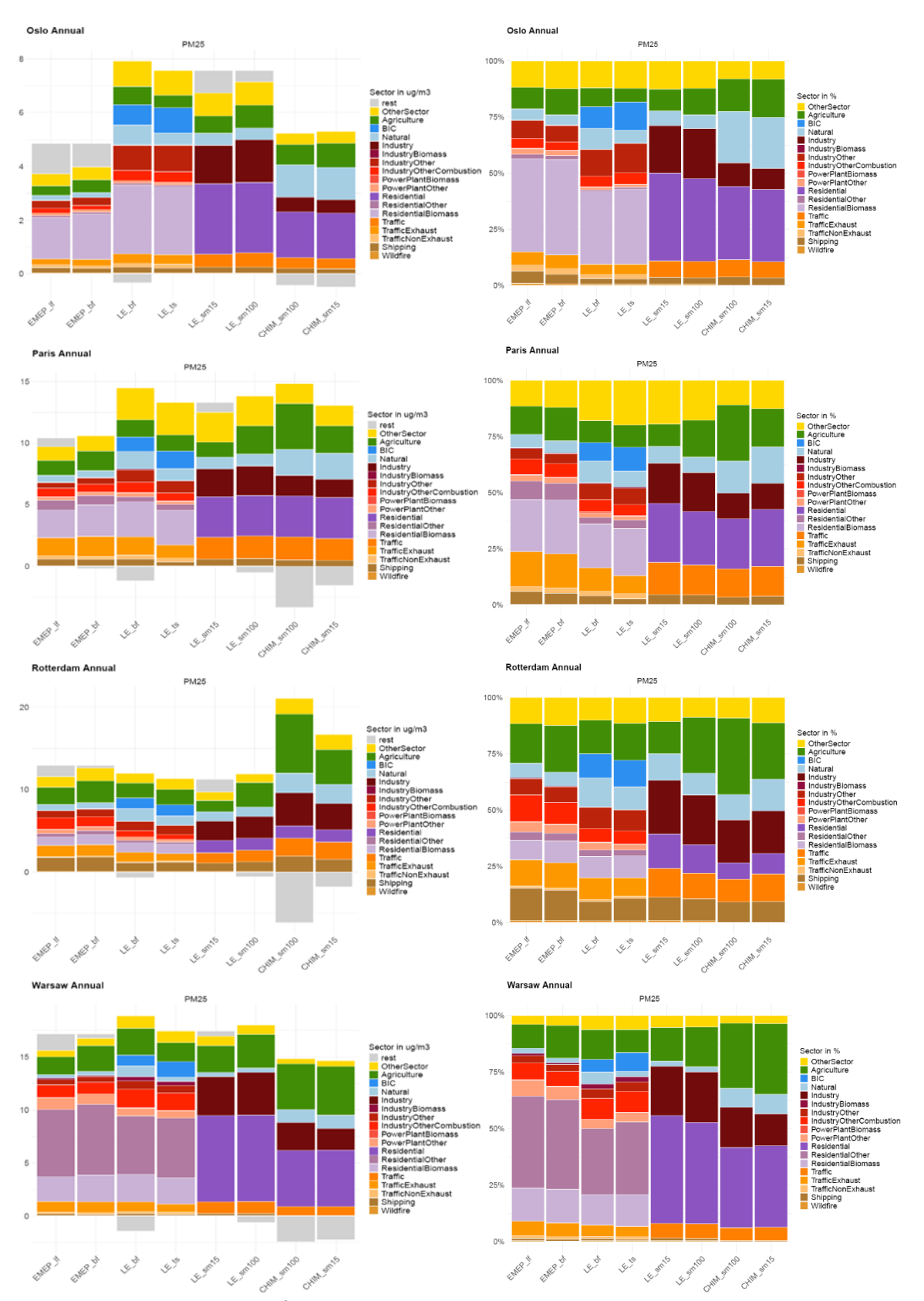


Figure A-1. Absolute (μ g/m³, left plots) and relative source sector contributions (%, right plots) to PM_{2.5} in Athens, Barcelona, Berlin, Milan, Paris, Oslo, Rotterdam and Warsaw from CHIMERE (CHIM), EMEP and LOTOS-EUROS (LE) model using either Brute Force method (_bf), Local Fractions (_lf), Tagging (_ts) or Surrogate Modelling with either 15% (_sm15) or 100% (_sm100) emission reductions scenarios. Sector categories refer to Table 3-2.

Appendix B – Impact of surface layer thickness

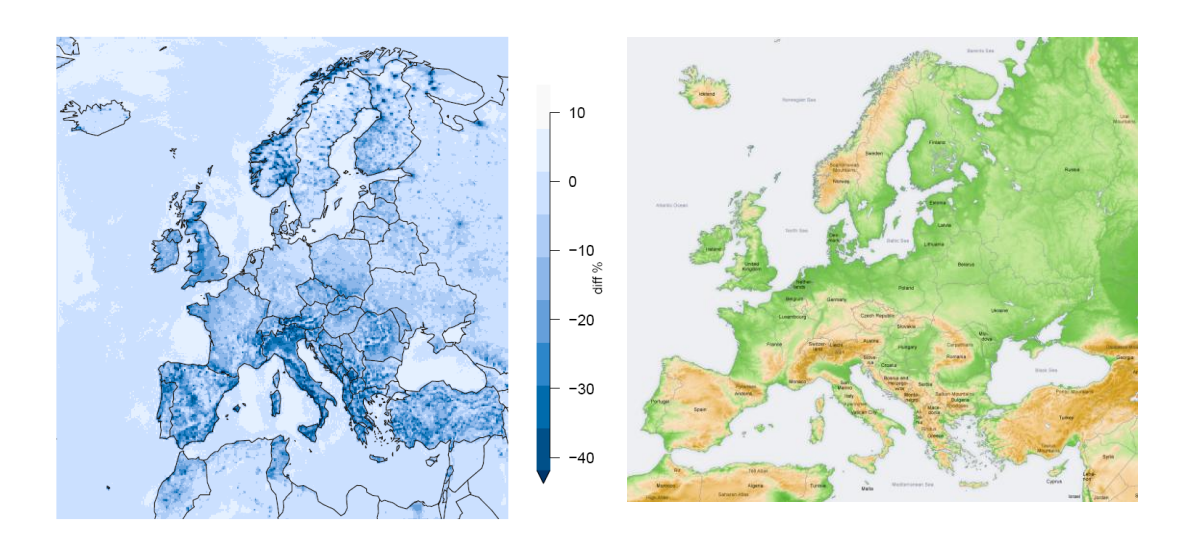


Figure B-1 Impact of doubling of the surface layer thickness in LOTOS-EUROS to POM concentrations in January 2019 (left plot) and orography (right plot)

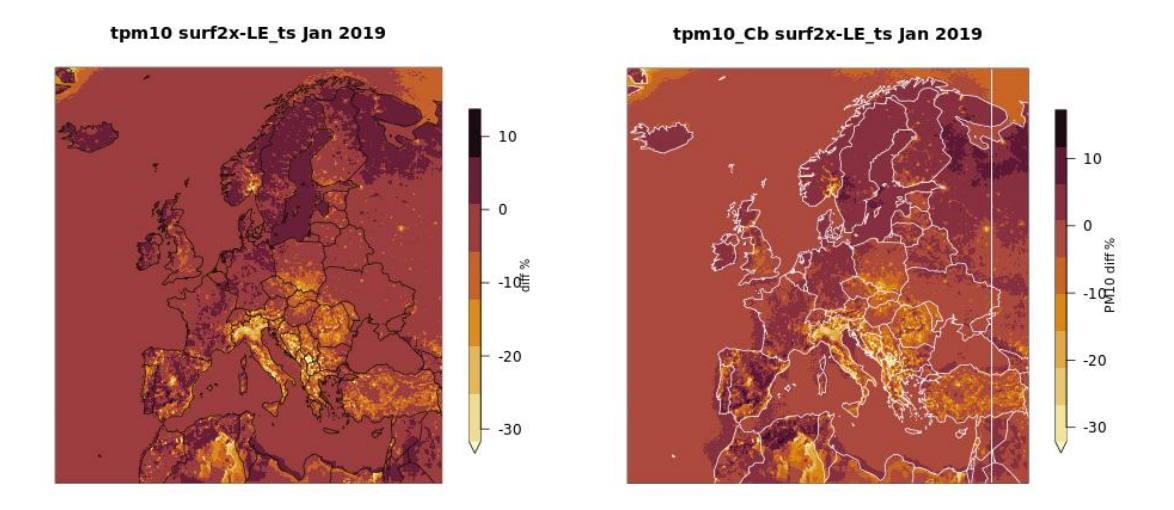


Figure B-2 Impact of doubling of surface layer thickness in LOTOS-EUROS to total PM_{10} (left plot) and PM_{10} residential combustion contribution (right plot) in January 2019

Appendix C – seasonal variation

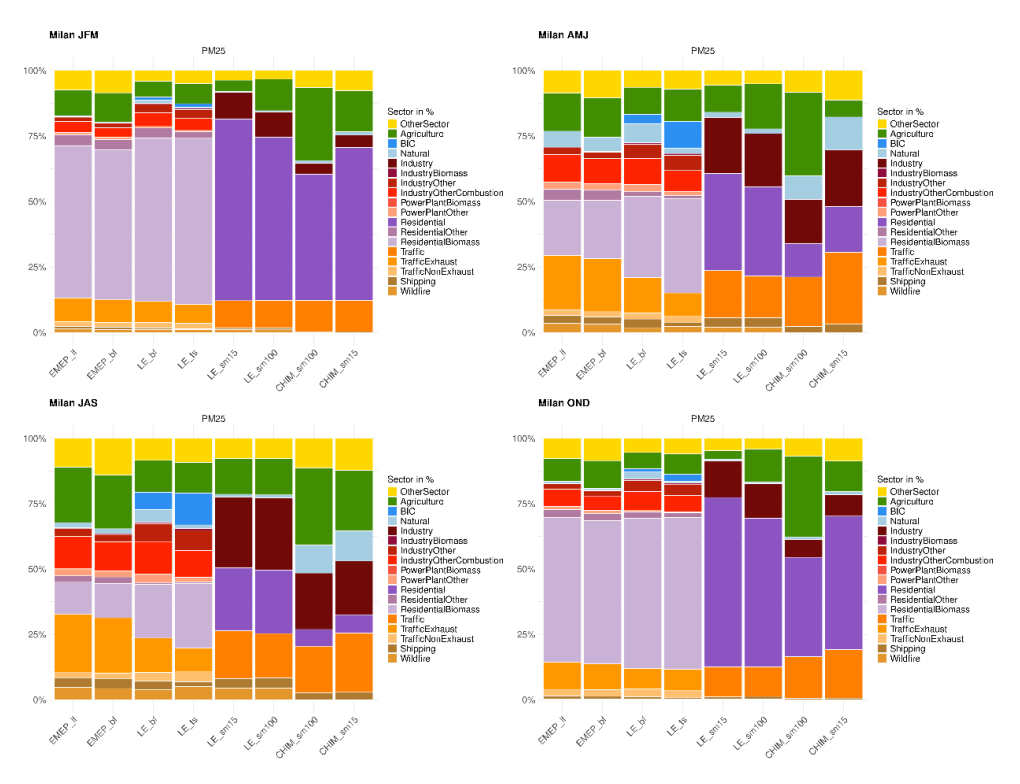


Figure C-1 Relative source sector contributions (in %) to $PM_{2.5}$ in Milan for January/February/March (JFM), April/May/June (AMJ), June/August/September (JAS), and October/November/December (OND)

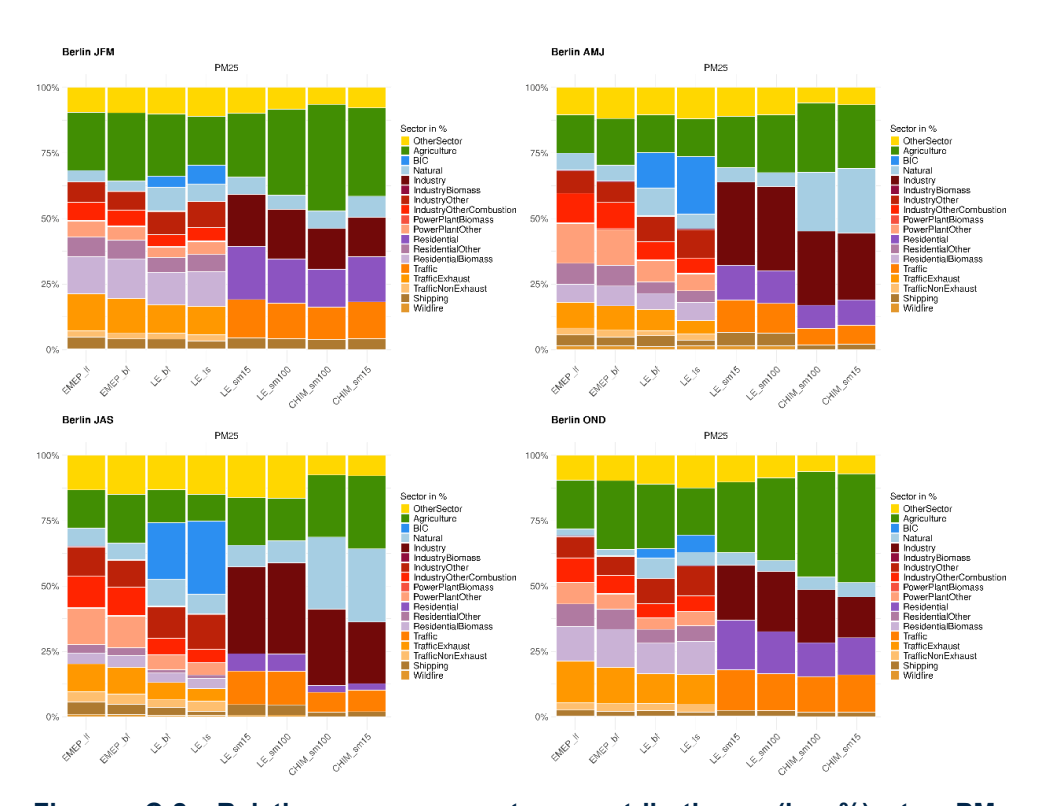


Figure C-2 Relative source sector contributions (in %) to PM $_{2.5}$ in Berlin for January/February/March (JFM), April/May/June (AMJ), June/August/September (JAS), and October/November/December (OND)

D6.3

Appendix D - EBAS Levoglucosan, Vanadium and Nickel tracer data

Table D-1 Overview of tracer data used for evaluation of modelled source contributions. N is number of data points in study period.

Station code	Species	N	Sample frequency (days)	Station typology	RMSE	Correlation
NO0002R	levoglucosan	53	7	rural	0.47	0.71 (r)
Station code	Species	N	Sample frequency (days)	Station typology	RMSE	Correlation (r)
CZ0003R	vanadium	365	1	Rural	0.33	0.29
CZ0005R	vanadium	182	1	N.S.	0.28	0.28
DE0001R	vanadium	250	1	N.S.	1.21	0.74
DE0002R	vanadium	49	2	Mountain	0.78	0.22
DE0003R	vanadium	53	2	N.S.	0.29	0.13
DE0007R	vanadium	49	7	Coastal	0.63	0.07
DE0009R	vanadium	53	7	N.S.	1.05	0.56
ES1778R	vanadium	53	7	N.S.	1.19	0.69
FI0018R	vanadium	53	7	N.S.	0.26	0.20
F10036R	vanadium	53	7	Coastal	0.10	0.05
F10050R	vanadium	52	7	N.S.	0.23	0.32
GB0048R	vanadium	52	7	rural	0.52	0.63
GB1055R	vanadium	52	7	rural	1.08	0.57
IS0091R	vanadium	52	7	rural	0.10	-0.02
IT0019R	vanadium	53	7	N.S.	0.90	0.71
NO0002R	vanadium	53	7	N.S.	0.46	0.65
NO0047R	vanadium	14	8.3	rural	0.07	0.01
NO0090R	vanadium	14	8.3	Rural	0.21	0.32
Station code	Species	N	Sample frequency (days)	Station Setting	RMSE	Correlation (r)
SI0008R	nickel	74	1	N.S.	1.04	0.14
CY0002R	nickel	338	1	rural	1.21	0.65
DE0001R	nickel	49	7	Coastal	0.77	0.30
DE0002R	nickel	52	7	N.S.	0.29	0.09

DE0003R	nickel	53	7	N.S.	1.05	0.54
DE0009R	nickel	53	7	N.S.	0.29	0.00
EE0009R	nickel	52	7	N.S.	0.50	0.42
ES0001R	nickel	60	1	rural	0.97	0.31
ES0007R	nickel	60	1	mountain	0.97	0.55
ES0008R	nickel	50	1	coastal	0.34	0.72
ES0009R	nickel	60	1	N.S.	0.93	0.45
ES0014R	nickel	61	1	rural	1.17	0.19
ES1778R	nickel	90	1	N.S.	0.26	0.04
FI0018R	nickel	52	7	N.S.	0.10	0.05
FI0036R	nickel	52	7	rural	0.23	0.25
F10050R	nickel	52	7	N.S.	1.12	0.60
GB0013R	nickel	14	7.3	N.S.	1.26	0.74
GB0017R	nickel	14	6.3	N.S.	0.52	0.84
GB0048R	nickel	14	8.3	rural	1.08	0.81
GB1055R	nickel	14	8.3	rural	0.90	0.50
IT0019R	nickel	49	2	mountain	1.93	0.20
NL0008R	nickel	176	1	N.S.	0.46	0.60
NO0002R	nickel	52	7	rural	0.07	0.03
NO0047R	nickel	53	7	N.S.	0.21	0.04
NO0090R	nickel	53	2	N.S.	0.07	0.38
NO0098R	nickel	53	7	N.S.	0.33	0.55

Appendix E – Data Providers PMF

The execution of CAMEO Task 6.3 was made possible through the generous contributions of PMF data from numerous research institutions across Europe. The provided datasets were instrumental in enabling the PMF and CTM comparisons and insights. We acknowledge the following contributors:

- Barcelona & Montseny (Spain): PMF data were provided by the IDAEA-CSIC research group (in 't Veld, 2023).
- **Melpitz (Germany):** Data from both the research station and the nearby village were obtained from Van Pinxteren et al. (2024).
- **Milan (Italy):** Data for the Milan station were supplied by the LIFE REMY project (manuscript currently unpublished).
- The Netherlands (Ijmuiden, Beverwijk, Wijk aan Zee): PMF data were kindly provided by Mooibroek et al. (2022).
- **Switzerland (Bern, Zurich, Payerne, Basel, Magadino):** Data were provided by Grange et al. (2021).
- Germany (Stuttgart, Gärtringen, Freiburg): Data were provided by the Landesanstalt für Umwelt Baden-Württemberg (LUBW). More information on the method can be found in (Schwarz et al., 2019)
- Athens (Greece): Data were provided by ENvironmental Radioactivity & Aerosol technology for atmospheric and Climate impacT (ENRACT) Lab National Centre for Scientific Research "Demokritos"; Athens, Greece. Authors: E. Diapouli, M. I. Manousakas, V. Vassilatou, S. Papagiannis, S. Vratolis, K. Eleftheriadis

We extend our sincere gratitude to all these institutions and projects for their invaluable support.

Document History

Version	Author(s)	Date	Changes
1.0			
2.0			

Internal Review History

Internal Reviewers	Date	Comments

This publication reflects the views only of the author, and the Commission cannot be held responsible for any use which may be made of the information contained therein.